

*University of Modena and Reggio Emilia*

*School of Graduate Studies “Multiscale Modelling, Computational Simulations and Characterization for Material and Life Sciences”  
(XXV cycle)*

***Study and development of industrial glass coating  
for industrial application***

***Candidate : Dr. Matteo Dignatici***

***Tutor : Prof. Cristina Siligardi***

***Co-Tutor : Dr. Monia Montorsi***

***Director : Prof. Ledi Menabue***

***Doctoral Thesis***

# 1 Introduction and objective

## 1.1 Introduction

Vitreous enamels play a very important role in the coating production process of steel, in accordance with the technical and aesthetic properties induced by enamel to the final material [1]. In particular, from the functional point of view, vitreous enamel coatings show excellent resistance to chemical degradation processes [2,3], as well as a good resistance to tribological phenomena such as abrasive wear [4]. Enamel coatings are generally defined as a substantially vitreous glassy inorganic layer bonded to various metal substrates by fusion at a specific temperature. The key factor for the functionality of the final material is the achievement of a good bond between the enamel and the metal substrate during the enamelling process. Several factors could affect the interface reactions and the bond mechanism between the glass coatings and the metal substrate, such as the chemical composition of enamel, the type of steel, the roughness of the metal surface, the heating process and the glazing temperature, the atmosphere of the oven and so on [5].



Figure 1. One rotational thermal exchanger of thermal power station

It's 25 years that Smaltiflex S.p.a. is enamelling vitreous enamel steel for industrial applications like thermal exchangers of thermal power stations (Figure 1). Ljungström is a kind of rotational thermal exchanger called air preheater (Figure 2). This air preheater is a regenerative heat exchanger which is mainly used in steam boiler plants for the preheating in combustion air. The hot gas and cold air ducts are arranged to allow both to flow simultaneously through the machine. The hot flue gas heats the rotor material and as the rotor rotates, the hot rotor section moves into the flow of the cold air and preheats it.

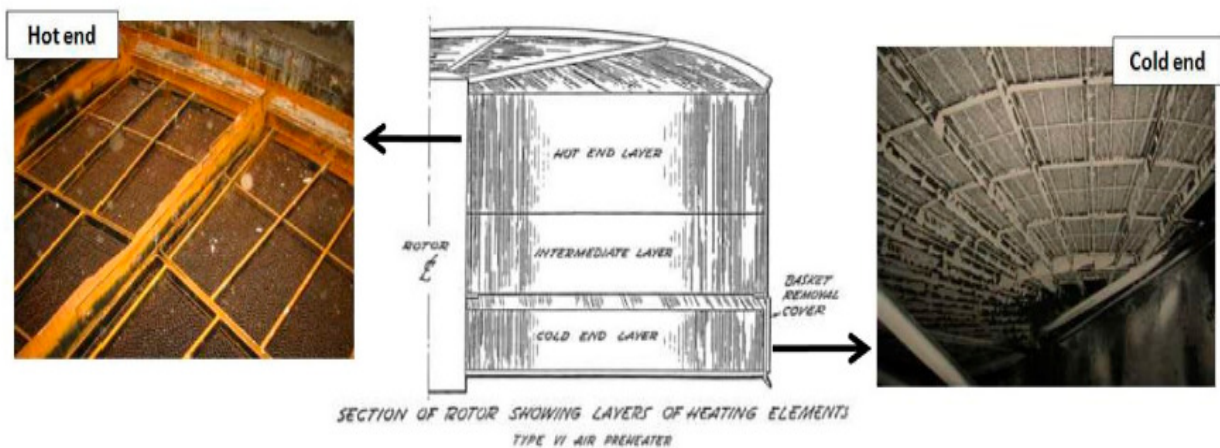


Figure 2. Ljungstrom preheater

## 1.2 Problems about final application of vitreous enamel steel

Generally, porcelain coatings are characterized by a glass structure with high hardness and by the presence of bubbles. The most important characteristic of these coatings is the strong structure between steel and enamel at the interface with a particular mechanism of adherence. Other important properties are represented by the high resistance to chemical solutions, in particular to acid pH [6-8].

The final application of vitreous enamel steel of Smaltiflex is a kind of preheater with energy recovery (Gas-Gas Heater, GGH) in thermal exchanger power stations. This preheater needs material for part-exchange with high resistance to corrosion, as during the heater process the pH is very low.

This part-exchange with vitreous coating is put together in baskets with different sizes. In these baskets, combustion exhaust gases heat the combustion air to improve the power station performance.

During this process, the temperature of exhaust gases gets to a dew point, and generates acid condense on the surface of baskets inside the rotors. Exhaust gases are typical of every air combustion, and are responsible for low pH  $\text{SO}_x$  and  $\text{NO}_x$  [9]. When these gases react with the water into the condense, they generate two strong acids such as sulfuric acid and nitric acid.

Usually these baskets are in stainless steel, but their lifetime is not suitable for the preheater maintenance. Studies about corrosion showed that the lifetime of part-exchange increased by six times [6,11].

Problems about vitreous coating are two: the mechanical and chemical structure of coating, and the status of the coating during the lifetime. In literature [6,7], vitreous enamel steel with no standard quality structure decreases quickly the lifetime of part-exchange. Fractures on the surface of part-exchange decrease the basket lifetime of about 50% [6].

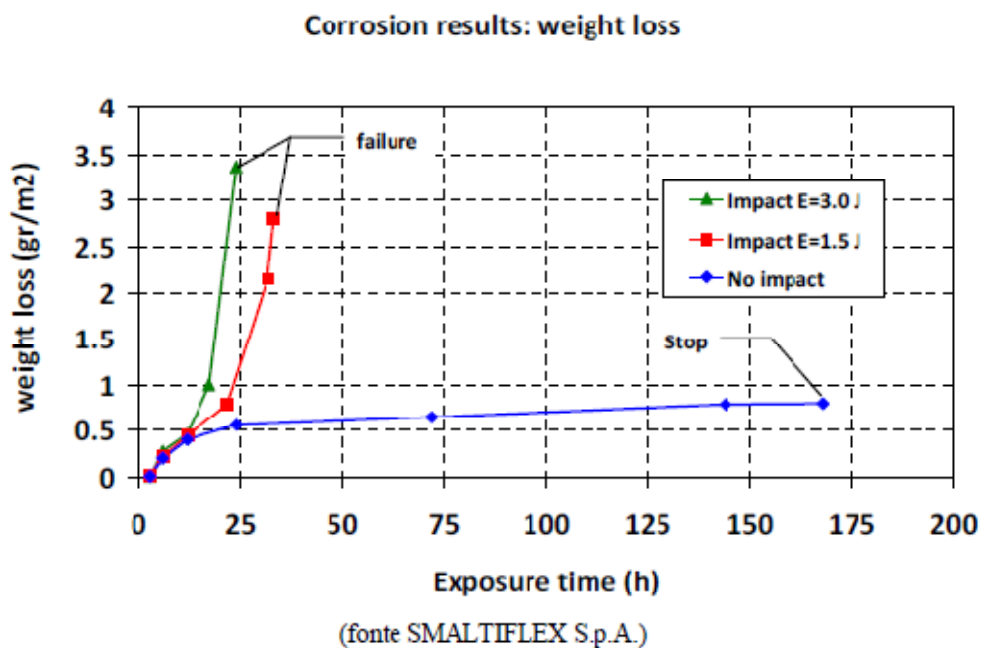


Figure 3. Test of corrosion carried out by Smaltiflex

In order to classify this kind of corrosion, Figure 3 shows the behaviour of the same vitreous enamel plate with and without mechanical stress (impact). The test was carried out to put the vitreous enamel plate in a room with 30% of  $\text{H}_2\text{SO}_4$  and with 105°C temperature. Two samples

with mechanical stress decrease quickly the weight, but without mechanical stress the variation is small for a long time.

From this test, it is possible to underline that :

- Thickness of enamel, thickness of steel and interface between enamel and steel are parameters which are important to improve the porcelain steel lifetime.
- Technology of enamelling could modify the properties of the interface.

After this introduction, I focus the objective on the study and characterization of vitreous coating over steel.

## **1.3 Objective**

The goal of this work is the study and characterization of industrial glass coating (enamel) over steel and enamel-steel interface.

This study is a cooperation between the Department of Engineering “Enzo Ferrari”, the University of Modena & Reggio Emilia and Smaltiflex S.p.A.. Smaltiflex produces vitreous enamel steel for thermal exchangers of thermal power stations and its knowledge of enamel starts in 1964.

For a long time, Smaltiflex has been enamelling steel for different applications: boiler tanks for domestic use, hobs, kilns, parts of washing machines and dishwashers. A classical problem of industrial enamel on steel is the bond between steel and enamel. Hereafter the main objectives of this work.

### **1.3.1 Specific objectives**

- ✓ Characterization of different frits and very low carbon steel DC04ED by using several experimental techniques.

- ✓ Mechanical and microstructural characterization of the enamel-steel interface of industrial samples, obtained by hand spraying system
- ✓ Electrophoretic (EP) deposition of industrial slurry over steel substrate: study and development of specific additives in order to increase the stability of the diluted slurry.
- ✓ Mechanical and microstructural characterization of the enamel-steel interface of samples obtained by (EP) deposition.

## References

[1] Andrew A.I. Porcelain Enamels. Garrad Press, Champaign, IL 1961.

[2] Kuchinski F.A. Corrosion resistant thick films by enamelling. In: Wachtman J.B., Haber Ra, editors. Ceramic films and coatings. Park Ridge (NJ): Noyes Publications (1993), p. 77-130.

[3] Scrinzi E, Rossi S. The aesthetic and functional properties of enamel coatings on steel. *Materials and Design* (2010); 31: 4138-46.

[4] Bazayants GV, Svetlichnyi VA, Demchuk VV, Ryzhikov VA. Abrasive wear of glass enamels and slag sitall used in heat energetics. *Glass and Ceramics* (1983); 40 [16]: 295-6.

[5] Ubertazzi A, Wojciechwski N. Vitreous Enamel. Hoepli Editor, Milan, 2002.

[6] A. Chelli, R. Poletti, L. Pignatti, F. Bruscoli, G. Pasqualetti, F. Bruni, A. Zucchelli, L. Rossetti, F. Lotti, G. Minak, V. Dal Re, S. Curioni, Elementi in acciaio smaltato per preriscaldatori d'aria e gas-gas heaters: un approccio integrato dalla loro formatura e smaltatura all'assemblaggio nei cestelli, XXI° International Congress on Porcelain Enamel, pp. 130-158, 18-22 maggio 2008, Shanghai-Cina

[7] Andrews A. I. Porcelain Enamel. The Garrard Press, 1961.

[8] R. Poletti, A. Zucchelli, A. Chelli, Experimental Investigation on Corrosion Resistance of Porcelain Enamel Composite Coating for Regenerative Air Heaters Parts, DanubiaAdria 2005

[9] M.C. Barros, P. Bello , E. Roca, J.J. Casares , Integrated pollution prevention and control for heavy ceramic industry in Galicia (NW Spain) Journal of Hazardous Materials 141 (2007) 680–692

[10] GiangiacoMo Minak, Andrea Zucchelli, Daniele Ghelli, STUDIO DEL COMPORTAMENTO DI LAMIERE SMALTATE OGGETTE AD IMPATTO A BASSA VELOCITÀ, AIAS – ASSOCIAZIONE ITALIANA PER L’ANALISI DELLE SOLLECITAZIONI XXXVII CONVEGNO NAZIONALE, 10-13 SETTEMBRE 2008, UNIVERSITÀ DI ROMA “LA SAPIENZA”

[11] A. Chelli, R. Poletti, Smaltiflex S.p.A., F. Bruscoli, G. Pasqualetti, F. Bruni, A. Zucchelli, L. Rossetti, F. Lotti, G. Minak, V. Dal Re, S. Curioni,  
Un approccio integrato dalla formatura e smaltatura all’assemblaggio nei cestelli , ELEMENTI IN ACCIAIO SMALTATO PER PRERISCALDATORI D’ARIA E GAS-GAS HEATERS , CISP

## 2. State of the Art

### 2.1 Glassy

Since the 1960, the Russian scientists of glass science favored a theory of the structure of vitreous silica based on the coincidence of the broad X-ray diffraction peaks for vitreous silica and the sharp peaks of cristobalite [1-3]. Vitreous pattern was got to line broadening due to the extremely small “particle size” of such crystallites. However, for vitreous silica, this “microcrystallite” theory has largely been supplanted by the random network theory of Zachariasen. According to Zachariasen, glass is a substance which an form extended three dimensional net works lacking periodicity with an energy content comparable with that of the corresponding crystal network. In essence, the density and the mechanical properties of glass are solid-like; however, the atoms form a continuous random network such that the unit cell (in crystal structure terminology) is infinitely large, containing an infinite number of atoms. Thus a working definition of glass is that it is a solid with a liquid-like structure. Unlike a crystal, glass may not be represented by a simple chemical formula. There are no restrictions with regard to the relative numbers of chemically different atoms other than the fact that the valences and/or coordination requirements may need to be satisfied. Unlike a crystal, glass does not have a sharp melting point when heated. The seemingly rigid solid gradually softens and flows at higher temperatures. At room temperatures, however, the viscosity of glass may be sufficiently high that measurable flow does not occur over millennia certainly not over practical time scales in typical laboratory experiments [1-2]. It is doubt full that glass windows in building structures of the middle ages have flowed to become thicker at the bottom [1]. Chunks of glass do not have habit planes. Nor does glass have identify able cleavage planes. In the absence of externally applied mechanical, electrical, thermal, magnetic, and gravitational fields, the properties of glass are essentially isotropic like those of a typical liquid. In principle, glasses and amorphous solids make up a class of substances called noncrystalline solids. Both glass and amorphous solids are “x-ray amorphous.” [1,2]. The distinction from an amorphous solid is made to recognize the smooth transition of glass to liquid state on heating; amorphous solids appear to crystallize before transformation to the liquid state. Care should, however, be taken in not confusing glass with an amorphous powder, a term commonly used to refer to a random assemblage of finely divided crystals.

### **2.1.1 Method and manufacture of glass**

The most common method for making glass is to:

- Melting of different raw materials in appropriate proportions
- Gather and form into useful products,
- Cool subsequently at a rate fast enough to avoid distortion of the shape yet slow enough to avoid cracking.

In reality, a substance may, however, be brought to a glassy state or amorphous state from any of the three equilibrium states of matter solid, liquid, or gas. Vapors of many substances when allowed to condense on a cold substrate often yield an amorphous structure. The structure may be a glass or an amorphous solid depending on experimental parameters. Inorganic glasses may also be obtained by

1. Hydrolyzing an alcoholic solution of an organometallic compound,
2. Stirring the hydrolyzed product to allow rapid chelation to a gel state,
3. Drying the gel mass to drive off the organics,
4. Sintering at an elevated temperature to obtain a compact.

This method, called the sol-gel route to glassmaking, is often used to deposit thin films such as antireflection coatings.

### **2.1.2 Glass properties**

From a thermodynamic viewpoint, glass is not the fourth state of matter. This may be understood by examining the volume-temperature relationship of a typical glass-forming melt upon cooling, as shown in Figure 4.

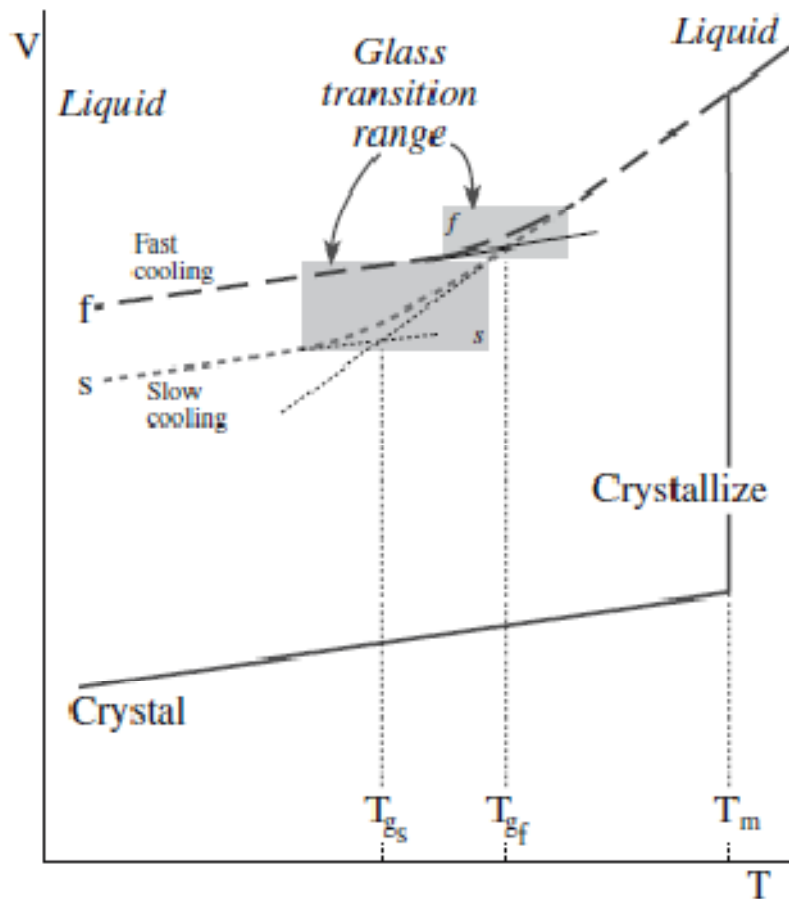


Figure 4. Different behaviour between solid state and glass state

Consider the graph of specific volume as a function of temperature as shown in Figure 4. It is a kind of a time–temperature–transformation diagram for a glass. On cooling the liquid from a high temperature, two event may occur at the point of solidification,  $T_m$  [1-3]. With crystallization of liquid reach a discontinuous change in  $V$  and a discontinuity in the rate of cooling (associated with the heat of crystallization). If no crystallization occurs the liquid passes into a supercooled state and  $V$  decreases at about the same rate as above  $T_m$ . At the glass transition point,  $T_g$ , the slope of the curve decreases to become close to that of the crystalline solid. This break in the cooling curve marks the passage Inorganic amorphous or glassy solid is a high-speed cooled liquid but is cooled fast to avoid that energy melting-solidification consented the crystallization of the system. The relationship between the oxygen and the cation of the oxide compound essentially influences the glass-forming ability of an oxide like Dietzel theory (Figure 2) from a supercooled liquid to a glass. Below  $T_g$  the glass structure does not relax very fast because it is now a solid. In the region of  $T_g$  the viscosity is about  $10^{13}$  Pa\*s [1-4]. The linear thermal expansion for the glassy state is usually about the same as that for the crystalline solid. If slower cooling rates are used so that the time for

the structure to relax is increased, the supercooled liquid persists to a lower temperature, and the resulting glass may have a higher density as shown graphically in Figure 5. The physics of vitreous examines the concept of fragility ; this is actually a property of glass-forming liquids above  $T_g$  and is a measure of the strength of the interatomic bonding.

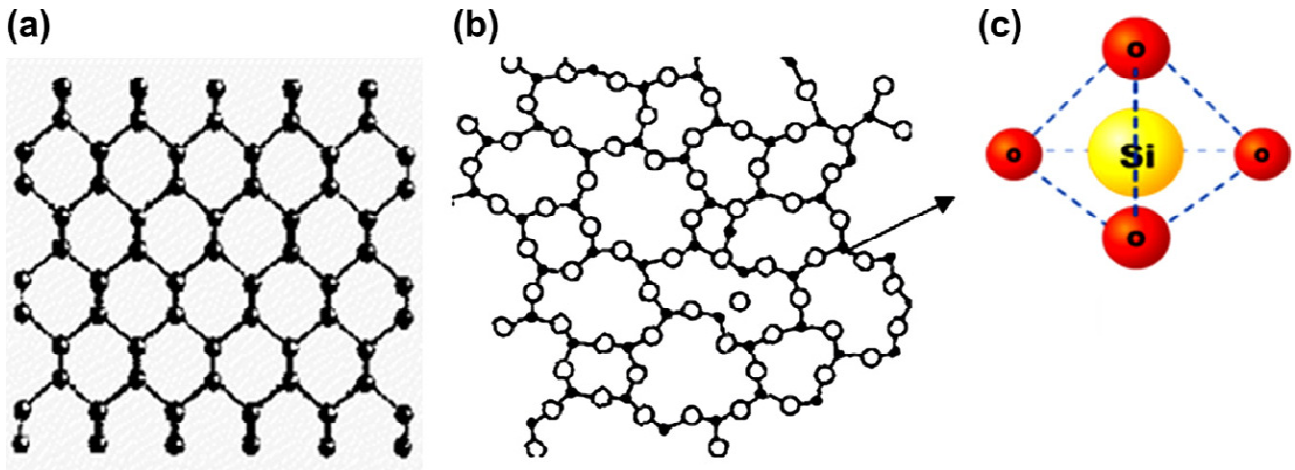


Figure 5. Glass structure

Fundamental characteristic of inorganic glasses, at room temperature, are very viscous structures ( $10^{18}$ Pa\*s glass viscosity vs 1Pa\*s water viscosity) [3]. Viscous flow of glass at room temperature occurs in a geological timescale.

With increasing temperature, the glass viscosity decreases as is shown in Figure 6.

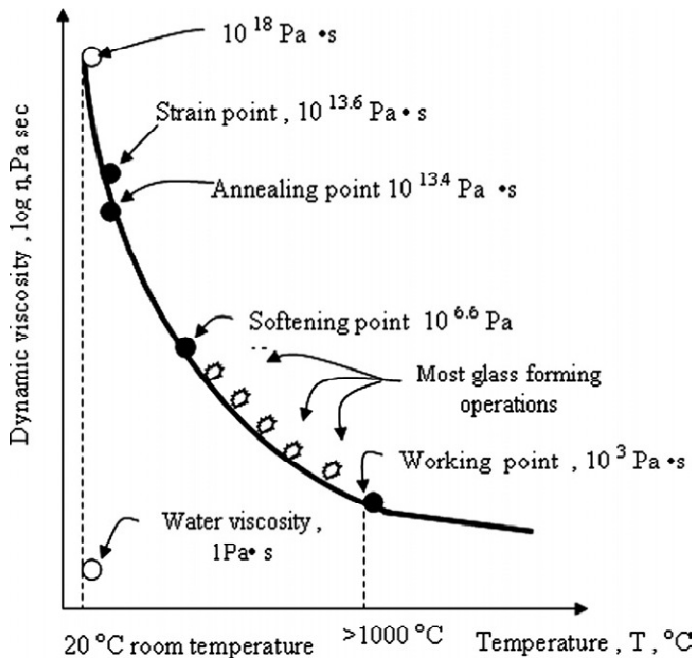


Figure 6. Viscosity vs Temperature and characteristic points

From figure 6 got five typical temperatures, called “standard points”, associated with the viscous flow (melting) of glass [4]. Structural applications for inorganic glass are allowed below Strain point. In the range room temperature and the temperature of Strain point, inorganic glass material was regulated by Hook equation. The strain point is the maximum temperature with relative viscosity to consented at glass the structural applications. The point to reduce the higher quantity of residual stress in 15’ minutes of thermal treatment are the Annealing point. To get mechanical properties suitable, this point are very important. Softening and Working points are the range that the modification of viscosity values are higher than other range.

Finishing the first thermal treatment the glass was formed, it is cooled to a temperature nearly above the strain point, where it will retain its shape and resist flow.

Before the first thermal treatment, the glass is annealed to relieve the internal stresses. To Avoid problem of fracture or crack at room temperature, glass is annealed will fracture or crack at ambient temperature [5].

Characteristic of specific viscosity of glass as a function of the temperature is illustrated in from Figure 7.

The standard points of glass.

No.	Standard point name	Viscosity (Pa s)	Temperature descriptions
1	Working point	$10^3$	At this temperature, the viscosity is sufficiently low for glass forming. Casting processes are possible below $10^3$ Pa s viscosity
2	Softening point	$10^{6.6}$	At this temperature, the viscosity is sufficiently low for glass to slump under own weight. Near below this temperature glass is stiff, but a little effort is necessary for yield and flow
3	Glass transition temperature	$10^{12}$	Range of temperatures at which glass transitions from super cooled liquid in a solid state
4	Annealing point	$10^{13.4}$	Internal stresses are relieved in minutes
5	Strain point	$10^{13.6}$	Internal stresses are relieved in hours

Figure 7. Effects of characteristic points

Mechanical and physical properties of glasses are essentially determined by their composition and the thermal treatments. Usually it was possible shown some parameters of inorganic glasses like :

1. Are harder than metals.
2. Have tensile strength in the range 24–69 MPa.
3. Are brittle and have low ductility.
4. Have a low coefficient of thermal expansion.
5. Are good electrical insulators.
6. Are resistant to chemical solution, water solution and other medium.

Selection of the main mechanical and physical properties of glass and glass–ceramic is presented in Table 1 and 2.

Material	Flexural Strength (MPa)	Compressive Strength (MPa)	Hardness HV	Young modulus (GPa)
Silica glass	98	1860	600	69
Crystalline glass-ceramic	103	344	250	64
Carbon Steel	275	275	100	200

Table 1. Mechanical properties of different kind of materials

Material	Density (Kg/m <sup>3</sup> )	Thermal conductivity (W/m °C)	Linear thermal expansion	Electrical resistivity (Ω m)
Silica glass	2304	34	1	10 <sup>7</sup>
Crystalline glass-ceramic	2592	33	9,4	10 <sup>12</sup>
Carbon Steel	8064	47	11,9	20

Table 2. Thermal properties of different kind of materials

## 2.2 Porcelain enamel : definition composition and properties

### 2.2.1 Definition

Porcelain enamel is an inorganic glass coating which is applied on metals and glass, for protective purposes, functional and decorative. Thermal treatments, to obtain glass coating, could be made after each kind of deposition [6]. Temperature of thermal treatment are different for each metal plate such as : steel (800-900)°C, glass (550-650)°C, aluminium (500-550)°C.

Melting and homogeneous coating has been obtained by thermal treatment and this allow a new composite material. Different chemical bonds, adherence are the typical characteristic of porcelain metal. Difference between porcelain steel and ceramic coating are the glass structure and the kind of substrate. UNI 8762 define: “porcelain enamel is a vitreous coating for metal and glass substrates to improve technical and artistic properties” [6-7]. This is an inorganic glass coating obtained by melting and fast cooling. Porcelain enamel has been melt on the substrate in

the thermal range [450-950]°C and has a cubic thermal expansion measured between (20-100) °C of between  $150$  and  $450 \cdot 10^{-7} \text{ K}^{-1}$ .

### 2.2.2 Composition

Basic composition of porcelain enamel are frit glass. These are a mixture of inorganic oxides and inorganic compounds after typical thermal treatment such as melting and fast cooled (Figures 8 and 9).

In furnace was melted the mixture of powder of raw materials and after the fast cooled by water (Figures 8 and 9). In few second temperature decrease about  $1000^\circ\text{C/s}$  and freezing to form little grains.



Figure 8. Melting of raw material



Figure 9. Frit glass during the cooling

### 2.2.3 Properties

Characteristic properties of vitreous enamel are [7]:

#### **Incombustibility**

Porcelain metal plate has been damage from the contact of heat and fire. Any kind of gases are released during these thermal stress.

#### **Resistance to high temperatures**

Heat resistance is a thermal property of porcelain enamel, and this are typical of glassy nature of the porcelain enamel. Inorganic glass before 400°C have not thermal stress to modify its structure.

#### **Resistance to thermal shock**

All porcelain enamel have got a good resistance to thermal shock. In particular, for civil use (pots and pans, grills, griddles, grills, ovens) can allow to thermal shock of 300°C.

### **Resistance to corrosion**

Iron-based metals will oxidize, rust and decay to the point of destruction if they are left exposed to the air. In this case vitreous enamel's primary function is to protect objects made of metal against this inevitable process, lengthening their working lives indefinitely. As the enamel adheres to the metal support surface perfectly, it blocks any possibility of rust formation, even at relatively high temperatures.

### **Resistance to chemical agents**

Different enamels perform noticeably differently towards chemical agents. Generally speaking, all vitreous enamels are fairly resistant to the majority acids, alkalis, organic solutions, varnishes, paints and salts. No enamel can stand up to nascent or elementary fluorine, to hydrofluoric acid and the acid solutions of fluorine (pH < 7), to strong alkaline solutions (pH > 12), to molten alkalis and hot concentrated phosphoric acid up to 230°C. The chemical resistance of enamel can be evaluated in compliance with UNI 5717. According to UNI 5717 can be used to give a classification of enamels (AA - A - B) according to their resistance to acids and the test method for obtain its [6].

### **Resistance to weathering**

Rain, air born pollutants, the salinity in the air in coastal areas, sunlight (UV rays) and sudden changes in temperature cause no damage whatsoever to enamelled surface colour or shine. This has been demonstrated and well-documented in a series of tests that involved exposing enamelled panels to atmospheric agents for 30 years. These are the properties that have opened a constant stream of new doors applications of vitreous enamelled steel in the building and street furniture sectors.

### **Impermeability to liquids**

As long as they are in good condition, enamelled surface are not porous and will be completely impermeable to liquids.

## **Hardness**

Enamelled products have a very hard vitreous surface with a high degree of resistance to knocks, scratches, abrasion and wear. However empirical, hardness classification is based on Mohs scale, which places enamels between 5 degrees and 7 degrees.

## **Resistance of abrasion**

Together with its resistance to temperatures and its hygienic qualities, enamel's resistance to abrasion is one of this material's most important functional qualities, enabling it to be used for a huge variety of applications in two important industrial sectors : domestic whitegoods and hygienic and sanitary fittings.

## **2.3 Porcelain enamels**

Porcelain enamels can be classify into two categories: enamel background called "ground" and "Final enamel"[7, 9-10].

### **Ground**

Composition of this enamel have got different metal oxide to improve the adherence between enamel and the metallic substrate. This adherence is obtained by specific thermal treatment. Colours of "ground" are limited because artistic effects aren't needed.

### **Refining enamel**

These enamel are useful to improve: chemical and mechanical property or artistic effects. Usually the application of final enamel need some specific pre-treatments.

## **2.4 Substrates for enamelling applications**

Industrial substrate used for enamelling applications are [7]:

- Steel
- Aluminum
- Cast iron

- Glass

## **Steel**

Steel for enamelling applications required some property such us :

- Homogeneous surface
- Suitable adherence with vitreous coating
- Limited phenomena of fishscale

Suitable steel can be classify about carbon mass concentration :

- Low carbon steel (C 0.035 ÷ 0.065 %)
- very low carbon steel (C < 0.0040 %)
- steel "Interstitial Free" (C 0.0015 ÷ 0.0050 %)

## **Aluminium**

Substrate of aluminium and aluminium alloys required some characteristic :

- Aluminium >99,5 %
- Alloy Aluminium – Manganese
- Substrates with aluminium coating

## **Cast Iron**

Only grey cast Iron is possible enamelling about UNI 8762 [7]. Perlitic or perlitic- ferric structure is required to obtain suitable adherence, and avoid the presence of cementite.

## **Glass**

Every kind of glass can be enamelling, without problems. Aim of glass substrate is improve the aesthetic surface but do not improve mechanical and chemical properties.

## **First treatment**

First treatments are some chemical and physical process to modify the substrate to obtain better condition to enamelling. Usually these process is carried out to get suitable adherence between enamel - steel.

In the first part the objective is the polish of surface to remove oil, and other substance no suitable for the adherence, and the last part is increase the surface roughness.

Chemical treatments is typical for steel and aluminium substrates, instead for cast iron is mechanical treatments like sandblast.

Chemical reactions are carried out in acid solutions or basic solutions separate from water washing to remove acid or basic solvents before dry process. Mechanical process consists in a sandblast treatment with sand or grain of hard metal.

### **2.5.1 First treatment for low carbon steel**

A typical sequence of chemical reactions for very low carbon steel are :

- Degreasing by solvent
- Degreasing by alkaline solutions
- Hot water and water at room temperature
- Pickling
- Nickelating
- Water room temperature
- Dry process

#### **2.5.1.1 Deagresing**

Degreasing is the first part of chemical treatment and remove, in 6-10 minutes, from the surface oils used during form of substrate. These oils are used to limited the oxidation of very low carbon steel by air, they are a little protective film versus the oxygen of the air. Solvent used for this application, allow the dispersion of oils in the washing machine ( Figure 10).



Figure 10. Industrial washing machine.

Other important contaminants are carbon and powders of metallic waste. These substances are removed by alkaline solutions at 80°C. These solutions is composed from three chemical species such us : Inorganic alkaline salts, additives, surfactants,.

Typical alkaline salts used are : Sodium idroxyde, Sodium methasilicate, Sodium Carbonate ; additive used is EDTA, and surfactant such as : Sulfate, Ammine, Carboxylate. Finally alkaline solutions are removed from substrate by hot water and water at room temperature. Other data about degreasing process is shown in Table 3.

Process	Time (min)	Temperature (°C)	Concentration (g/l)
Degreasing	6-10	40- 70	20-60
Degreasing by Alkaline	6-10	40-70	20-60
Water	1-3	50	
Water	1-3	20	

Table 3. Specific data of degreasing process

### 2.5.1.2 Pickling for very low carbon steel

Pickling is a treatment, after degreasing, to remove contaminant substance on the surface of substrate. These substance are : Iron oxide (II), Magnetite. This process is carried out by sulphuric

acid at 10% wt at the temperature of 65-70°C for 3-5 minutes. Amount of Iron remove from substrate is the key to obtain suitable nickeling and suitable enamelling. Usually amount about 10-20gr/m<sup>2</sup> consent to obtain good results.

#### **2.4.1.3 Nickeling**

This process is carried out by NiSO<sub>4</sub> to deposit little amount of Ni<sup>+2</sup> on the surface of substrate. Presence of Nickel on the surface improve the adherence between steel –enamel during the thermal treatment.

#### **2.4.1.4 Water**

After Nickeling, substrate is neutralized by water to remove every waste substance of previous process.

#### **2.4.1.5 Dry**

Dry process is the last process of First treatment, and is carried out by kiln with ho air. Finally the substrate is ready for enamelling treatment.

### **2.5 Enamelling**

The Techniques used to apply vitreous enamel to different metals vary according to whether the enamel is ground in a dry condition or wet condition. Application of enamel is carry out in both methods. In the case of a wet application, the next operation is drying . Final step of both methods is the thermal treatment in furnace, to densify the specimens. An important difference between these type of enamelling is based one the number of layers of enamel carry out (i.e. one to three), which usually require drying and different thermal treatments.

## 2.5.1 Wet enamelling

There are various variations on the theme of wet coating :

- Dipping
- Flow enamelling
- Spray enamelling
- Electron enamelling

### 2.5.1.1 Dipping

Dipping is a technique of enamelling that require the enamel slip, then removing it at a certain speed and angle, so that the excess amount of slip will drip off. This application is used for cover coats, when both sides of the product need to be enamelled and also in general when finished product's surface is not relevance. Over the years, whenever the type of product and the process have made it possible, this application has evolved from manual to automatic (Figure 11). The system used for dipping technique usually comprises simple chains fitted with hooks that support the products before the application and while excess amount of slip is dripping off. Mechanical mechanism then take the products from the chain, plunge them into the slip bath, then put them back on the chain to drip off. Thus, the specimens is ready for drying process in a oven.



Figure 11. Dipping enamelling process, chain with specimens.

### 2.5.1.2 Flow coating

This is an enamelling technique that require flowing slip enamel by pressure o gravity force on the surface of substrate. System that keep motion the specimens at certain angles make excess amount of slip drain off. This plant is development to provide for enamelling wide-scale specimens that are difficult to handle, it only lends itself to automation in the case of certain single product types, such as boiler. The piece are attached to the application line, on hook that are designed so that they can turn and slope during the coating process or just afterwards, to enable the excess amount of slip enamel to drain off. The chain on which the pieces are hooked is stopped at certain points ; the enamel is then pumped inside the specimens (Figure 12).



Figure 12. Flow enamelling for tube application

Alternative solution is, the pieces can be enamelled with a jet of enamel from above while they are on the move. Jet enamelling is a particular kind of flow enamelling. In the automatic plant allow this method to be used, the slurry is introduced inside the pieces with aid pumps or by flowing enamel from tanks situated above the pieces. Like dipping and flow enamelling, this technique do not consent high aesthetic quality of enamel surface.

### **2.5.1.3 Spray enamelling**

Function of the air atomiser spray gun is to limited the liquid into minute drops, while at the same time aiming them in the desired direction whit a jet of compressed air. The improve of relative speed difference between air and the slurry as it exits the nozzle, the smaller the drops will be. In order to achieve this, the enamel jet must be as wide possible, so that the greatest possible quantity of slurry is eliminated at lowest possible velocity. The pistol is fitted with a pair of valves that are designed to allow the desired amount of air and slurry to exit, or stop them completely. Air can be mixed with the vitreous enamel either inside or outside the pistol. In the first case, the method is called atomising with internal mixture, in the later atomising with external mixture. Last case is frequently used because, if as adjusted correctly, it will produce a very fine mist that guarantees an excellent finish. Although the mist produced by internal mixture jets is not as fine, they have the dual advantage of using less air and having a high rate of output.

The principle is very straightforward : the enamel is sucked into the pistol by vacuum created at the front of the nozzle, passing through a tube connected to a container set in a position higher than the jet.

This type of enamel feed is called siphon spraying. If the liquids to be sprayed are dense or high rate of productivity is required, the pistol is usually fed by a pressurized container or a pump. In this case is called pressure spraying.

### **2.5.1.5 Electro-enamelling**

The process of electro-coating enamelling is the last method to have been introduced on an industrial scale. The mechanism behind this technology is based on the migration of enamel particle in a suspension (slurry) : when they are given a negative charge, they are attracted by the substrate to be coated, which has a positive charge. Two electrodes are used to maintain a continuous current through a bath that contains the slurry : in this way, the particles of frit and of any other solid substances that have been added move along the force lines towards the specimens to be coated, which acts as an anode submerged in the slurry.

At the same time as the solid particles are being deposited on the specimen to be coated, the water in the slurry is moving in the other direction, from the anode towards the cathode. This phenomenon is carried out by using suitable cathodes to eliminated the water in proportion to the

amount of solid that has been deposited and thus maintain the viscosity of the slurry at a constant. Up to now, there are eighteen plants of this operating in the world, one which is in Italy. But the system is spreading because it offers several considerable advantages such as :

- Possibility of control of the thickness, which can be guaranteed uniform even on very complex specimen
- The surface are smooth, without any orange peel effect
- The edges are covered well
- Even small diameter holes can be drilled into the surface without having to clean up afterwards
- As the process is highly automated, compact plants be constructed in which pre-treatments can be integrated with the coating process

### **2.5.2 Dry enamelling**

System used for dry enamelling are electrostatic powder coating. The principle behind how this coating process functions is that of the in which electrostatically charged particles interact with each other. The enamel powder is taken from a fluid bed container and sent pneumatically to a distributor, which gives it an electric charge. The crown electrode is connected to a continuous current generator powered negatively at 60 to 100KW. This created a strong force field that ionizes the air. The electrically charged enamel particles are projected by the air flow that conveys the powder to the piece to be enamelled. While it is being transported in this way, the enamel deposit is influenced not only by the dynamic action of the air flow, but also by the force field lines and by force of gravity. In this way, the powder reaches the surface to be enamelled , where is deposited, losing its negative charge in the process, which is yielded to the substrate and then discharged to the earth.

### **2.5.3 Coating steel**

Multi-layered enamelling involved applying at least of enamel (one ground and the other cover coating) in a dry or wet process, each one followed by drying and firing. Multilayered wet enamelling is the commonest coating method of all : it can envisage up to two coatings with one firings or three coatings with two firings. Double-layer powder coating is a relatively recent method that has spread rapidly because of the advantages its : the most important of these is the improved surface appearance of the enamel, which is unquestionably smoother and more compact.

### **2.6 Dry process for wet enamelling**

Specimens obtained are only dried if the enamel were applied from slurry or liquid form. This is because the coating achieved with enamel conveyed in a liquid medium cannot be sent directly for thermal treatment, because the high temperature used (about 850°C) inside the furnace during this process would make the watery phase of the slurry decompose and give off Hydrogen gas. If this were to penetrate into a steel support, it might cause the typical problem called fish scaling.

For these reason and also because it would be operatively difficult to move specimens that are still wet from the coating phase directly to the heating. The pieces hooked onto the conveyor coming from the coating stations are transported through a drying tunnel that my be heated by gas or by recycling hot air from furnace. The heat is usually transmitted by convection natural or forced , conduction.

The first system to have been used in dryers is the natural convention that uses the air's natural convection movements : at one time, this is often done quite simply by leaving the material standing in the enamelling department for a long time. This processes was accelerated whenever possible by passing the specimens to be dried over the top of the furnace for thermal treatment, making use of its upward heat loss.

The second system is forced convection uses the air's natural convection movements, it augments them with artificially generated air flows. The primary aim of forced ventilation is to remove the layer of steam generated during the process from the surface or the product without delay, replacing it with new air that is better suited to absorbing wide amount of humidity : this considerably reduce the amount the time that the products have to stay in the dryer. It is also possible to make beneficial use of an efficient external heat exchanger, which enables the temperature to be adjusted to the best values.

## **2.7 Thermal treatment process**

For an enamel applied as a dry enamelling or dried after wet enamelling to adhere to the support, it must be heated to a high temperature for a determinate period of time, usually about 5 minute at about 850°C [6-8] . This thermal treatment, which is the last process in the enamelling process, is known as firing or densification. Important chemical and physical reactions take place on surface of the metal during heating, to which the development of adherence between the steel and the enamel is due.

Vitreous enamelling concern to the application of a thin layer of glass onto a steel substrate in order to provide a protective layer against chemical corrosion from the surrounding environment [6-8]. By this reason, enamelling has been used for the steel substrate, in particular for very low carbon steel. Porcelain enamel is a mass glass, with a particular microstructure not crystalline and high concentration of ionic bond. Low carbon steel is material with crystalline structure, with metallic bond between atoms. The mechanism of adherence between this two different material are in two phase.

Oxidation of a few micrometers of metallic substrate by oxidant ambient during thermal treatment. This treatment was obtained by specific furnace. Ground enamel melting over 800°C, and dissolve the Iron oxide (II) in the liquid phase. New liquid phase with Nickel and Cobalt oxides, get a few redox (Figure 13).

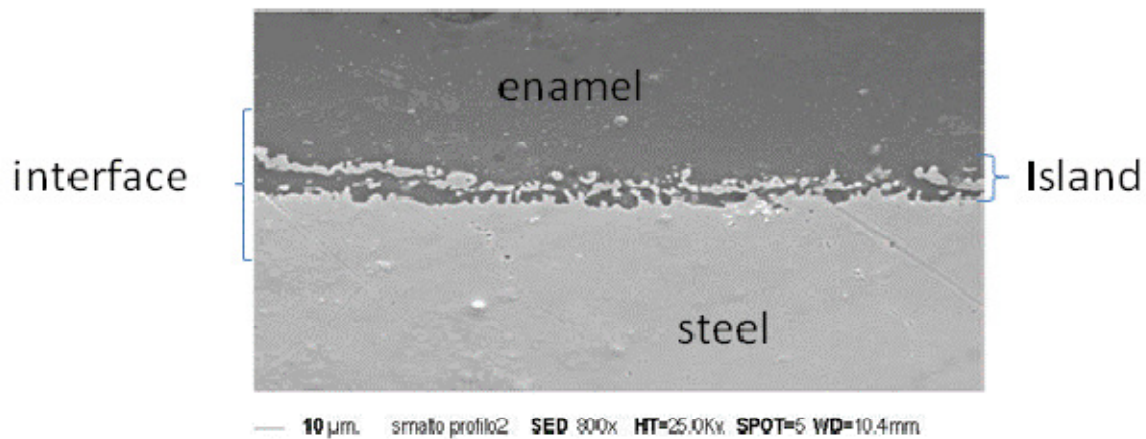
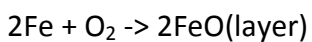
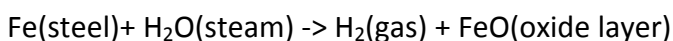


Figure 13. SEM of interface of vitreous enamel steel

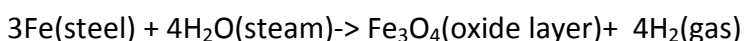
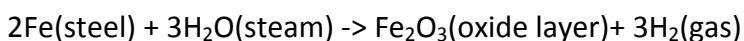
The first step consist in the oxidation on a little layer of steel. During the thermal treatment in a few minute was obtained about 1 μm of FeO layer [8-10]. The oxidant agent is the oxygen present in furnace.



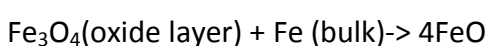
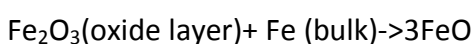
At higher temperature than 540 °C [8-14]:



At temperatures below 540 °C, the iron improve its oxidation number from 0 to +2 and +3 [8-15]



During the thermal treatment at the temperature above 540 °C, the oxides of iron ( $\text{Fe}^{+2}$  and  $\text{Fe}^{+3}$ ) formed decompose and reduce them oxidation number in the presence of iron and form FeO by reactions [15] :

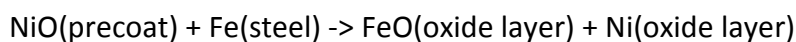


At higher temperature, FeO can total dissolves in the liquid enamel at the interface until all the available oxides are exhausted [9 ; 14-15].

According to chemical reactions show the evolution at interface above 540 °C, by which time most of moisture present in the precoat layer is exhausted by producing Fe<sub>2</sub>O<sub>3</sub> and Fe<sub>3</sub>O<sub>4</sub>.

The layer of precoat does not contain any iron oxides and the concentration of iron oxide in the top enamel layer is much lower. The higher Fe concentration at the interfacial enamel cannot be achieved by reduction of Fe<sup>3+</sup> or Fe<sup>2+</sup> by silica-rich glass enamel.

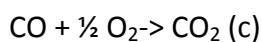
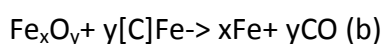
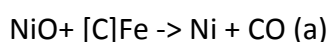
This concentrations is caused by reaction between the enamel and the steel as well as the dissolution of any iron oxide scales formed during firing. In the presence of NiO, the electrochemical exchange reaction [9]:



This reaction contribute to the complete dissolution of FeO in the interfacial-enamel.

Liquid enamel with low viscosity, which is rich in FeO, the bubble nucleation is much easier than when the amount of FeO is less because of the concomitant reduction in surface tension.

This fact indicates that the dissolved Carbon can be removed rapidly from surface layer of steel via following reactions [9;14-15]:



Chemical reaction with the oxidation of carbon from the surface layer of steel has an advantageous effect on hydrogen absorption because it promotes the formation of ferrite, which reduces hydrogen solubility at high temperatures. From presence of a NiO precoat, reach of more CO<sub>x</sub> in a low viscosity enamel liquid leads to the formation of a larger number of bubbles at the interface [9 ; 14-15].

During the cooling, hydrogen expelled from the steel resulting from a change in the crystal structure (fcc to bcc) will allow high quantity of hydrogen to mix with the CO gas [16-20]. This mix are confirmed due to reaction a and b and aid the formation of gas bubbles at the interface. The first consequence are the decrease of the density of the interface, and the increase of the hole and porosity. This results decrease the mechanical properties of the interface and the enamel

The amount remaining NiO, which has been left after the electrochemical exchange reactions, can dissolve in the glass at the interface [16]. During the cooling the dissolved NiO and FeO are reduced by H<sub>2</sub> and/or CO in the atmosphere to form the Fe<sub>x</sub>Ni<sub>y</sub> metal-rich dendritic area for the preferential segregation of these particles around the bubbles. The concentration of FeO increase quickly between the interface to enamel because redox potential of H<sub>2</sub> and CO not enough to reduce FeO (Figure 14).

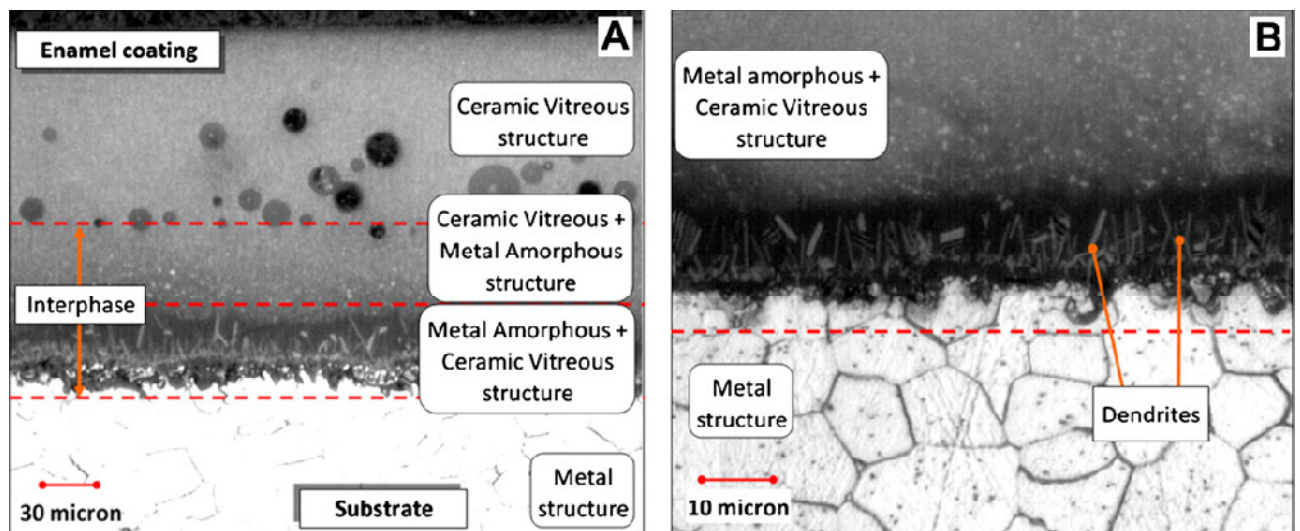


Figure 14. Interface enamel steel with presence of dendritic area

## References

- [1]. C. Barry Carter , M Norton Gran, Ceramic Materials – Science and Engineering, Springer
  
- [2]. James F. Shackelford • Robert H. Doremus, Ceramic and Glass Materials, Structure, Properties and Processing, Springer
  
- [3]. G. Aliprandi, Lezioni di Ceramurgia
  
- [4]. Fundamentals of Materials Science and Engineering, 5th edition, W.D. Callister jrJohn Wiley & Sons, Inc.
  
- [5]. Corso di Vetri, Siligardi Cristina
  
- [6]. Eugen Axinte ; Glasses as engineering materials: A review Materials and Design 32 (2011) 1717–1732
  
- [7]. Tratto da “Smalto Porcellanato – Tecnologia & Mercati” N 1 -2007
  
- [8]. X. Yang, A. Jha, R. Brydson, R.C. Cochrane, J. Thin Solid Film, inpress.
  
- [9]. Tratto da “Smalto Porcellanato - Tecnologia & Mercati” – N. 3/2000
  
- [10]. Tratto da Smalto Porcellanato Tecnologia e Mercati numero 3/1997 anno XXXIX inserto no. 6
  
- [11]. J. Wratil, Vitreous Enamels, Borax Holdings Ltd, London, 1984, pp. 14–17.
  
- [12]. H.H. Liu, Y. Shueh, F.S. Yang, P. Shen, Mater. Sci. Eng. A 149 (1992) 220.
  
- [13]. X. Yang, A. Jha, R. Brydson, R.C. Cochrane, The effects of a nickel oxide precoat on the gas bubble structures and fish-scaling resistance in vitreous enamels, Materials Science and Engineering A366 (2004) 254–261

- [14]. C.A. Zapffe, C.E. Sims, J. Am. Ceram. Soc. 23 (1940) 187.
- [15]. P.K. Chu, J.H. Keeler, H.M. Davis, J. Am. Ceram. Soc. 36 (1953)48.
- [16]. J.Q. Dumm, P.W. Brown, J. Am. Ceram. Soc. 82 (1999) 987.
- [17]. E.D. Lacey, ActaCrystallogr. 18 (1965) 141.
- [18]. N.T. Shardakov, E.K. Kurumchin, G.K. Vdovin, V.A. Deryabin, GlassCeram. 53 (1996) 46.
- [19]. Andrea Zucchelli, Giangiacomo Minak, Daniele Ghelli, Low-velocity impact behaviour of vitreous-enamelled steel plates, International Journal of Impact Engineering
- [20]. From “Smalto Porcellanato - Tecnologia & Mercati” – N. 3/2003 – Anno XLV

## 3. Materials and Methods

### 3.1 Enamel SM014

Enamel SM014 is an industrial slurry obtained by mixing water with a frit and some additives such as  $\text{SiO}_2$ , 4% wt of a commercial caolinitic clay (provided by Colorobbia S.p.A.), 0.6 % wt of  $\text{NaNO}_2$ , 0.6 % wt of  $\text{NaAlO}_2$  and 0.6% wt of  $\text{H}_3\text{BO}_3$ .

Water is used in this slurry because is cheap and safely for industry rather than other medium like ethanol.

On the other hand, high value of its dielectric constant with respect to other solvents (e.g. ethanol and methanol) greatly improve the quality of the medium because polar solvents with high dielectric constant dissolve better polar solute. Frit is a glass for vitreous coating over steel, prepared by heating suitable batches in a room to melting temperature in a furnace (Figures 15 and 16). The batch constituents are chosen to obtain a suitable chemical composition. After thermal treatment, the melt is quickly quenched in water at room temperature in order to obtain the frit.



Figure 15. Production plant of glass frit



Figure 16. Quenching process to obtain the frit

In order to obtain the enamel, the frit was mixed with water and milled in a ball milling using ball in alubit in order to obtain particles size down to  $D_{90} = 75 \mu\text{m}$ .

The additives were added in order to avoid the settling of the slurry after the milling process.

The obtained enamel slip was applied to the sheet steel by a hand-spraying system.

The density of enamelling slip is  $1.70 \text{ g/cm}^3$  [1-2].

### 3.2 Carbon steel

The substrate used for enamel coating was very low carbon steel (type DC04ED, obtained in the form of rectangular plates by cold rolling), which chemical composition is the following : C = 0.004wt%, Si = 0.008wt%, S = 0.015wt%, Mn = 0.22wt%, P = 0.008wt%, Al = 0.037wt%, Ni = 0.036wt%, Cr = 0.021wt%, Cu = 0.032wt%, and Fe as the remaining amount (according to the EN 10209). Fe rest second (EN 10209). The dimensions of the sheet of steel were 30mm x 30mm x 1 mm. The first treatment of the metal sheet consisted of the elimination of grease and impurities by immersing the specimens in a chemical degreasing bath at 70°C for 10 minutes. The addition of nickel mitigates the problems of fish-scaling and promotes adhesion between the enamel and the steel surface [3-5].

### 3.3 Vitreous enamel steel by hand-spray system

Vitreous enamels play a very important role in the coating production process of steel in accordance with the technical and aesthetic properties induced by the enamel to the final material [4]. In particular, from the functional point of view, vitreous enamel coatings show excellent resistance to chemical degradation processes [7,8] as well as a good resistance to tribological phenomena such as abrasive wear [9]. Enamel coatings are generally defined as a substantially vitreous glassy inorganic layer bonded to various metal substrates by fusion at a defined temperature [10-14].

In this work the enamelling steel was dried in an oven at 120°C for 15 minutes. There for, the heating process, which promotes the bond creation between steel and enamel, was performed in an industrial furnace. Particularly, the sample was heated at 860°C for 6 minutes; and then cooled in air, resulting in a coating thickness of about 200µm per side. This final product is named “industrial sample” [14] (Figure 17).

Moreover, other enamelling steels named laboratory samples with a thickness coating of 200µm, 250µm and 300µm respectively, have been obtained in order to analyze the influence of the thickness on the mechanical properties. The results will be discussed in chapter four.

During the thermal treatment the enamel melts and interacts with the metal substrate, thus enabling the formation of a continuous varying structure.

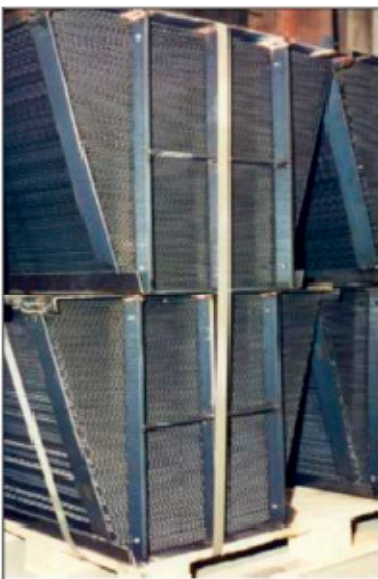


Figure 17. Vitreous enamel steel plate after thermal treatment

### 3.4 Vitreous enamel steel by Electrophoretic technique

Electrophoretic deposition (EPD) is an electrochemical method attracting increasing interest as a material processing technique to prepare coatings and films [15–17]. This technique is usually carried out in a two electrode cells (Figures 18 and 19). EPD can be applied to colloidal suspensions of metals, polymers, ceramics and glasses. In the case of ceramics, after deposition, a heat-treatment step to densify the deposit and to eliminate porosity is needed.

The stability of the suspension is the basic condition to apply the EPD technique (Figure 20) [18]. Usually, traditional industrial slurries for steel and ceramic applications contain more than 50% w/w frit glass /water. The high concentration and low stability of industrial slurries make them unsuitable for EPD technique [19-22]. The suspensions were prepared by 1 g of concentrate slurry diluted ten time by deionised water added little amount of additive (0,01 – 2)wt% such as :

CaCl <sub>2</sub>
MgCl <sub>2</sub>
Ca <sub>3</sub> (PO <sub>4</sub> ) <sub>2</sub>
TPF
Sodium Polyacrilate
Bentonite
Densicer
Cmc 150
Cmc 30
Cmc 5s

Table 4. Additivies used for EPD technique

Homogenization was conducted by 5min magnetic stirrer, 30 minutes of sonication in a ultrasound bath (Bandelin sonorex) and finally other 5min of magnetic stirring to disperse the particles and to break up any possible solid agglomerates. This allowed to obtain suitable suspensions for deposition mass. All electrophoretic experiments were carried out by applying voltage (15 - 30)V between the two parallel electrodes (held at 10 mm distance) using a TTiEL561 power supply (Thurlby Thandar Instrument, Huntingdon, UK) working at constant voltage and connected to a TTi1906 computing multimeter (Thurlby Thandar Instrument, Huntingdon, UK). After deposition the samples were dried at room temperature in the laboratory. In order to determine the yield of the process samples were weighed before and after deposition and the coating area was measured. Sintering process was carried out by kiln at 800 and 850°C for 4 minutes. The rheological behaviour of an industrial slurry has been modified by the addition of different additives such as bentonite, densicer, carboxy methyl celluloses Cmc 30, carboxy methyl celluloses Cmc 150, carboxy methyl celluloses Cmc 5s in order to obtain appropriate suspensions for EPD. Better performance is obtained from Densicer additive, the results will be discussed in chapter four.

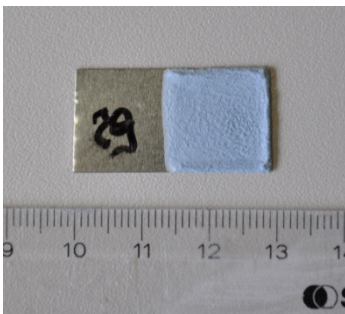


Figure 18. Sample of vitreous enamel steel by EPD technique

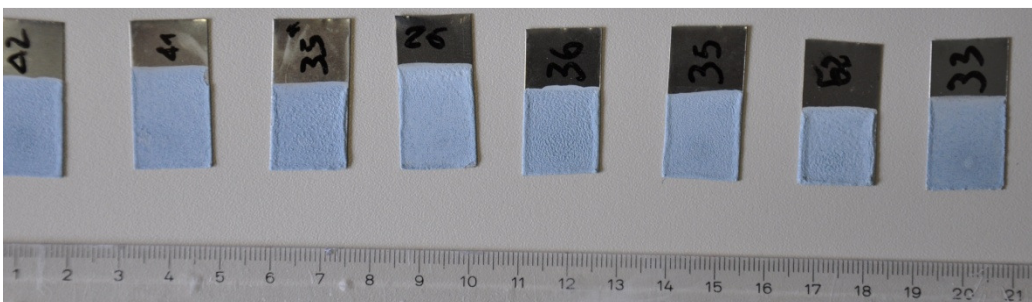


Figure 19. Vitreous enamel steel obtained by EPD technique after dryer process

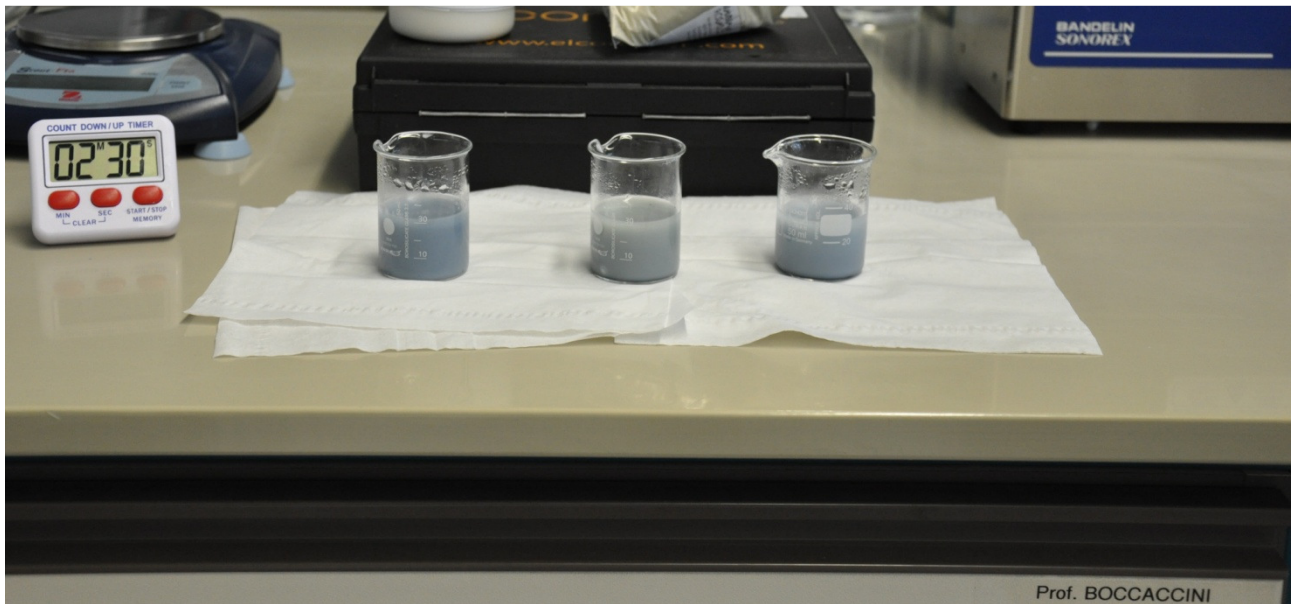


Figure 20. Comparison of stability of the same enamel SM014 with and without additives. From left side SM014 with Densicer, SM014 with Bentonite, SM014 without additive.

## 3.5 Characterization Methods

### 3.5.1 Characterization of enamels

#### 3.5.1.1 Thermal analysis

##### 3.5.1.1.1 Hot stage microscopy (HSM)

The thermal behaviour and the coefficient of thermal expansion ( $\alpha$ ) of the enamel were measured using a hot-stage microscope (HSM) using powdered enamel ( $< 25 \mu\text{m}$ ) (Model Misura, Export System Solutions, Modena, Italy) and an optical dilatometer (Model Misura, Export System Solutions, Modena, Italy) (figure 21).

Hot stage microscopy is a fast and simple procedure that makes it possible to measure some points of the viscosity temperature curve for vitreous materials. In this work the viscosity-temperature curve for the studied enamel was measured by using the De Pablos method [23]. Choosing four characteristic points: the transformation point ( $\log \eta = 13$ ) (from DTA measurement), first sintering ( $\log \eta = 10$ ), softening point ( $\log \eta = 6$ ), half-ball ( $\log \eta = 4.2$ ) and flow ( $\log \eta = 3.0$ ) from hot stage microscopy. The coefficient of thermal linear expansion of the

enamel was measured on a bar of 15 × 15 × 5 mm, in the (50-400)°C temperature range with a heating rate of 10°C/min.

The different stages of the process are recorded photographically or by means of a video camera. The definition of the characteristic temperatures appeared for the first time in 1954 in the German rule DIN 51730. Other well-known norms, which define the characteristic temperatures identifiable with the heating microscope, are ASTM D 1857 and ISO 540. The norms define also shape and size of the samples to be analyzed and the heating cycle to be applied. According to them, it is possible to identify four characteristic temperatures, which are: Deformation, Sphere, Hemisphere and Flow Temperatures (figure 22). A typical series of photographs shows the evolution of the glass compact during heating. In these investigations, the shape change of the silhouette of the sample is the indicator used for assessing the physical changes occurring in the material (from sintering to melting). Hot stage microscopy is a fast and simple procedure that makes possible approximately to measure some points of the viscosity temperature curve for vitreous materials.

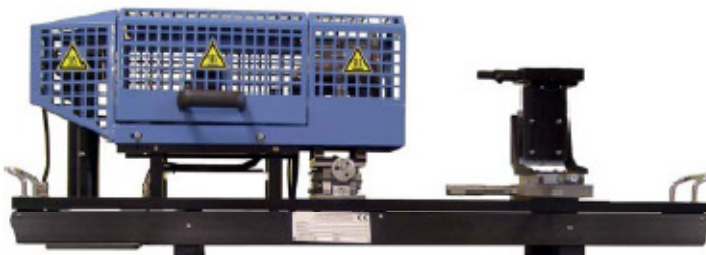


Figure 21. Hot stage microscope

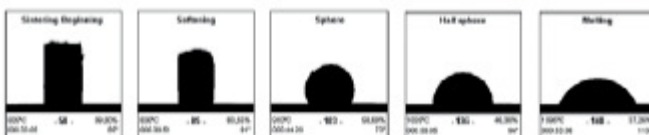


Figure 22. Characteristic temperature obtained from HSM investigation.

### **3.5.1.1.2 Optical dilatometer (ODHT)**

The non-contact Vertical Optical Dilatometer Misura® ODHT, designed, patented by Expert System Solutions, allows to carry out thermo mechanical measurements following the process of expansion, sintering or bloating of materials and analyzing the sample throughout the entire industrial firing cycle (up to a maximum temperature of 1650 °C and heating rate up to 80 °C/min). The practical applications of this technique are various and include all fields in which it is important to know the thermo-mechanical behaviour of the materials, reproducing industrial firing cycles, even when they have a viscous behaviour or they develop liquid phases during firing or they lose the property of reflection.

Misura® ODHT is based on the double beam concept : the first optical path is always aligned to the top of the specimen, while the second optical path, which is focused on the sample holder, is taken as a reference beam to correct the mechanical drift of the instrument. Doing so, there is no need of any correction nor calibration and it is also possible to set several different heating rates and dwells/stasis during the heating and cooling cycle, widening the temperature range for analyses. Furthermore, the magnification of the optical system does not change because of time or the number of test performed, and, to demonstrate it, a NIST Standard Reference Material is supplied.

Optical Dilatometers Misura® ODHT are useful for all materials that present considerable expansions and contractions. Vertical Optical Dilatometers Misura® ODHT allow to get a more complete characterization of the evaluated materials and to identify automatically:

- sintering, sintering kinetics, expansion, shrinkage;
- temperature of glass transition ( $T_g$ );
- temperature of dilatometric softening ( $T_s$ );
- dimensional variation during heating and cooling;
- Alpha ( $\alpha$ ) and cubical Alpha value;
- Delta ( $\Delta$ ) L/L0.

### **3.5.1.1.3 Thermal analysis : Differential Thermal analysis (DTA)**

In a DTA-experiment (Differential Thermal Analysis) the temperature difference between the sample under investigation and an inert reference material is measured as a function of temperature. Both samples are treated with the same temperature program and the same heating and cooling rates.

During the analysis such heating flows are detected by two thermocouples which measure the temperature difference between the sample and a standard material, heated together under identical thermal conditions in the same oven. The reference standard must be chosen in such a way that it does not suffer any transformation over the temperature range employed to examine the sample. Alumina and silicon carbide are satisfactory reference standards for solids whereas dinonyl phthalate and certain silicone oils have been used as standards for liquids. The technique is based on the fact that as a substance is heated, it undergoes transformations that involve absorption or emission of heat. For example, in correspondence of a phase transformation, the latent heat of transformation will be absorbed or released and the temperature of the sample will lag or lead that of the reference material. The temperature sensors embedded in the two substances are connected in a way so that any temperature difference generated during the heating cycle are graphically recorded as a series of peaks on a chart. The reactions associated to heat absorption (i.e. melting) are endothermic and are characterized by negative peaks. The reactions associated to heat development (i.e. oxidations) are called exothermic and are characterized by positive peaks. Although differential thermal analyses have been made for many materials, the major applications have been concerned with glass and ceramics. DTA is a powerful tool in studying the crystallization and glass transition temperatures [24-27].

The glass transition temperature,  $T_g$ , is the temperature below the physical behaviour is ruled on Hooke law such as solid behaviour. Over this temperature, variation of viscosity show a different rule. In the region of  $T_g$  the viscosity is about  $10^{13}$  Pa\*s. The glass transition temperature of enamel,  $T_g$ , was determined with a Netzsch, STA 409 differential thermal analyzer (DTA) on samples milled to an average particle size of less than 25  $\mu\text{m}$ .

### **3.5.1.2 Chemical analysis**

Plasma is a conducting gaseous mixture containing significant concentration of cations and electrons. In the argon plasma used for atomic spectroscopy, argon ions and electrons are the principal conducting species, although cations from the sample also contribute. Argon ions, once formed in a plasma, are capable of absorbing sufficient power from an external source to maintain the temperature at a level at which further ionization sustains the plasma indefinitely; temperature as great as 8,000 k is encountered. Three power sources have been employed in argon plasma spectroscopy. One is a dc electrical source capable of maintaining a current of several amperes between electrodes immersed in the argon plasma. The second and third are powerful radio-frequency and microwave-frequency generators through which the argon flows. By the time the analyte atoms and ions reach the observation point in the plasma, they have spent about 2 ms in the plasma at temperatures ranging from 6000 to 8000 k. These times and temperatures are two to three times greater than those attainable in the hottest combustion flames (acetylene/ nitrous oxide).

This analysis was carried out to obtain chemical composition of the slip enamel.

A few quantity of slurry was dried in a oven for 3h at 110°C to obtain dry powder was analyzed by ICP OES spectrometer, Varian liberty 200.

### **3.5.1.3 Particle size distribution**

The grain size distribution of the frit powder after the milling process was characterized by using a laser particle size analyzer (MASTERSIZER 2000, Malvern). During the laser diffraction measurement, particles are passed through a focused laser beam. These particles scatter light at an angle that is inversely proportional to their size. The angular intensity of the scattered light is then measured from a series of photosensitive detectors. The number and positioning of these detectors in the Mastersizer 2000 has been optimized to achieve maximum resolution across a broad range of sizes. The map of scattering intensity versus angle is the primary source of information used to calculate the particle size. The scattering of particles is accurately predicted by the Mie scattering model. This model is rigorously applied within the Mastersizer 2000 software,

allowing accurate sizing across the widest possible dynamic range. This analyzer uses a laser diffraction technique with multiple light detectors to obtain the diameters of particles. Laser particle size measurements were conducted in order to verify if the particle distribution was in the range (1-20  $\mu\text{m}$ ) usually used for EPD technique [18].

#### **3.5.1.4 Density**

Density was measured by inox pycnometer BYK Gardner. Volume of Pycnometer 100  $\text{cm}^3$  like ISO 2811. Rotational rheometry was used to homogenize industrial slurry for 5 minutes before the measurement.

Pycnometer was filled fully of slurry to get 100  $\text{cm}^3$  of enamel slurry. Pycnometer was measured by technical scale before filled fully and after filled fully of slurry.

#### **3.5.1.5 X- Ray diffraction (XRD)**

The technique of diffraction of the powders essentially is carried out by a narrow beam of monochromatic X-rays, incident on a powder. In these particular conditions, diffracted rays are generated by the series of planes with distance  $d(hkl)$  of  $(n)$  phases of the system investigated according to the geometric conditions dictated by Bragg's law  $2d_{(nhnknl)} \sin(\theta) = \lambda$  and imposed by the instrumental conditions (wavelength used).

The result of this experiment is a pattern with relation between energy versus the angle  $2\theta$ .

Powder of slip enamel were investigated by an XRD diffractometer with Cu-K $\alpha$  radiation and conventional  $\theta$ - $2\theta$  geometry (PANalytical, X'Pert PRO, CuK $\alpha$  radiation equipped with an X'Celerator detector).

## 3.5.2 Characterization of carbon steel

### 3.5.2.1 Mechanical characterization

Hardness characterization was conducted by indenter 400 Series, 402MVD Wolpert Wilson Instrument (Figure 23). The instrument is a Knoop/Vickers hardness tester with crisp optics that have a total magnification of 100x and 400x. The system features eight dial selectable test forces ranging from (0,01- 2) kg. For easy sample mounting, the instrument is equipped with a 100 x 100 mm precision XY-Stage with 25 mm movement in each direction. Instruments get some information about: Hardness diagonals value, statistics on backlit display.



Figure 23. 402MVD, Wolpert Wilson

### 3.5.2.2 Measurements of roughness

Vitreous enamel is generally defined as a substantially vitreous or glassy inorganic coating bonded to various metal substrates by fusion at a defined temperature. Thin inorganic glass layer protects the very low carbon steel metallic substrate against chemical corrosion from the surrounding corrosive environment.

Enamel coats were prepared under conditions that gave different degrees of adherence, for this reason the adherence and roughness of the interface have been evaluated in this study. Suitable

correlation was found between adherence and roughness of interface, and it was concluded that roughness of interface is a necessary, but not a sufficient condition for the development of good adherence between a porcelain enamel ground coat and iron. Most of the roughness that is associated with good adherence apparently develops during the firing process [28]. According to EN10209 [2, 29], the investigation in Europe standard of vitreous coating adherence strength, the enamelling specimen is investigated by the steel ball falling impact. After the destruction, the adherence strength was chosen according the relics of enamel on the destroyed surface. Vitreous coating adherence strength can be graded into 1st, 2nd, 3rd, 4th and 5th grade and the 1st grade is the best. Measurements of surface steel roughness were performed by using DIAVITE DH-5 equipment. Characteristic of instrument : Measuring range Z : 400  $\mu\text{m}$ , Working distance : 5 mm, Repeatability: 2 nm, Vertical resolution: 0.025 nm, Spot size: 7  $\mu\text{m}$ .

### **3.5.3 Characterization of the slurry for EPD**

#### **3.5.3.1 Zeta potential**

Zeta potential is the electric potential in the interfacial double layer at the location of the slipping plane versus a point in the bulk away from the interface [30]. The zeta potential represents the potential difference between the dispersion medium and the stationary layer of fluid attached to the dispersed particle and it is a parameter that correlates with the stability of suspensions [31, 32]. Zeta potential measurements were performed on slurries using a Zetasizer, (Nano ZS, Malvern). Settling time is the most important parameter relevant to assess the suitability of the suspensions in electrophoretic deposition. This parameter has an effect in modifying the quality of mass sedimentation and affects the homogeneity of the surface, and the thickness of the deposit. The sedimentation time was measured by using a chronometer. This is the time elapsed between the end of the procedure to obtain the slurry and the complete settling of the slurry.

### 3.5.3.2 Rheological characterization

The rheological characterization of the slurry was carried out in continuous shear by using a rotational viscometer (VT550, Haake, NV sensor). This characterization allows obtaining a direct measure of the relationship between shear rate and shear stress, the apparent viscosity and time.

The flow curve tests were done in flow conditions using a four step cycle with  $\dot{\gamma} = 200 \text{ s}^{-1}$  as maximum shear rate, 30 s at  $200 \text{ s}^{-1}$  to exclude the effects of sample preparation phase; at rest for 1 min.; the shear rate increased from 0 to  $200 \text{ s}^{-1}$  in 5 min or 10 min. (up curve) and shear rate decreased from 200 to  $0 \text{ s}^{-1}$  in 5 min or 10 min. (down curve) with constant acceleration.

The Time-dependent behaviour was tested by single step time curves at constant shear rate ( $200 \text{ s}^{-1}$ , 5 min) in isothermal conditions ( $30^\circ\text{C}$ ). Rheological characterization was carried out for all additives used in the slurries, except for the suspensions with CMCs which could not be characterized due to their high instability. This relationship was obtained at  $30^\circ\text{C}$  because the use of ultrasound improves the temperature of specimen.

### 3.5.3.3 Settling after preparation of suspension for EPD

Settling time was the most important parameter relevant to assessing the suitability of the suspensions in EPD. This parameter has an effect in modifying the quality of mass sedimentation and affects the homogeneity of the surface, and the thickness of the deposit. The sedimentation time was measured by using a chronometer. This is the time elapsed between the end of the procedure to obtain the slurry and the complete settling of the slurry.

### **3.5.4 Vitreous enamel steel by hand-spraying system: surface characterization**

#### **3.5.4.1 ESEM with hot stage**

In order to study the thermal transformation of enamel on the steel, “*in situ*” environmental scanning electron microscopy (ESEM) with hot stage was used. An FEI Quanta 200 ESEM equipped with a thermal tungsten gun, a gaseous secondary electron detector (GSED), and a 1500°C hot stage was used for *in situ* electron imaging. An AS-type thermocouple was used to monitor the temperature, and calibration was performed using the melting point of gold (1064°C) [7].

The instrument was operating at 20 kV acceleration potential and with a working distance of about 20 mm. The samples were heated at a rate of about 20°C/min. SE images were collected at several temperatures. The heating rate and temperature range were selected on the basis of an industrial cycle: heating rate 50°C/min from room to 900°C.

The ESEM experiments were repeated twice giving reproducible results. The sample was cut obtaining a small piece of steel in a square shape (3/4mm per side). The enamel powder was dispersed in acetone to create slurry and applied over the steel by using a laboratory air-spray. It makes no difference that the thickness of the enamel is thinner than the industrial one, since it is more or less 150 micrometers. This sample was named “laboratory sample”.

#### **3.5.4.2 Indentation tester**

The CSM Indentation Tester (Figure 24) is a high precision instrument used for the determination of mechanical properties of thin films, coatings and substrates. Properties such as hardness and elastic modulus can be determined on almost any type of material: soft, hard, brittle or ductile. The operating principle of the instrument is as follows: an indenter tip, normal to the sample surface, is driven into the sample by applying an increasing load up to some preset value. Hardness values were determined using the Oliver and Pharr method [33], according to the ISO 14577 standard.

The load is then gradually decreased until partial or complete relaxation of the material occurs (Figure 24). A piece of enamelling steel (10 x 10 x 1)mm were cold mounted using epoxy resin to

show cross section. The surface of the resin was polished by SiC abrasive papers (80 –2500 mesh grade) and three different Diamond polish papers.



Figure 24. Indentation tester, CSM instruments

### 3.5.5 Vitreous enamel steel by hand-spraying system: interface characterization

#### 3.5.5.1 SEM/EDS characterization

Accelerated electrons in an SEM carry significant amounts of kinetic energy, and this energy is dissipated as a variety of signals produced by electron – sample when the incident electrons are decelerated in the solid sample. These signals include secondary electrons (that produce SEM images), backscattered electrons (BSE). Secondary electrons and backscattered electrons are commonly used for imaging samples: secondary electrons are most valuable for showing morphology and topography on samples and backscattered electrons are most valuable for illustrating contrasts in composition in multiphase samples

Scanning electron microscope is suitable for producing an image of high resolution by detecting secondary electron and backscattered electrons generated from a specimen at low accelerating voltage in a separate or synthesis fashion.

To study the enamel-steel interface, a conventional high resolution scanning electron microscope (SEM) with an energy dispersion spectroscope (EDS), SEM+EDS, (Philips XL 40/604 + INCA

instruments) was used. A transversal cross-section of an industrial specimen was incorporated into a resin. After the solidification, the sample was polished on the surface with silicon carbide and alumina gel papers. Finally the specimen was mounted on aluminium stub and gold-coated (30nm thick). A semi-quantitative chemical analysis (EDS) was then performed on each single indentation in order to correlate the mechanical properties with the chemical compositions of the sample interface.

### 3.5.5.2 Indentation tester

The microhardness as well as the Young modulus of the interface was determined on the polished cross-sections by depth sensing Berkovic nano-indentation (Nanoindenter, CSM Instruments, Peseux, Switzerland) (Figures 25 and 26), using a penetration depth of 200 nm. For this test, the sample was embedded in a thermosetting resin in order to block and prevent the movement of the sample during the measurement.

For the test, an indentation matrix of 7 rows x 5 columns on the steel-enamel interface was used.



Figure 25. Indentation tester CSM instruments

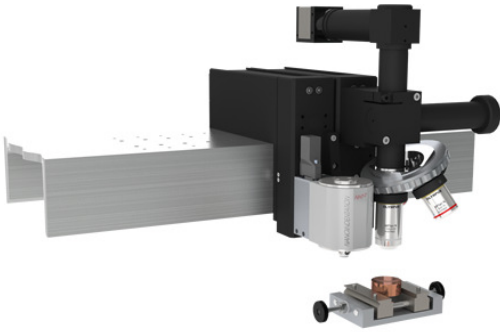


Figure 26. Indentation Tester with sample in resin

### 3.5.6 Characterization of the vitreous enamel steel obtained by EPD

#### 3.5.6.1 Indentation tester

The samples obtained by EPD technique were investigated by nano-indenter (Nano-indenter, CSM Instruments, Peseux, Switzerland).

After thermal treatment these specimens ( 30 x 10 x 1 )mm were cold mounted using epoxy resins to show cross section. Surface of resins was polished with SiC abrasive papers (80-2500 mesh) and three different Diamond slurries. Microhardness and Young modulus were obtained from each indentation with this setting of the instrument:

- Approach speed : 3000 nm/min
- Dz sensor in fine range
- Delta Slope Contact : 60%
- Acquisition Rate : 30,0 [Hz]
- Linear Loading
- Max depth : 500,00 nm
- Loading rate : 25,00 mN/min
- Unloading rate : 25,00 mN/min
- Pause : 15,0 s
- Type :Berkovich Serial number : BJ-15\_Cal 2-02-2012
- Material : Diamond

Characterization is carried out by a matrix with 10 vertical lines and 10 horizontal lines. The distance between each horizontal and vertical line of the matrix is 5 micrometers, so they are equidistant in the xy plane. Aim of this characterization was the interface between SM014 and AISI 316L.

### **3.5.6.2 Scanning electron microscope (SEM)**

To study the Electrophoretic deposition samples, a conventional high resolution scanning electron microscope (SEM) with an energy dispersion spectroscopy (EDS), SEM+EDS, (Philips XL 40/604 + INCA instruments) was used.

Samples after thermal treatment was embedded in a cold resin and after solidification, were polished on the surface with silicon carbide papers (80 – 2500 mesh) and alumina papers. Finally the specimen and gold-coated (30nm thick).

## References

- [1]. Leila Samiee, Hossein Sarpoolaky, Alireza Mirhabibi ; Microstructure and adherence of cobalt containing and cobalt free enamels to low carbon steel ; Materials Science and Engineering A 458 (2007) 88–95
- [2]. From “Smalto Porcellanato Tecnologia e Mercati” numero 1/2000 no. 12
- [3]. Kautz K. The effect of iron surface preparation upon enamel adherence J. Am. Ceram. Soc. (1937); 20: 288-95.
- [4]. Richmond JC., Moore DG., Kirkpatrick HB., Harrison WN. Relation between roughness of interface and adherence of porcelain enamel to steel. J. Am. Ceram. Soc. (1953); 36, [12]: 410–416.
- [5]. Salamah MA., White D. Catalytic activity of nickel at the glass/metal interface in the porcelain enamelling system J. Am. Ceram. Soc. (1981); 64, [4]: 224-26.
- [6]. Andrew A.I. Porcelain Enamels. Garrad Press, Champaign, IL 1961.
- [7]. Kuchinski F.A. Corrosion resistant thick films by enamelling. In: Wachtman J.B., Haber Ra, editors. Ceramic films and coatings. Park Ridge (NJ): Noyes Publications (1993), p. 77-130.
- [8]. Scrinzi E, Rossi S. The aesthetic and functional properties of enamel coatings on steel. Materials and Design (2010); 31: 4138-46.
- [9]. Bazayants GV, Svetlichnyi VA, Demchuk VV, Ryzhikov VA. Abrasive wear of glass enamels and slag sitall used in heat energetics. Glass and Ceramics (1983); 40 [16]: 295-6.
- [10]. Andrews AI. Porcelain enamel. Champaign, Illinois: The Garrard Press; 1961.

- [11]. Poletti R, Zucchelli A, Chelli A, Experimental investigation on corrosion resistance of porcelain enamel composite coating for regenerative air heaters parts. In: G. Nicoletto, editor. Danubia Adria; 2005.
- [12]. Chelli A, Poletti R, Pignatti L, Zucchelli A, Rossetti L, Dal Re V, et al. Studio delle Proprieta` Meccaniche e Tribologiche di Lamiera in Acciaio rivestite mediante Smalti Porcellanati [Experimental study of the mechanical and tribological properties of enamelled steel plate]. Smalto Porcellanato, CISP 2006.
- [13]. Chelli A, Poletti R, Pignatti L, Bruscoli F, Pasqualetti G, Bruni F, et al. Composite enamelled steel elements for air preheaters and gas-gas heaters: an integrated approach from sheet forming and enamelling to basket assembly. In: CEIA China Enamelware Industry Association XXI international congress on porcelain enamel, 18–22. Shanghai, China: maggio; 2008. p. 130–58.
- [14]. A. Zucchelli, M. Dignatici, M. Montorsi, R. Carlotti, C. Siligardi ; Characterization of vitreous enamel-steel interface by using hot stage ESEM and nanoindentation techniques ; Journal of the European Ceramic Society
- [15]. Sarkar, P. and Nicholson, P. S., Electrophoretic sedimentation (EPD): mechanism, kinetics and application to ceramics. J. Am. Ceram. Soc., 1996, 79, 1987–2002.
- [16]. Boccaccini, A. R. and Zhitomirsky, I., Application of electrophoretic and electrolytic sedimentation techniques in ceramics processing. Curr. Opin. Solid State Mater. Sci., 2002, 6, 251–260.
- [17]. Van der Biest, O. O. and Van de perre, L. J., Electrophoretic sedimentation of materials. Ann. Rev. Mater. Sci., 1999, 29, 327–352.
- [18]. Laxmidhar Besra, Meilin Liu ; A review on fundamentals and applications of electrophoretic sedimentation (EPD) ; Progress in Materials Science 52 (2007) 1–61

- [19]. Guven, N., Pollastro, R.M ; Molecular aspects of aqueous smectite suspensions. In: (Eds.), Clay–Water Interface and its Rheological Implications. Clay Minerals Society Workshop Lectures, vol. 4. Clay Min. Society, Boulder, Colorado, pp. 2–79
- [20]. Prashant Shankar , Jeremy Teo , Yee-Kwong Leong , Andy Fourie b, Martin Fahey ; Adsorbed phosphate additives for interrogating the nature of interparticles forces in kaolin clay slurries via rheological yield stress ; *Advanced Powder Technology* 21 (2010) 380–385.
- [21]. Emilia Caballero, Concepcion Jimenez de Cisneros Hydration properties of bentonites from Cabo de Gata (SE, Spain). Isotopic study ( $^{18}\text{O}/^{16}\text{O}$ ;  $2\text{H}/\text{H}$ ) of the hydration water ; *Chemie der Erde* 71 (2011) 389–395.
- [22]. Guang-Peng Jiang, Jian-FengYanga, Ji-QiangGao, Koichi Niihara ; Characterization of porous silicon nitride ceramics using bentonite as binder and sintering additive ; *Materials Characterization* 60 (2009) 456–460.
- [23]. De Pablos A., Duran A., Nieto MI. Adjusting of laboratory filature furnace for obtaining fibreglass *Bol. Soc. Esp. Ceram. Vidr.* (1997); 36 (5): 517-523.
- [24]. Agafanov, V., and Jourausky, G., 1934, The thermal analysisof the soils of Tunisia :*Pedology, Acad. Sci. Paris, Comptesrendus*,V. 198, pp. 1356-58.
- [25]. Agatonoff, V., 1935, Mineralogical study of soil: *3d Internat.Cong. Soil Sci. Trans.*, v. 3, pp. 74-78.
- [26]. Arora A., Shaaban E.R., Singh K., Pandey O.P.: *J. Non–Cryst. Solids* 354, 3944 (2008).
- [27]. Erol M., Kuchukbayrak S., Ersoy-Mericboyu A.: *J. Non–Cryst. Solids* 355, 569 (2009).
- [28]. J. C. RICHMOND, D. G. MOORE, H. B. KIRKPATRICK, W. N. HARRISON, Relation Between Roughness of Interface and Adherence of Porcelain Enamel to Steel ; *Journal of the American Ceramic Society*

[29]. J. Weizhong, W. Ying, D. Qi, Mater.Lett. 58 (2004) 1611–1615.

[30]. Mingzhao He, YanminWanga, Eric Forsberg,Slurry rheology in wet ultrafine grinding of industrial minerals: a review, Powder Technology 147 (2004) 94–112

[31]. Guang-Peng Jiang, Jian-FengYanga, Ji-QiangGao, Koichi Niihara ; Characterization of porous silicon nitride ceramics using bentonite as binder and sintering additive ; Materials Characterization 60 (2009) 456–460.

[32]. Ilaria Corni, Mary P. Ryan, Aldo R. Boccaccini ; Electrophoretic deposition: From traditional ceramics to nanotechnology ; Journal of the European Ceramic Society 28 (2008) 1353–1367

[33]. W.C. Oliver, G.M. Pharr, A new improved technique for determining hardness and elastic modulus sing load and sensing indentation experiments, J. Mater. Res. 7(6) (1992) 1564-1582.

## 4 Result and discussion

### 4.1 Hot stage microscopy

In the present thesis work, a preliminary study needed for the selection of the suitable frit has been performed. All the evaluated frits has been supplied from Smaltiflex. The first analyses have been performed in order to assess the frits thermal behaviour and their suitability to the required condition of the productive process. Following the list of the evaluated frits:

- 1524
- 8100
- 8010
- Mix
- Enamel SM014

The heating industrial process, which promotes the bond creation between steel and enamel, was performed in an industrial furnace. The firing time was 6 minutes at 860°C, the sample was then cooled in air. These values of thermal treatment are typical for vitreous enamel steel [1,2,3]. Better frit glass need a melting point near to the high temperature of thermal treatment. Low temperature of melting do not allow at gases, like CO<sub>2</sub> and H<sub>2</sub>, to go out from the very low carbon steel.

For the hot-stage microscope, the enamel powders were compacted to little cylinders (1mm diameter and 3 mm of height) by uniaxial pressing. The measurements were performed with 20°C/min heating rate from 20°C to 1400°C [1].

An example of the results obtained by hot stage microscope analysis is reported in figure 27.

<b>Codice:</b>	00901S	<b>Tipo prova:</b>	Provino singolo
<b>Descrizione:</b>	MS_Silgardil(Smaltiflex-Matteo)_sma ...	<b>Temperatura min.:</b>	28 °C
<b>Data:</b>	28/06/2010	<b>Temperatura max.:</b>	874 °C

Ciclo termico			
	Salita	Temp	Stasi
1	20,0	1600 °C	0,0
2			
3			
4			
5			
6			
7			
8			

Valori caratteristici	
Forma	Temperatura
Sinterizzazione	664 °C
Rammollimento	722 °C
Sfera	796 °C
Mezza Sfera	832 °C
Fusione	862 °C

Durata prova	
<b>Totale</b>	000.42.22
<b>dal 1° scatto</b>	000.42.21

Intervalli			
	Inizio	Interv.	Fine
1	20°C	2°C	1600°C
2			
3			

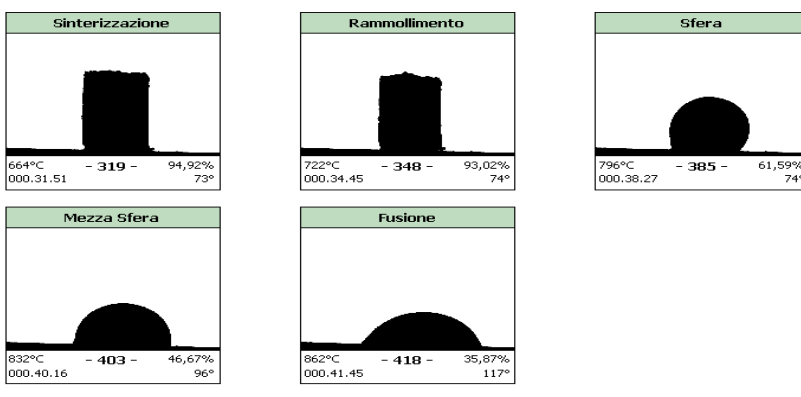


Figure 27. Hot stage microscope of Enamel SM014

*Sintering point* is the point that specimen start to reduce its size. Usually ceramic-glass samples improve their size in the first part of thermal treatment then reduce when the temperature increase.

Vitreous enamel phases reaches the *softening point* when the liquid phases resulting from the heat treatment beyond the temperature of glass transition of the glassy components above mentioned appear on the surface of the sample. From this point on, the shape of the sample undergoes substantial changes due to the surface tension of the liquid phases. If this instrument is used in order to reach this point, the rounding of the corners of the sample and the smoothing of the upper part of the walls of the sample are taken into consideration. At the *Sphere point*, the specimen is formed almost entirely of liquid phases and the shape of the sample is controlled by the surface tension. While the surface tension tends to reduce the surface to a minimum forming a sphere, the hydrostatic pressure related to the density of the liquid phase tends to flatten the

shape. For this reason some glasses do not reach the sphere point: it is the case of glasses with a high density and a low surface tension. The *Half Sphere point* is reached when the height of the sample is half the width of the base. If a glassy material behaves normally, at the half sphere temperature the contact angle is approximately 90°. In other hand, at this point the contact angle is often much higher and in some cases the shape of the sample can resemble a bell. These anomalies can be attributed to the formation of non-homogenous phases inside the sample, such as crystallization or glass-glass separations. *Melting point* can be defined in different ways. Better way is considering the sample melted when its height is 33,3% (one third), respect to its initial height. Some norms require the height to be one third of the height at the Hemisphere Temperature.

Results obtained from hot stage microscope for all tested samples are summarized in Table 5.

From the hot stage microscopy experiments it was possible to observe that the sintering temperature of the SM014 enamel occurs at about 660°C, the softening occurs at about 760°C while the sphere is reached at about 790°C. Finally, the hot stage microscopy experiments showed that the half-sphere of the enamel occurs at about 830°C and the melting temperature is about 844°C (Table 5 and Figure 27).

Sample	Temperature(°C)				
	Sintering	Softening	Sphere	Half sphere	Melting
<b>1524</b>	572	672	726	774	796
<b>8100</b>	572	750	780	782	792
<b>8010</b>	562	764	780	792	804
<b>mix</b>	568	/	762	776	788
<b>SM014</b>	662	766	796	826	844

Table 5. Summary of peculiar temperatures for enamels studied

Figure 28 shows a qualitative viscosity-temperature curve obtained by hot stage microscopy for the SM014 enamel samples. According to De Pablos method [1, 4, chapter 3.5.1.1.1 ] characteristic temperature was reached from DTA and hot stage microscope.

Since only a small temperature range was considered, the viscosity-temperature behaviour is linear.

It is important to underline that the atmosphere of the kiln of the hot stage microscope influences and the surface tension and the wet angle, while the possible emission of gases from the enamel mainly affects the points based on the observation of definite geometrical forms such as the half ball and melting points [1].

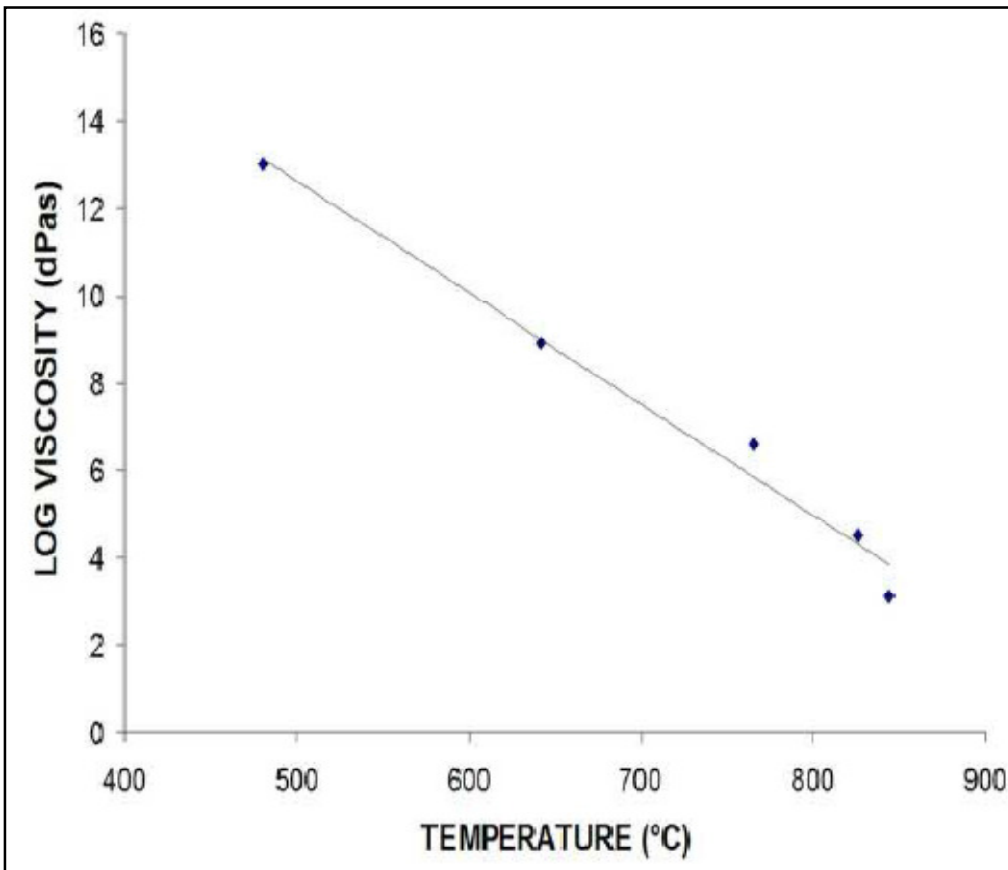


Figure 28. Qualitative viscosity-temperature curve and the related ESEM taken during the heating of the enamel-steel system.

In any case, this technique makes it possible to obtain a qualitative viscosity-temperature curve for the enamel in an easier way than the other more “sophisticated” techniques (beam bending, fiber elongation, high temperature rotational viscosimeter, etc...[5-7]). With this data was possible obtained the values of viscosity of the enamel in the range [800 – 860]°C. The control of fluidity of enamel during the thermal treatment is important to reach homogeneous surface and thickness on the specimens.

## 4.2 Optical dilatometer

Linear thermal expansion tests were carried out in order to reach information about the residual stress after thermal treatment. From literature [8, 9] glass material has better resistance of compression stress than tension stress. Linear thermal expansion of very low carbon steel DC04ED is  $130 \times 10^{-7} / ^\circ\text{C}$  [1] and the values of vitreous enamel is  $12.4 \times 10^{-6} / ^\circ\text{C}$  (Table 6). Vitreous enamel-steel composites, therefore, contain residual stresses which influence the overall physical and mechanical properties of the system.

This small difference between the thermal expansion coefficients makes it possible to obtain the coating under compression while the steel is under tension (see Figure 18 in [8] from which, for this specific case, it is possible to estimate a maximum residual stress acting on the coating of about -20 MPa). The introduction of surface compression is a well-established technique for strengthening of enamel because the presence of a layer of surface compression mitigates failure from coating cracks [8, 10].

Better performance was obtained from SM014 (Table 6 and Figure 29) because gap between linear thermal expansion of enamel and steel is smaller than other frit investigated. This condition allows to reduce the residual stresses.

Results obtained from Optical dilatometer for all tested samples are summarized in Table 6 and Figure 29.

Temperature(°C)	Alfa (1/°C)
1524	$88,77 * 10^{-7}$
8100	$76,25 * 10^{-7}$
8010	$117,62 * 10^{-7}$
mix	$88,44 * 10^{-7}$
SM014	$124,70 * 10^{-7}$

Table 6. Values of linear thermal expansion.

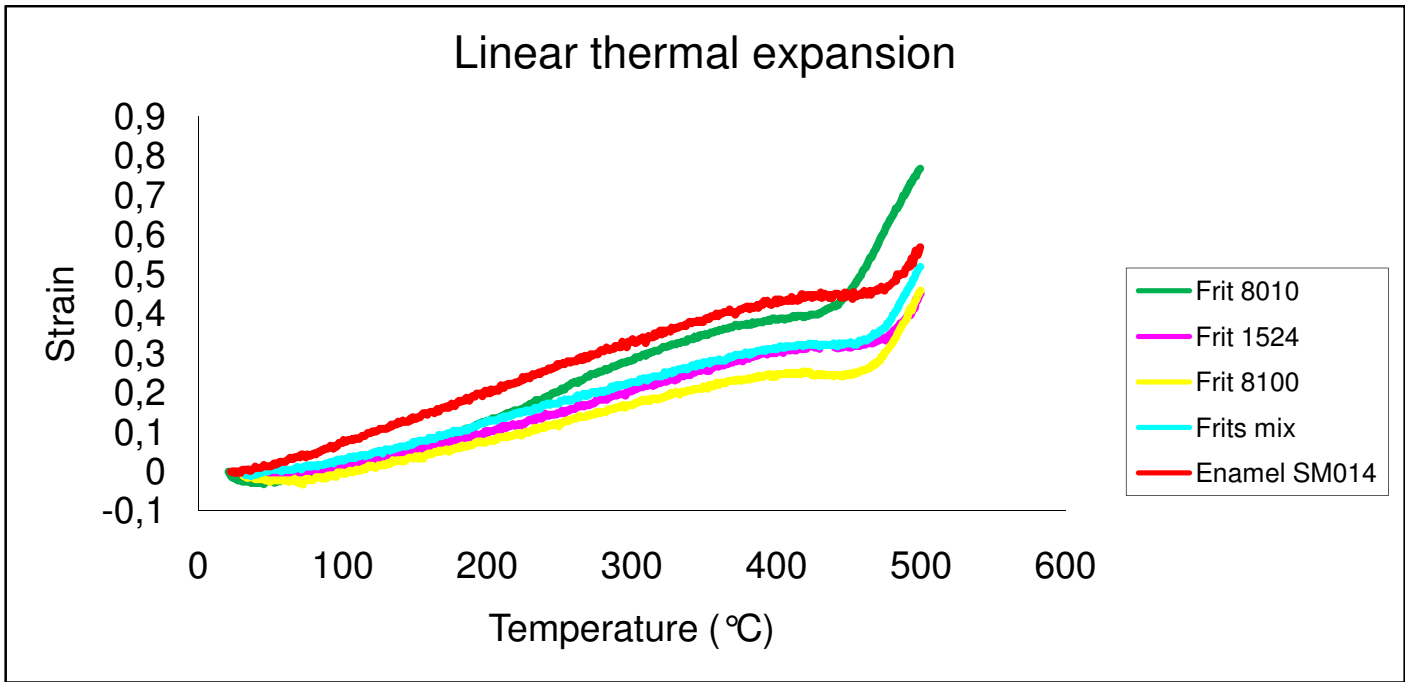


Figure 29. Matching of linear thermal expansion.

### 4.3 Differential thermal analysis

Differential Thermal Analysis (DTA) allows the study of either reversible or irreversible transformations that are associated to heating exchanges within the material during thermal treatment. From DTA investigation was possible reached values of  $T_g$  and  $T_{exo}$  of each frit investigated. The temperature of peak after the temperature  $T_g$  in the thermogram is known  $T_{exo}$ . The effect of this characteristic peak is crystallization of frit. Only three frit investigated have been got this peak such as : frit 8100, frit 8010, frit 1524.

Other values obtained are peaks typical of crystallization of glass during the thermal treatment.

Each thermogram is shown in Figure 30-34 and are summarized in Table 7.

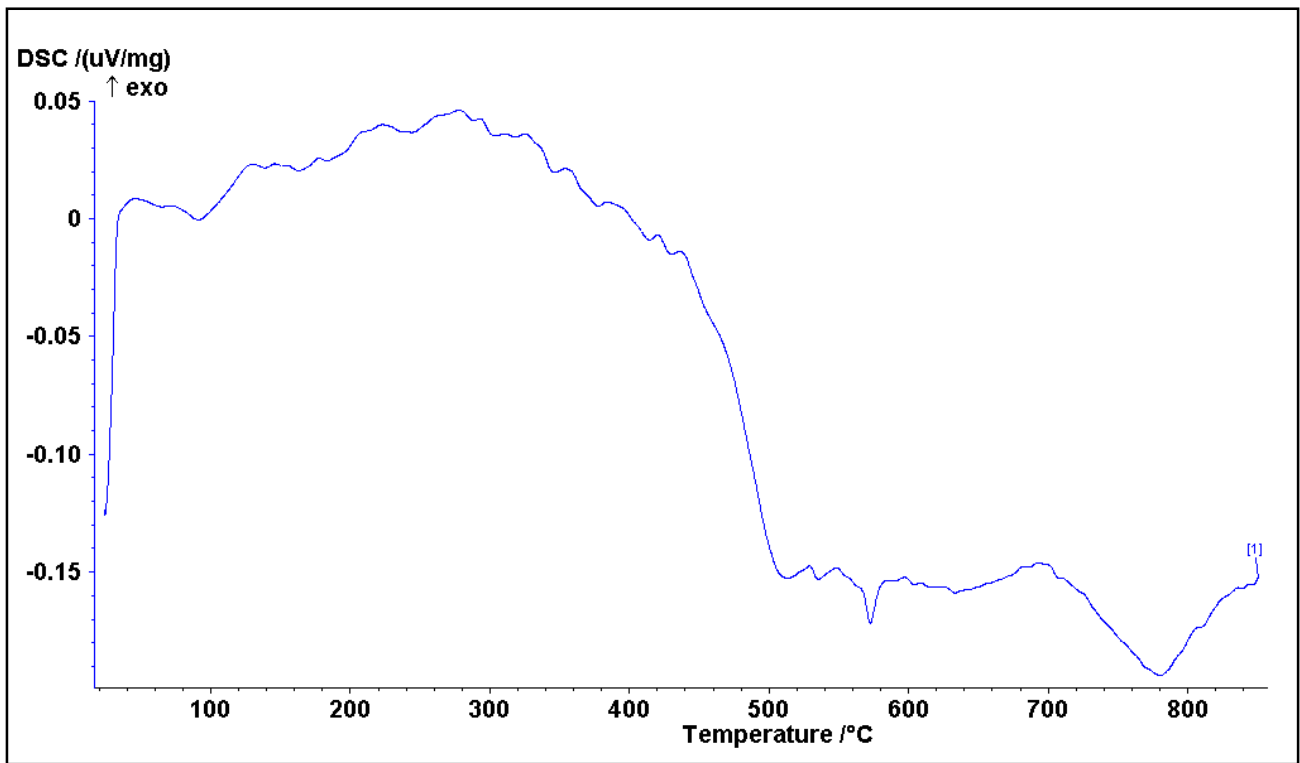


Figure 30. Differential thermal analysis of enamel SM014

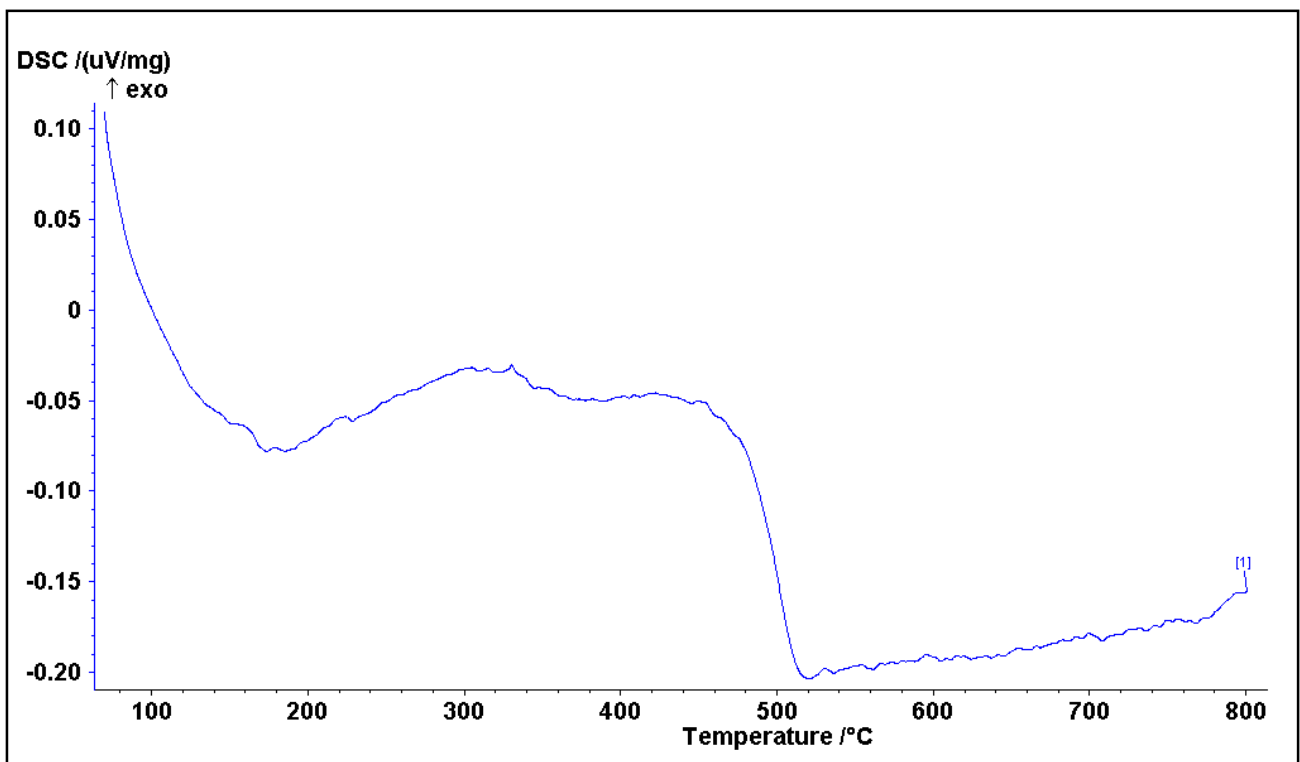


Figure 31. Differential Thermal analysis of frit 1524.

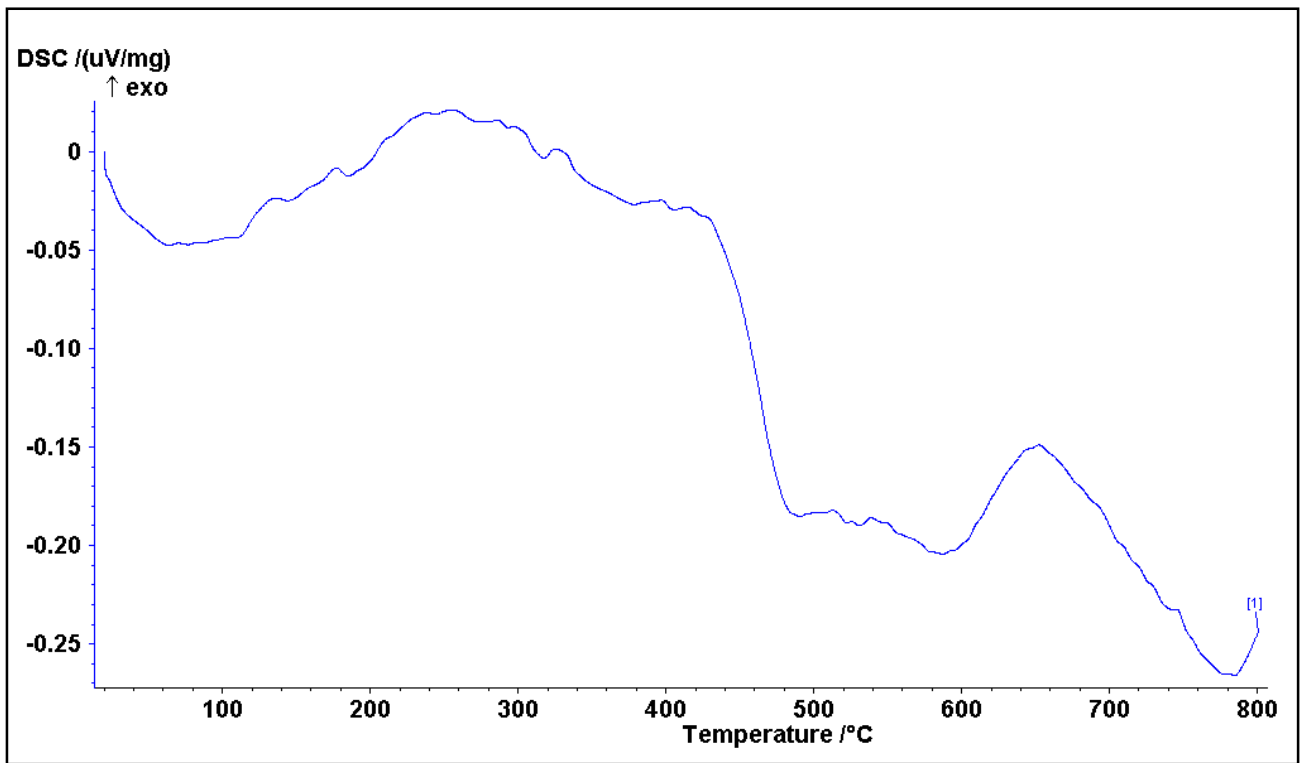


Figure 32. Differential thermal analysis of frit 8010.

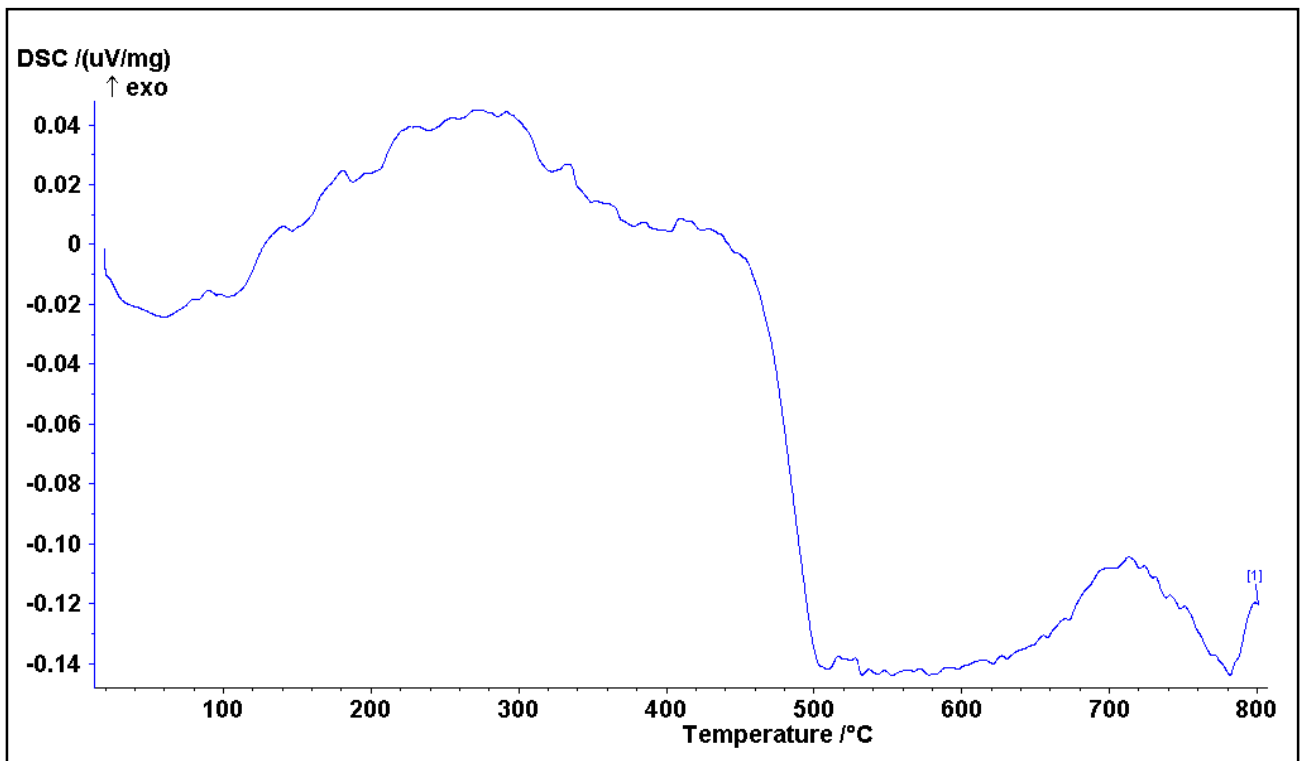


Figure 33. Differential thermal analysis of frit 8100.

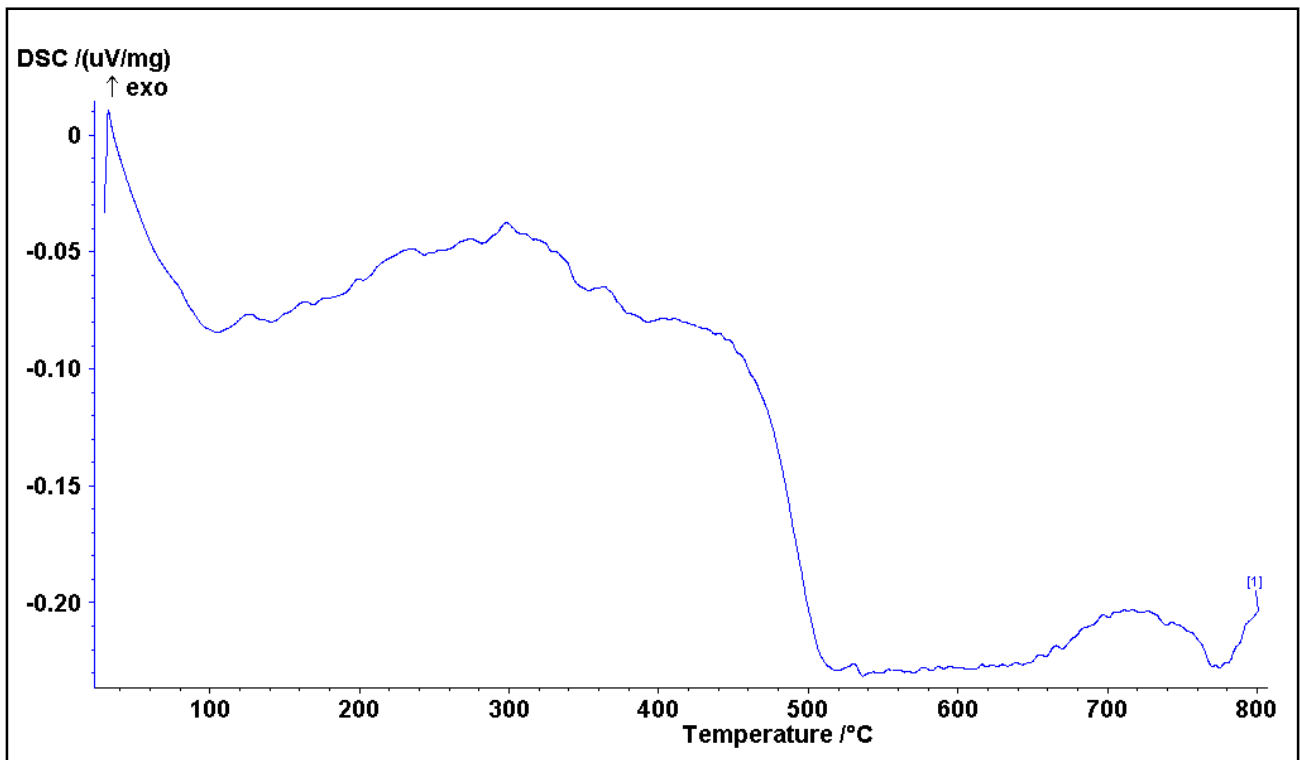


Figure 34. Differential thermal analysis of frit mix.

Samples	Tg (°C)	Texo (°C)
1524	460	No
8100	430	700 - 720
8010	450	660
mix	450	720
SM014	450	No

Table 7. Summary of DTA results.

From data of thermal treatment (Table 7, and figure 30-34), is possible to confirm that only enamel SM014 is suitable for vitreous enamel coating process. About Tg obtained, the samples have been reached similar values (Table 7) and the little gap is not relevant.

Other frit glassy investigated have a low values of melting temperature (Table 5). In order to obtain suitable coating only SM014 was completely investigated with other techniques.

After these tests, only SM014 was used for hand spraying and EPD techniques because better performance is reached from it.

## 4.4 Chemical analysis

In table 8 is reported the chemical composition of SM014 enamel.

Oxide	SiO <sub>2</sub>	B <sub>2</sub> O <sub>3</sub>	Na <sub>2</sub> O	TiO <sub>2</sub>	BaO	Al <sub>2</sub> O <sub>3</sub>	CaO	K <sub>2</sub> O	Fe <sub>2</sub> O <sub>3</sub>	MnO	MgO	(Co <sub>3</sub> O <sub>4</sub> +NiO+CuO)	Total
ICP wt %	62.41	10.06	7.65	4.51	2.57	2.2	4.37	3.01	1.21	0.92	0.14	0.95	100

Table 8. Chemical composition of SM014 enamel.

The sample shows high concentration of alkaline and alkaline earth metals oxides [1,11,12,13]; these substances allow suitable chemical reactions typical of the thermal treatment. This chemical composition of enamel is suitable at the industrial thermal treatment (Paragraph 2.7 and 4.1).

The reaction of the iron, cobalt and nickel ions in the metal/enamel interface is designed to form small galvanic cell that strongly corrodes the base metal [2,35]. The current ionic transition flows from iron through melt to cobalt and back to iron. These local cells exhausted during firing because the anodic iron and diffusing oxygen are abundant [14,15]. After iron goes in to solution, the surface becomes roughed, and the glass anchors itself into the depressions produced so final adhesion is basically mechanical.

## 4.5 Grain size distribution

The grain size distribution of enamel SM014 in slurry is reported in Figure 35. Two measurements have been performed. The particle size distribution of the frit powders is reported in figure 9 and shows a quite large bimodal distributive curve. The first maximum lies at around 25  $\mu\text{m}$ , while the second one at around 8  $\mu\text{m}$  even if 90% of the particle is finer than around 77  $\mu\text{m}$ .

## Result Analysis Report

Sample Name: Barbo2		Measured: giovedì 30 giugno 2011 12.51.23
Sample Source & type:	Measured by:	Analysed: giovedì 30 giugno 2011 12.51.23
Sample bulk lot ref:	Result Source: Measurement	SOP Name:

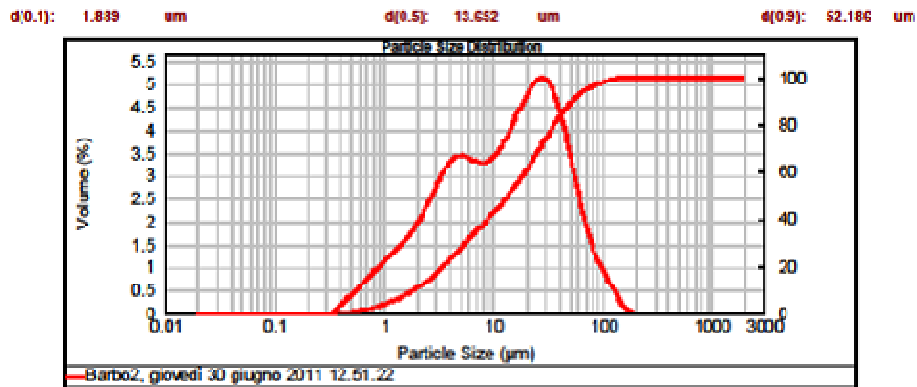


Figure 35. Grain size distribution of industrial slurry SM014.

According to the cumulative curve in Figure 35 was reached typical values of : D10, D50, D90. These values represent the ten, fifty, ninety percents of volume of particle with diameter less the values 1.889 $\mu\text{m}$ , 13.652 $\mu\text{m}$ , 52.186 $\mu\text{m}$ . Results obtained from grain size distribution for all tested samples are summarized in Table 9.

First measurement ( $\mu\text{m}$ )	Second measurement ( $\mu\text{m}$ )
d(10): 1.893	d(10): 1.889
d(50): 12.909	d(50): 13.652
d(90): 45.085	d(90): 52.186

Table 9. Laser particle size tests.

An optimal particle size value for EPD technique occurs in the range of 1–20  $\mu\text{m}$  as reported in the literature [16, 17]. The studied frits powders are quite large for an EPD application and tend to sediment in water, however using some additives into the aqueous suspension it is possible to increase their “colloidal” properties, i.e. to obtain stable suspensions.

As reported by Besra and Liu [16] particle with small values of size limited the problem of settling due to gravity. It is important that the particles remain dispersed and stable for homogeneous deposition. The mobility of small particles in EPD technique is higher than large size particle.

## 4.6 Density

Density of industrial slurry SM014 was measured by using a pycnometer (volume 100  $\text{dm}^3$ ) and a balance ( $\pm 0,01\text{g}$ ). It was obtained by this formula:

$$\text{Density of slurry (g/cm}^3\text{)} = \frac{\text{Mass of fully pycnometer} - \text{Mass of empty pycnometer}}{\text{Volume of pycnometer.}}$$

The specific gravity of enamelling slip is 1.70  $\text{g/cm}^3$  [1]. High values of density are suitable only for air brush and immersion enamelling, but electrophoretic deposition enamelling needs only diluted slurry [11,12,14,16,18]. The 50% of solid phase are present in the slurry, and this amount contribute to reach the values of density. The highest amount of solid phase formed by frit have density about 2.5  $\text{g/cm}^3$ .

## 4.7 X-ray diffraction

The mineralogical characterization of the enamel was performed using a X-ray diffraction (XRD, PANalytical, X'Pert PRO diffractometer, using  $\text{Cu-K}\alpha$  radiation from a Cu emission tube and an X'Celerator detector on the diffracted beam path). It was performed on dried enamel

specimens to detect and identify the nature of enamel. The XRD pattern of enamel is reported in figure 36.

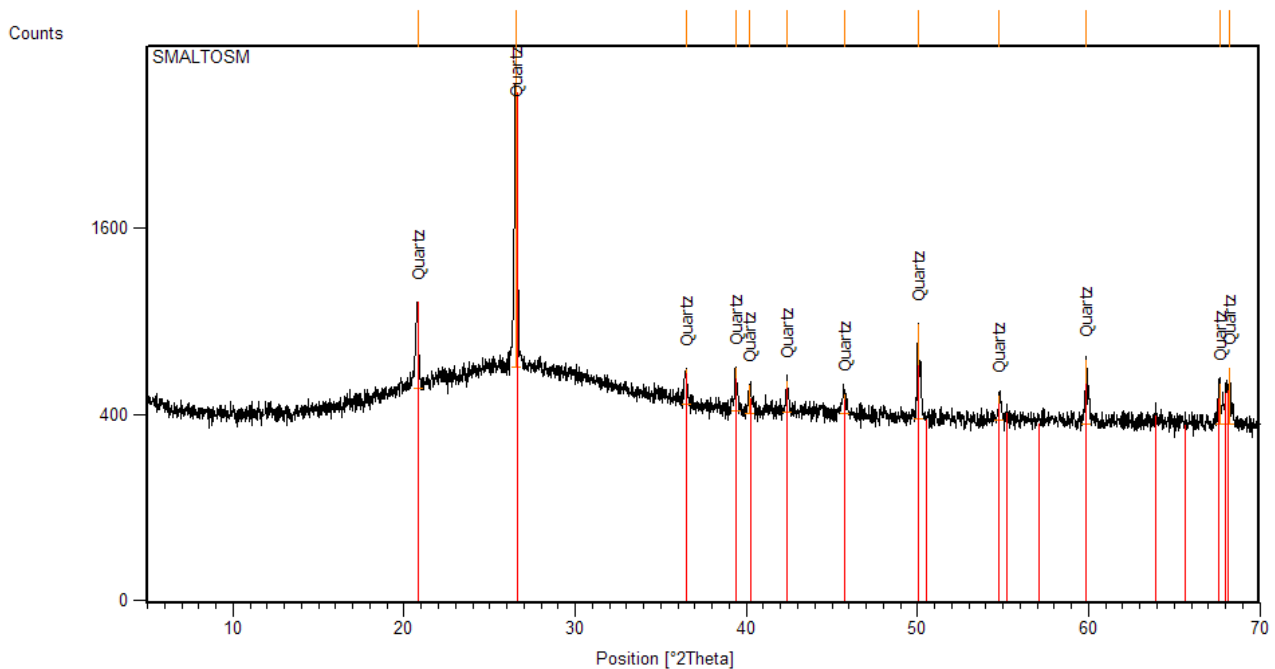


Figure 36. X-ray diffraction of Enamel SM014.

X-ray diffraction analysis performed on the sample Figure 36 shows a broad band typical of glassy samples and crystals of quartz. This crystalline phase is added into the enamel with small amounts of kaolin clay as well to increase some properties of final enamel (this is a Smaltiflex industrial procedure).

## 4.8 Characterization of steel

### 4.8.1 Optical observation

Very low carbon steel DCO4ED produced by Arcelormittal is shown in figure 37. This steel have a characteristic ferritic structure with equiaxial grain [19].

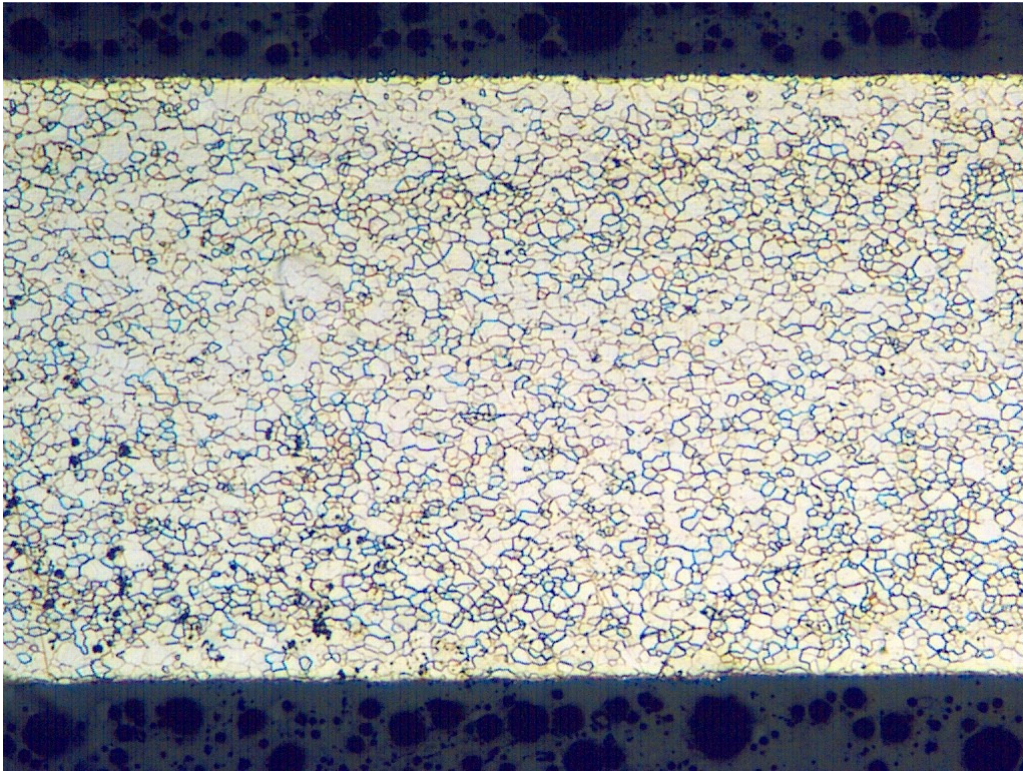


Figure 37. Very low carbon steel DC04ED .

#### 4.8.2 Micro-hardness

Thin plate of very low carbon steel (30 x 30 x 1)mm, was investigated by Vickers loads. Was used two different loads to confirm the data of the tests. Data obtained in table 10 are similar in both measurements. From ASTM A 370, the values of micro-hardness Vickers is about 115 - 120 HV. Values of ASTM A 370 are similar to values reach in laboratory.

DC04ED	100g Vickers HV	200g Vickers HV
Average (30 data)	129,7	119,5
Standard deviation	20,3	13,4

Table 10. Hardness of Very low carbon steel.

### 4.8.3 Measurements of roughness

Surface roughness of the enamel is:  $R_a = 0.39 \pm 0.04 \mu\text{m}$ ,  $R_z = 2.15 \pm 0.26 \mu\text{m}$ ,  $R_{\text{max}} = 2.8 \pm 0.8 \mu\text{m}$ ; while the surface roughness of the steel is:  $R_a = 1.07 \pm 0.19 \mu\text{m}$ ,  $R_z = 5.73 \pm 0.43 \mu\text{m}$ ,  $R_{\text{max}} = 7.32 \pm 0.84 \mu\text{m}$ . The measured steel roughness fits the range [20] that is known to be able to support the enamel-steel adhesion. Suitable values of roughness are about  $1,6 \mu\text{m}$  according to UNI EN 10130.

## 4.9 Investigation of Enamel SM014 for electrophoretic deposition technique

### 4.9.1 Zeta potential

Due the high concentration of slurry SM014, it was not possible investigated about zeta potential. Only diluted slurry with additive to modify the stability and limited the settling was investigate. A little quantity of slurry of enamel SM014 was diluted ten times because normal running of measurement have a limit at high concentration. No suitable results was obtained from measurements of this specimen. These values was incompatible for electrophoretic deposition. The use of additives to improve the absolute value of zeta potential was a solution to obtain suitable data. The results are reported in table 11 :

Additive with SM014 diluted 10 times	Z potential
Bentonite	-57.6
Densicer	-93.4
Cmc 150	-1.20
Cmc 30	-11.8
Cmc 5s	-86,2

Table 11. Zeta potential values (mV) for suspensions added with additive.

In Table 11, the zeta potential values for each slurry are reported. It is possible to observe that Densicer is the best additive in terms of improving the dispersion of slurries. Bentonite and the CMCs additives show also a fairly good performance, in particular when they have low molecular weight (i.e. CMC5s). No suitable values wasn't obtain from use of CMC 150. Considering that the settling time lower than 30 second the suspensions is not stable for the application for EPD technique. So from the observation of the results it can be deduced that only Densicer and Bentonite are suitable to prepare the slurries in additive in order to avoid a fast sedimentation. The additive chemistry is a key factor influencing the electrophoretic deposition process, however this aspect was not further investigated here. In any case, for successful EPD it is imperative to achieve a high and uniform surface charge of the suspended particles.

#### **4.9.2 Rheological characterization**

Rotational rheometry was used to determine the effect of each additive on the time and shear dependent behaviour of the suspensions. From the experimental flow curves it was verified that the enamel suspension without additive is not stable during the test and it was not possible to plot the curves due to the suspension instability. In this part only suspensions with a good time of sedimentation were analyzed. The tests were carried out only for three suspensions, like SM014, SM014 with Densicer®, SM014 with Bentonite.

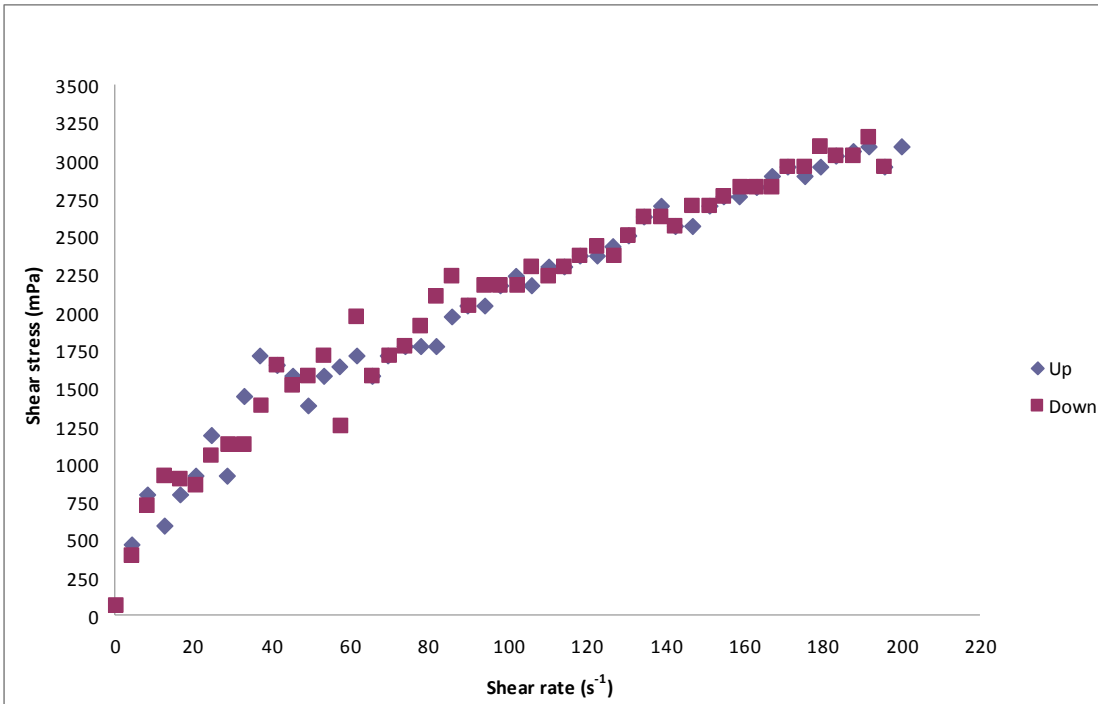


Figure 38. Flow curve (up and down) of slurries prepared with Densicer 0.10%.

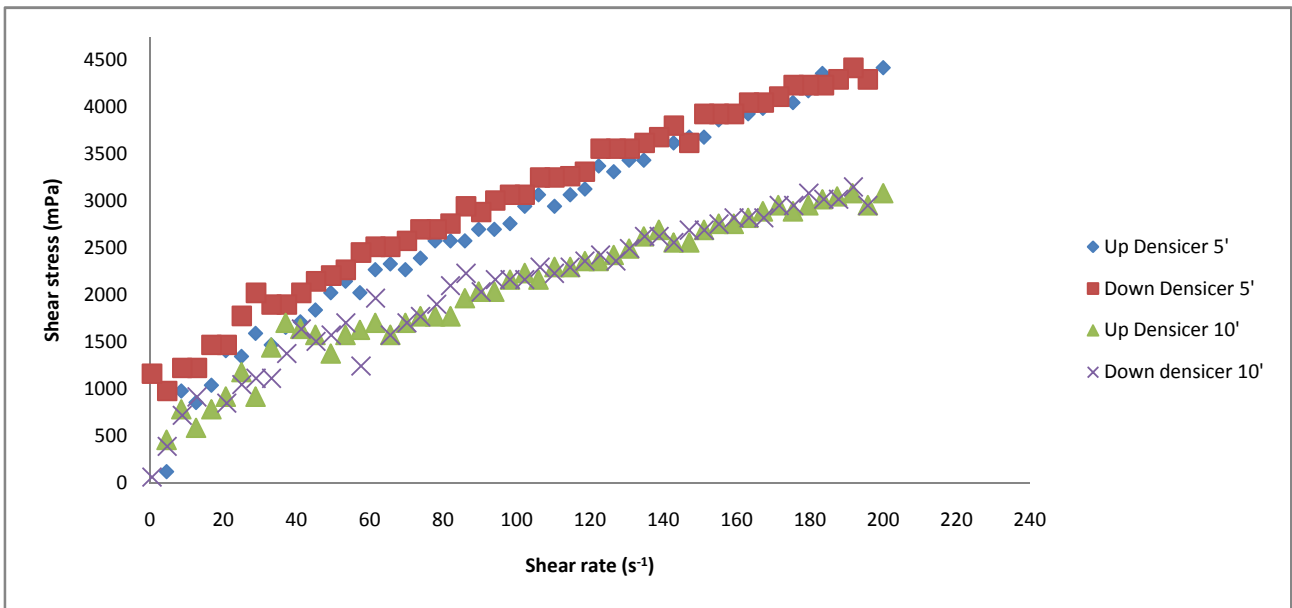


Figure 39. Flow curve (up and down) of slurries prepared with Densicer 0.10% at different times.

In Figure 38 the flow curve for enamel aqueous suspensions added with Densicer (up and down curves) was plotted. This suspension shows a shear thinning behaviour (viscosity decreases when applied shear stress increases and no a yield stress is present). The hysteresis between the up and

down curves normally indicates the time dependence, in this case the curves are quite overlapped indicating low thixotropy and good stability confirming zeta potential data. Flow curves with a test time of 5 min and 10 min (Figures 38 and 39) were also performed, in order further to check the suspension stability. It is possible to note a good reproducibility for the two tests confirming that this additive permits a settling time longer than usually required for EPD. On the other hand the rheological behaviour of slurries prepared with the other additives was shown to be incompatible with EPD technique because the time of sedimentation is not long enough.

A set of experiments to obtain single step curves (shear stress vs. time) was carried out in order to evaluate the time dependence of these enamel slurries. In figure 40 time curve with SM014 (without additive), SM014 with Densicer and SM014 with Bentonite suspensions are plotted because the other additives showed values near to zero. This test, in which very diluted suspensions were used was carried out to obtain data about suspension stability vs time. In this case it was assessed if there is sedimentation or not within a predetermined time period. The higher values of shear stress and viscosity of the suspensions containing Densicer, in comparison to the confirmed other suspension shown the higher stability of Densicer suspension. Low values of shear stress and viscosity improve the sedimentation of the suspensions. These results were confirmed from the very low values, of shear stress and viscosity, for suspensions containing CMCs. The suspensions without additive and with bentonite showed the lowest values respect to the slurry with Densicer. Besides, it is possible to observe low stability because the shear stress values decreased as a function of the measured time, indicating settling. The suspensions contain glass powders (frits) having relatively high density ( $2.5 \text{ g.cm}^{-3}$ ), so a strong suspensivant agent is required to avoid the phenomena of quick sedimentation. From these results it is possible to confirm that SM014 suspension without additive shows a high instability and it is not suitable for application in EPD.

Regarding the use of bentonite as additive, no improvement of suspension stability was observed. The amount of bentonite added (2 wt%) is not high enough for developing the stability of the suspension. For the curve reported it is possible to calculate the corresponding viscosity values. These values are very low (2.5 mPa.s) and very close to the viscosity of water (1 mPa.s) being more than 10 times lower than the viscosity values obtained with the other additive used (Densicer) Figure (41, 42). Generally bentonite prevents the sedimentation giving to the suspension visco-structural behaviour that increases the stability.

Finally, the enamel suspension added with Densicer shows higher viscosity values (33 mPa.s) and a constant trend versus time, this fact allows to predict no sedimentation, during the measured time (300 s.).

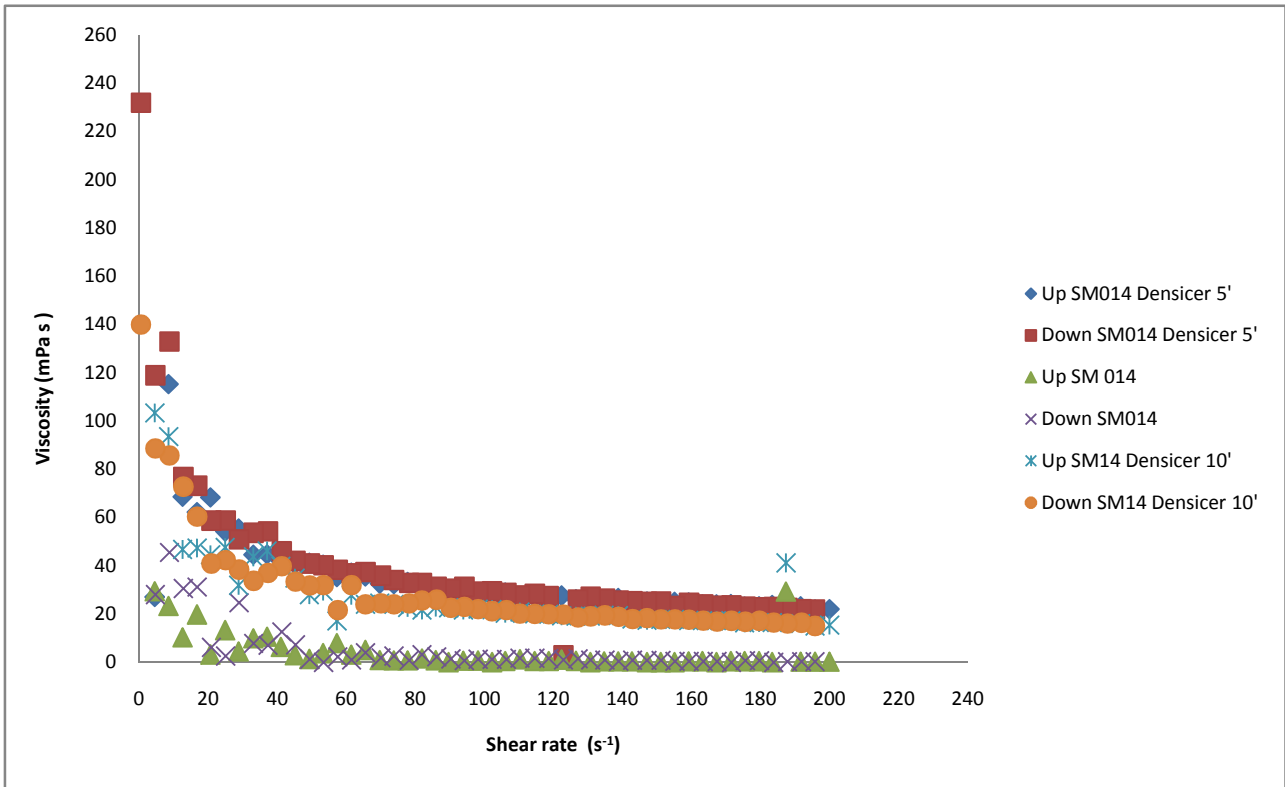


Figure 40. Flow curves (Viscosity vs. shear rate) for the slurrries without additive and with Densicer 0,10% at the two measured time points (5' and 10').

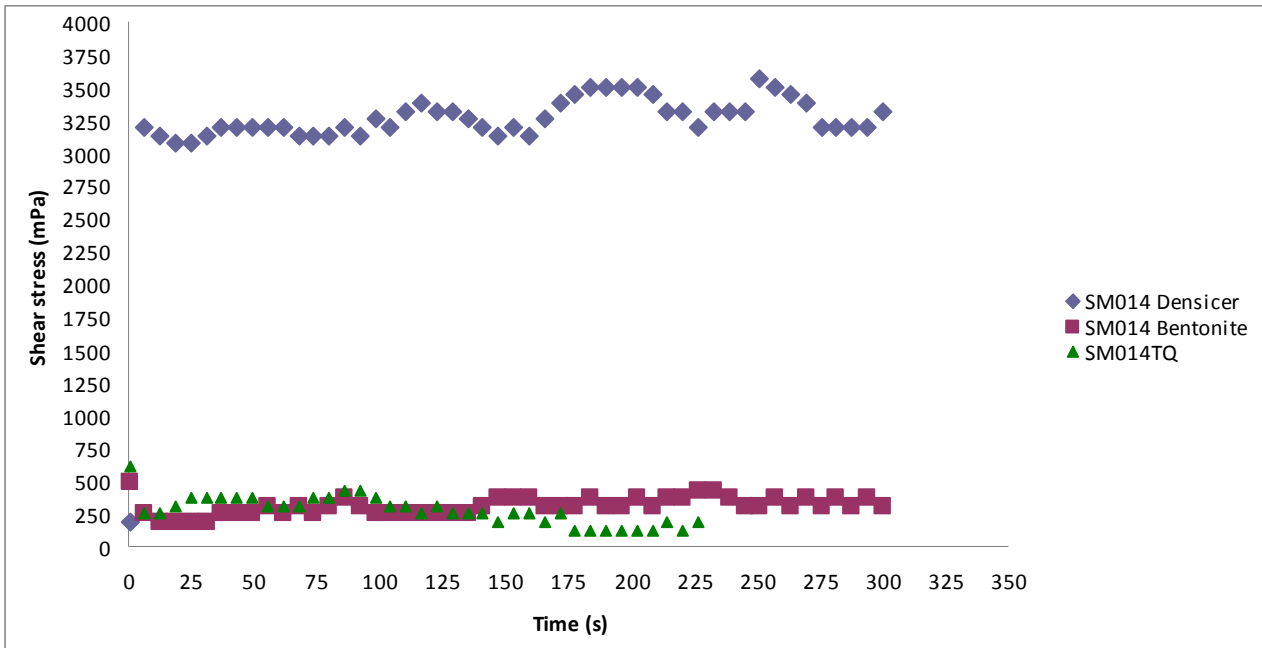


Figure 41. Time curves (Shear stress vs. time) for the slurries without additive (SM014 TQ) and with Densicer (SM014 Densicer) and bentonite (SM014 bentonite).

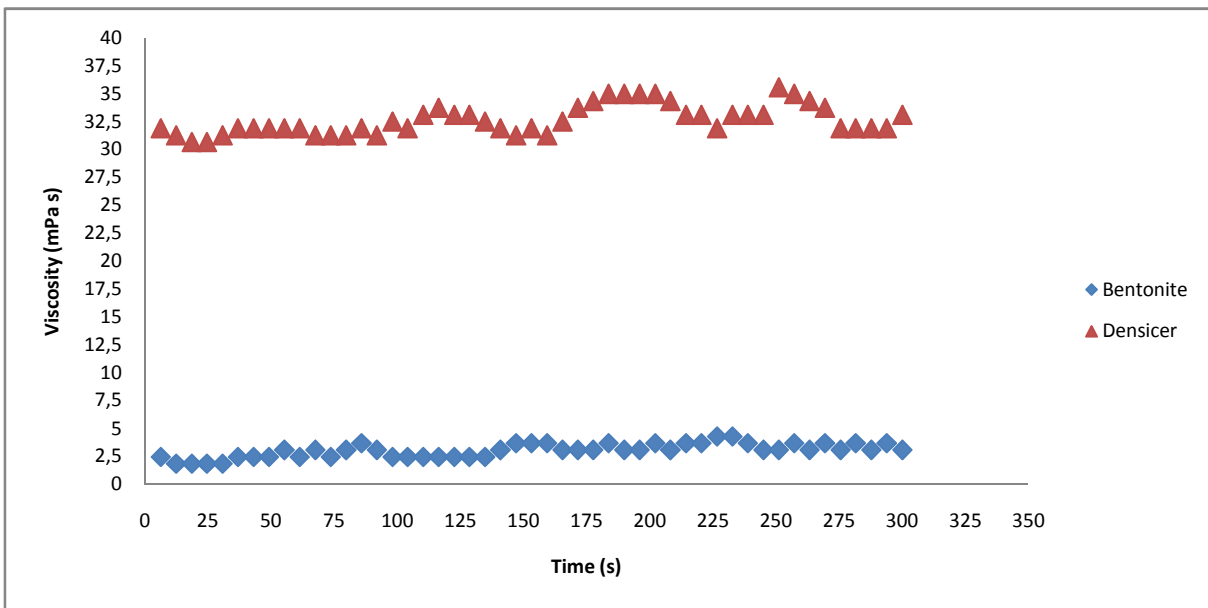


Figure 42. Time curve, matching between two better additive like : Densicer and Bentonite.

Homogeneous slurry improve the quality of enamelling and complete rheological characterization. Electrophoretic deposition needed stable and homogeneous suspension to control the deposition. In this technique was possible choose the thickness of deposition mass[1-5].

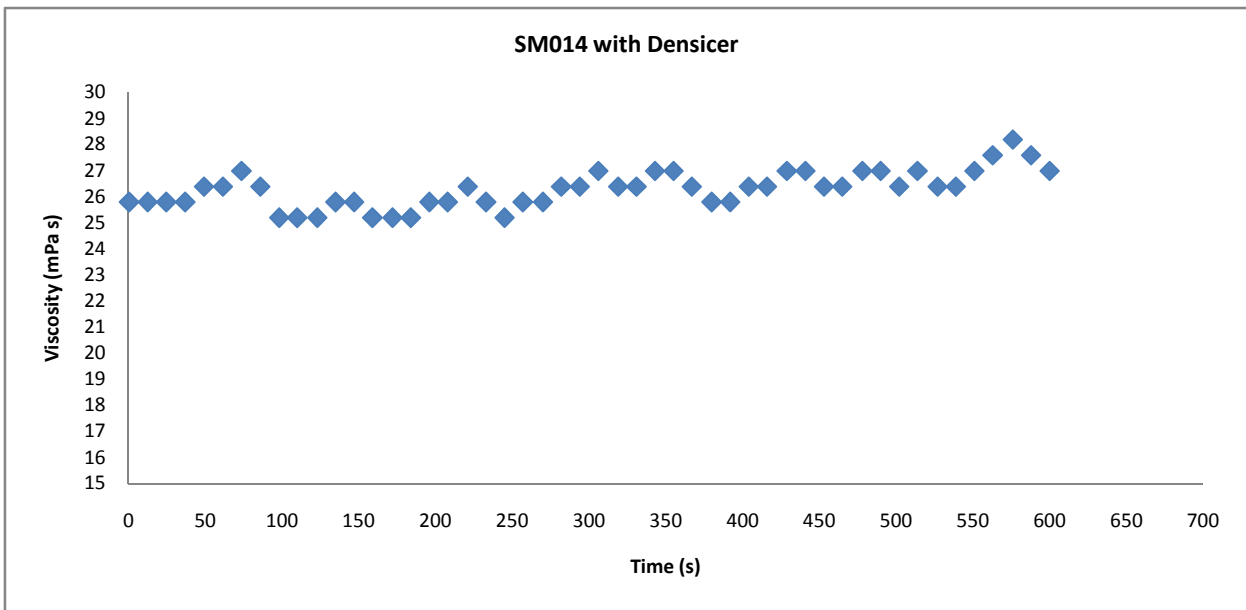


Figure 43. Time curve of 10' minutes of industrial Slurry with Densicer

Densicer additive, consented to improve the time of rheological characterization from 300 seconds and 600 seconds with 200 of shear rate (Figure 43).

#### 4.9.3 Settling after preparation of suspension for EPD

Table 12 reports the time of sedimentation values for several studied suspensions added with 2 wt% of the different additives. Only the highest concentration of additive permits to obtain results reproducible results because the lower concentration values gave worst results so they were not reported. Except for Densicer where the tests were conducted with 0.1 wt%. It is important to underline that suspensions having a settling time lower than 30 seconds are not generally suitable for the application of EPD technique [12,15]. From the results presented it is possible to conclude that Densicer is suitable additive for the preparation of rather stable slurries for EPD.

<b>Additive</b>	<b>Time of sedimentation [seconds]</b>
CaCl <sub>2</sub>	15- 20
MgCl <sub>2</sub>	15-20
Ca <sub>3</sub> (PO <sub>4</sub> ) <sub>2</sub>	15-20
TPF	10-15
Bentonite	10-40
Densicer	15 (0.01) – 200 (0.1)
Cmc 150	15- 20
Cmc 30	15- 20
Cmc 5s	15- 20
Sodium Polyacrilate	15- 20

**Table 12.** Time of sedimentation for the suspensions studied added with 2wt% of additive (except Densicer).

Last rheological investigation carried out was a typical procedure of preparation of suspensions for EPD to show the behaviour of different additives in order to corroborate the previous experimental data (zeta potential, rheological investigation). Usually, to obtain a stable dispersion of ceramics particles in suspension for EPD, an ultrasonic device is used. Three kinds of suspensions, (Figure 44) normally suspension with with Densicer, slurry with bentonite, slurry without additive, were analyzed during five minutes of magnetic stirring, thirty minutes of ultrasonication, and finally five minutes of magnetic stirring. The results of this analysis are shown in the following digital images. By counting down the time, it was investigated the time of stability of the three suspensions. Starting from 150 seconds, bentonite suspension and slurry suspension without additive showed only 30 seconds of stability (Table 12). This time is quite low for EPD tests and it would be difficult to obtain a homogeneous layer on the substrate. The slurry with Densicer showed better performance than the other two suspensions, exhibiting five minutes of stability. Thus the behaviour in time of sedimentation of the slurry added with Densicer showed positive results in terms of sedimentation time by EPD and it is just a suitable system for vitreous enamels.

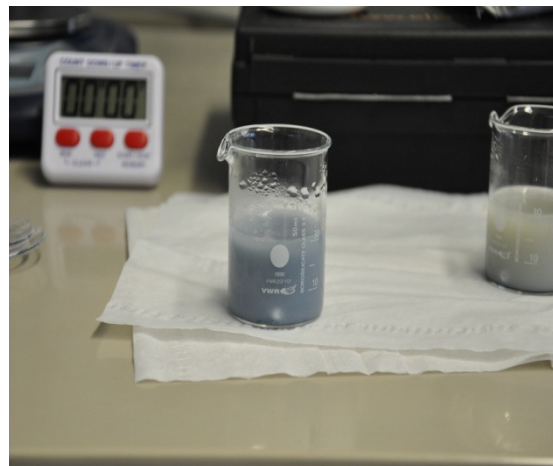
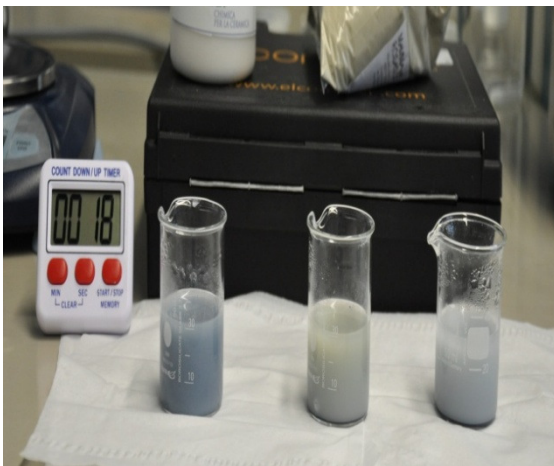


Figure 44. Test of time settling in three different condition : SM014 Densicer, SM014 with Bentonite, SMO14 without additive.

## 4.10 Vitreous enamel steel by hand-spraying system : surface characterization

### 4.10.1 ESEM with hot stage

The “in situ” ESEM observation of the laboratory sample, during the enamelling, provides an important tool to study the full melting process and this equipment makes it possible to record a “movie” of all the observations as well of the measurements. Figure 45 shows in detail the

morphological evolution of the enamel powder during melting, starting from room temperature up to 900°C.

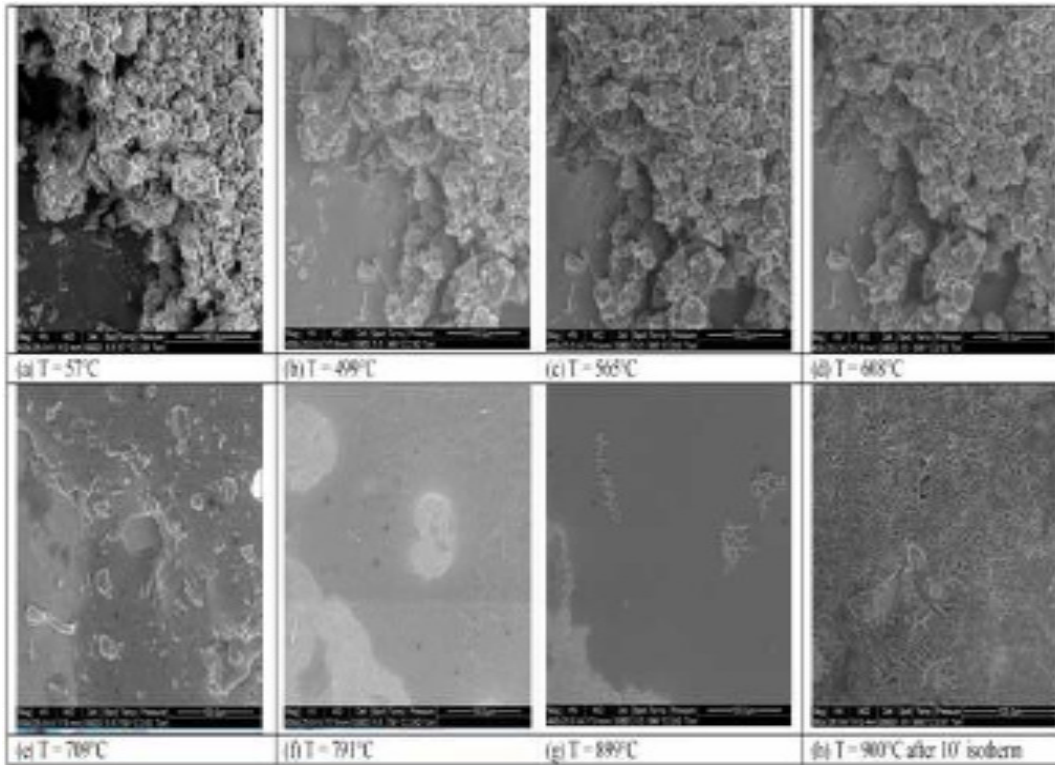


Figure 45. ESEM “in situ” image of studied enamel during heating at different temperatures

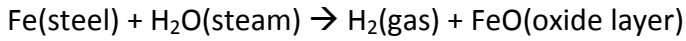
Figure 45a shows a classical crushed-glass powder; increasing the temperature above the  $T_g$  temperature the viscous flow resulting from the driving force of the surface tension causes grain rounding and neck growth (Figure 45b-d). At about 700°C (Figure 45e) the enamel starts to melt even if quartz particles are clearly visible, but it becomes homogeneous and totally melted at about 900°C.

An isotherm at 900°C for 10 minutes produces strong crystallization observed by XRD of  $Fe_2O_3$  and  $Fe_3O_4$ , while the quartz is already present in the enamel as raw material (data not reported). As already reported by Barkova et al. [18] these crystalline phases are formed during heating because an intensive thermal effect induces an oxidation process on the enamel surface, which takes place according to the following pathway:  $\alpha\text{-Fe} \rightarrow Fe_3O_4 \rightarrow \alpha\text{-Fe}_2O_3$ . The oxygen supply is very important during the thermal process because we obtain different chemical reactions at different temperatures.

Water can be a good supply of oxygen to obtain the oxidation of the Iron [1].



$$dG^\circ(\text{J/mol Fe or C}) = dH^\circ - TdS^\circ \quad dG^\circ(\text{J/mol Fe or C}) = -28137 - 21.8T$$



$$dG^\circ(\text{J/mol Fe or C}) = dH^\circ - TdS^\circ \quad dG^\circ(\text{J/mol Fe or C}) = -16245 + 8.6T$$



$$dG^\circ(\text{J/mol Fe or C}) = dH^\circ - TdS^\circ \quad dG^\circ(\text{J/mol Fe or C}) = -35861 + 41.6T$$

In fact, ferric and ferrous cations play different roles in the structure of melt, so the ferric-ferrous ratio influences the physical properties of melts. The redox state of iron in melts depends on some external and internal parameters: temperature, oxygen fugacity and composition. They [1] would like to underline that the oxygen concentration in the sample was measured in an industrial sample, after heat treatment in SEM equipment not in situ in ESEM equipment. ESEM was used only to understand how the enamel melts on steel during the heat treatment.

#### 4.10.2 Micro-hardness

Thin plate of vitreous enamel plate (30 x 30 x 1)mm with 200 microns of SM014 enamel, was analyzed by Vickers loads. A Polish and planar surface was requested to obtain suitable specimen. Was used three different loads like : [100 ; 200 ; 300] to confirm the data of the tests (Table 13). Progressive loads was used to reach the maximum value before the fracture of the specimen. According to Wang and Zucchelli [21 - 24] values of Micro-hardness Hv reach are [582 – 995]. These range of micro-hardness are reached with different vitreous coating and specific thermal treatments.

Vitreous enamel plate	100g Vickers HV	200g Vickers HV	300g Vickers HV
Average (30 data)	609	623	604
Standard deviation	35	44	46

Table 13. Hardness of Very low carbon steel.

### 4.10.3 Nano Indenter test

In table 14 the results of HV test on samples having enamel with different thickness (200, 250 and 300 $\mu\text{m}$ ) are shown. Industrial porcelain steel require suitable values of mechanical properties because the stresses in preheater exchanger are high [43]. Tests about these stresses was carried out with different thickness of vitreous coating to obtain better agreement between micro-hardness and Young modulus.

According to Wang [21] and Zucchelli at all [1, 24] values of micro-hardness is similar for each thickness of vitreous coating, but the gap between Young modulus (250  $\mu\text{m}$  vs 300  $\mu\text{m}$ ) is important. High values of Young modulus are request for final application of vitreous enamel steel from Smaltiflex. Afterwards these data is possible underline the thickness of the vitreous coating modify the Young modulus in porcelain steel.

Thickness enamel $\mu\text{m}$	HV vickers	STD deviation	Young modulus (GPa)	STD deviation
200	759	28	81	3
250	750	28	80	2
300	770	15	<b>85</b>	2

Table 14. Characterization of different thickness of vitreous enamel plate bulk

## 4.11 Vitreous enamel steel by hand-spraying system: interface characterization

### 4.11.1 SEM and EDS observation

A typical micrograph of the enamel-steel interface using back scattered electrons for imaging is shown in Figure 46. This Figure shows small islands in the interfacial region, Zone 1. It can be noted that the islands form the so-called anchor points; thus the roughness of steel in the interface is increased. [25].

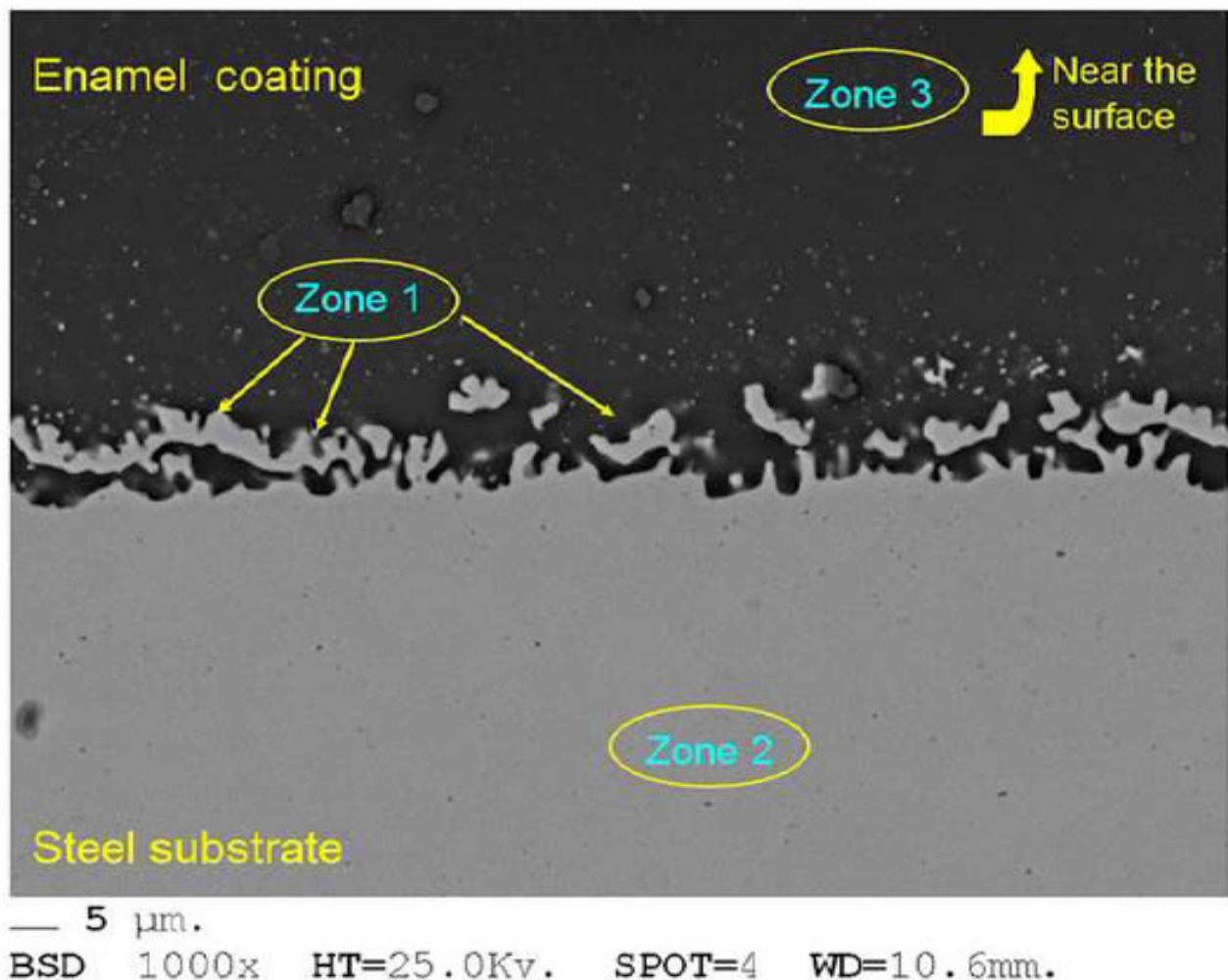


Figure 46. SEM micrograph of cross sectioned enamel/steel interface

Analyzing the same zone by using X-ray mapping, Figure 47 shows a distribution of Si, O, Na, Fe and Ni elements in the interface. While anchor points are mainly composed of Fe and Ni (observed

by EDS but the spectrum is not reported), enamel can be found around these “small islands”, as confirmed by the presence of Si, O and Na. Observing the Ni-map, it was found that the interface is 10 mainly composed of Ni and Fe even if very small Ni-richer areas are clearly evident in the enamel phase.

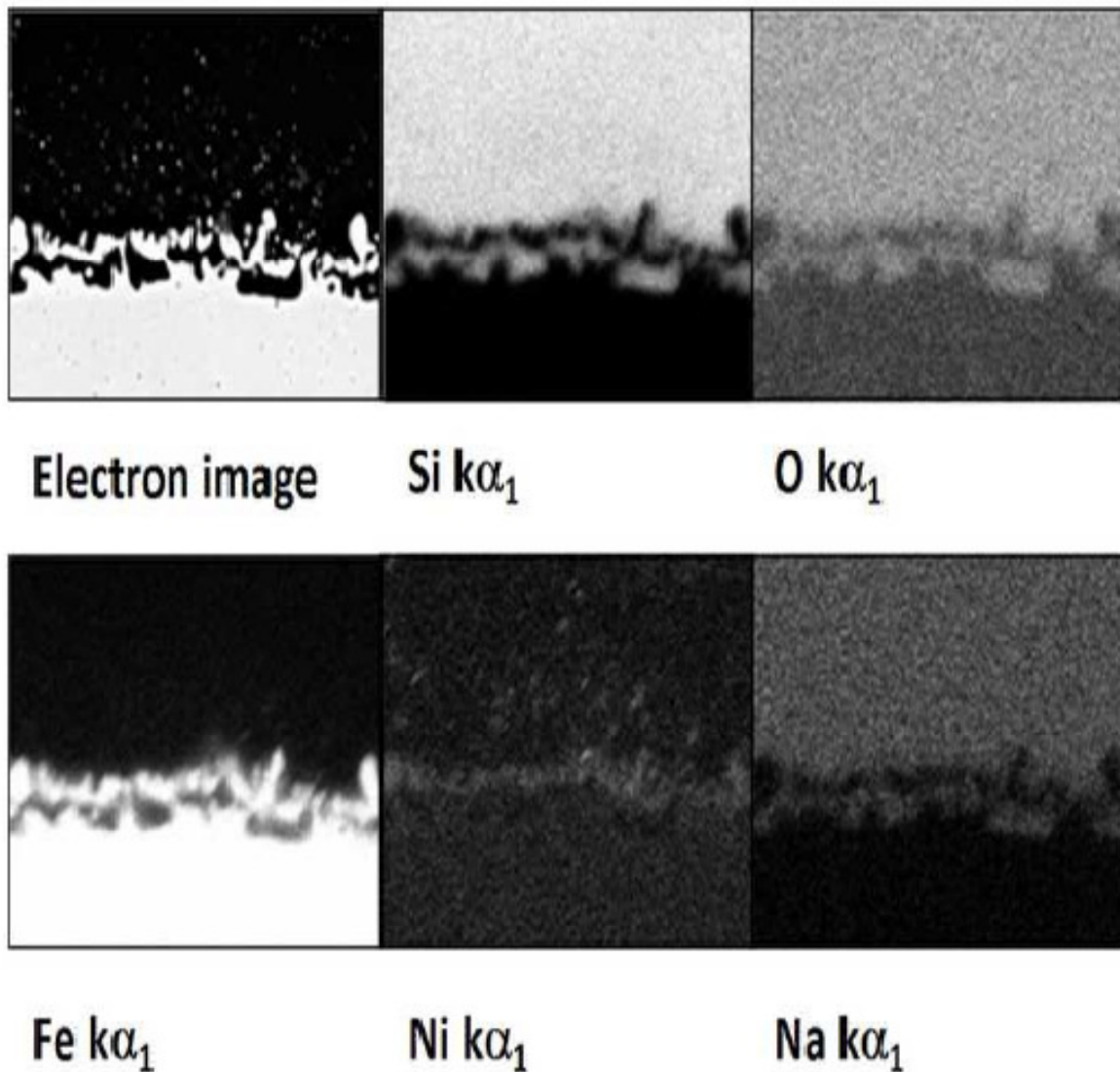


Figure 47. X-ray mapping of interface

Several EDS spectra, twenty, were collected in three different zones of enamel, Figure 46 : near metal ; above “islands” and near the surface; the average semi quantitative chemical analysis of the main oxides is reported in table 15.

<b>Oxide Wt% (<math>\pm 1\%</math>)</b>				
<b>Zones</b>	<b>Na<sub>2</sub>O</b>	<b>SiO<sub>2</sub></b>	<b>Fe<sub>2</sub>O<sub>3</sub></b>	<b>Others</b>
Zone 1	6.9	38.6	45.4	9.1
Zone 2	7.8	57.5	22.4	12.3
Zone 3	9.0	71.0	1.8	18.2

**Table 15. Semiquantitative chemical analysis of the three different zones of the enamel (see Figure 30)[7]**

The equipment used to detect the amount of element on the studied samples is an energy dispersive spectroscope (INCA instruments). The microanalysis software has a built-in routine to transform the element % concentration in weight oxide %. As reported in [26] the x-ray intensity generated for each element in the sample is proportional to the concentration of that element. The quantitative analysis used in this work is a “standard less analysis”. Standard less analysis is the simplest of the correction procedure.

The spectrum of the unknown is recorded without concern for the electron dose as long as the dead time is acceptable. To perform a quantitative analysis, it is necessary only to supply the correct beam energy and the elements to be analyzed. The analysis total will always be exactly 100%. This approach is that we can calculate the intensity measured from standards with accuracy equal to that measuring them directly, based on certain properties of the single spectrum obtained from an unknown. The most general approach makes use of four equations to predict the x-ray intensity that would be obtained from a pure-element standard [26].

From the results it is clear that the concentration of iron oxides at the top of the enamel layer is 1wt%, while the presence of higher Fe concentrations at the interfacial enamel must be caused by a reaction between enamel and steel as well as the dissolution of any iron oxide phases formed during firing.

As reported by J.Q. Dumm et al. [27], iron concentration was measured mainly as Fe<sup>2+</sup>, since Fe<sup>3+</sup> is not stable at 850°C in the presence of iron.

At the interface we had the presence of FeO and islands rich in FeNi at the intergrowth phase. The equilibrium at the interface, in the pretreatment, is shown by this reaction [28]:

NiO precoat + Fe steel → FeO oxide layer + Ni oxide layer)

$$dG^\circ(\text{J/mol Fe or C}) = dH^\circ - TdS^\circ \quad dG^\circ(\text{J/mol Fe or C}) = -28\,137 - 21.8T$$

As reported by P.M. Sorensen [29], the  $\text{Fe}^{2+}$  ions behave as network modifiers, while the  $\text{Fe}^{3+}$  ions preferably behave as network formers; this means that the viscosity of enamel in the interface should have a lower viscosity with respect to industrial enamel during firing, especially at higher temperatures, increasing the diffusion of iron from the steel. For the same reason, the coefficient of linear expansion of enamel in the interface having higher amounts of network modifier will present a CTE value lower than the steel one ( $13.0 \times 10^{-6} \text{ }^\circ\text{C}^{-1}$ ). This fact can contribute to increase the compressive stress in the enamel layer at the interface region.

At the same time, it is important to underline that, as reported by Romero et al. [30], thanks to TEM observation of glasses with similar composition, iron oxide in the glass seems to promote a liquid-liquid phase separation in the original enamel where drops richer in iron are dispersed in the silica vitreous phase.

The industrial sample was also subjected to a fractographic analysis after an impact test as described in [31]. From the SEM observation of the fractured surface, a morphology close to a known liquid-liquid phase separation was observed [32]. The liquid formed during melting of a glass batch can, in some cases, spontaneously separate into very viscous liquids or phases. Cooling the melts to a temperature below the glass transformation leads to a phase separation as a result of a liquid-liquid immiscibility. Understanding of immiscibility is based on thermodynamics of regular solutions.

The separation process can yield glass with either droplet/matrix or interconnected microstructures. [33] In particular, in glasses containing high amounts of iron, the EDS analysis indicates the presence of two phases rich in iron oxide (mainly crystalline) and silicon oxide (mainly vitreous), respectively.

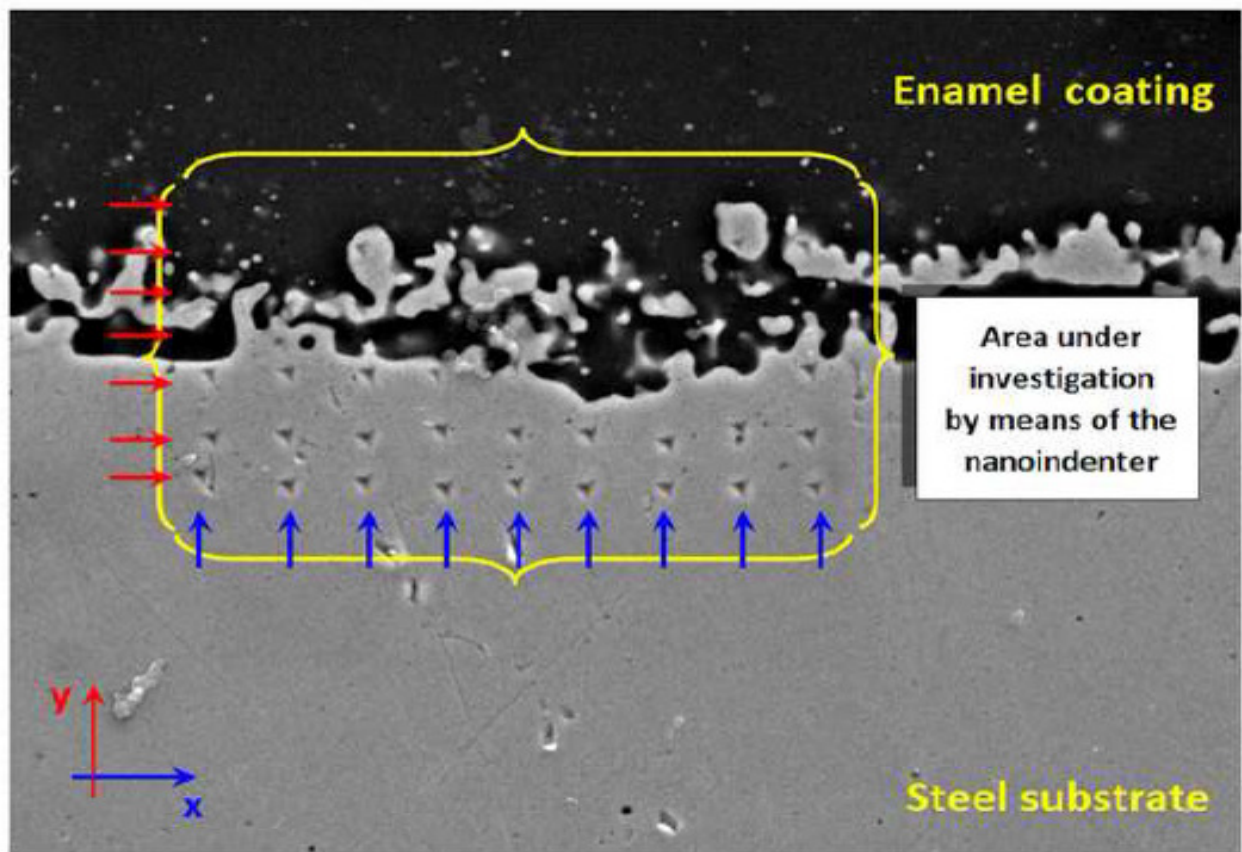
This phase separation can act as a nuclear agent for the crystallization of iron rich phases.

Since the steel-enamel interface presents a very complex chemical composition due to the diffusion of Fe ions, the micro-hardness of this zone will show different mechanical properties with respect to the other enamel and the steel constituents.

#### 4.11.2 Nano indenter test

As reported above, the thickness of the interface is in the range of 35-40 micrometers and it is quite difficult to measure its mechanical properties by Vickers micro-hardness because the indentation area is usually larger than 20  $\mu\text{m}$ .

For these reasons, a Nano-indentation technique is used to map cross-section hardness from the enamel-steel junction to the outer enamel surface. Figure 48 shows a cross-section of the industrial sample tested by using a nano-indententer; in particular, the indentation matrix area is formed by 9 columns in x direction and 7 rows in y direction.



— 5  $\mu\text{m}$ .

SED 1500x HT=25.0Kv. SPOT=5 WD=10.7mm.

Figure 48. SEM indentation matrix zone on enamel-steel interface at 1500X of magnification

Figure 49 reports Vickers Hardness with matrix points of single indentation. The distance between each horizontal and vertical line of the matrix is 5 micrometers, so they are equidistant in the xy plane.

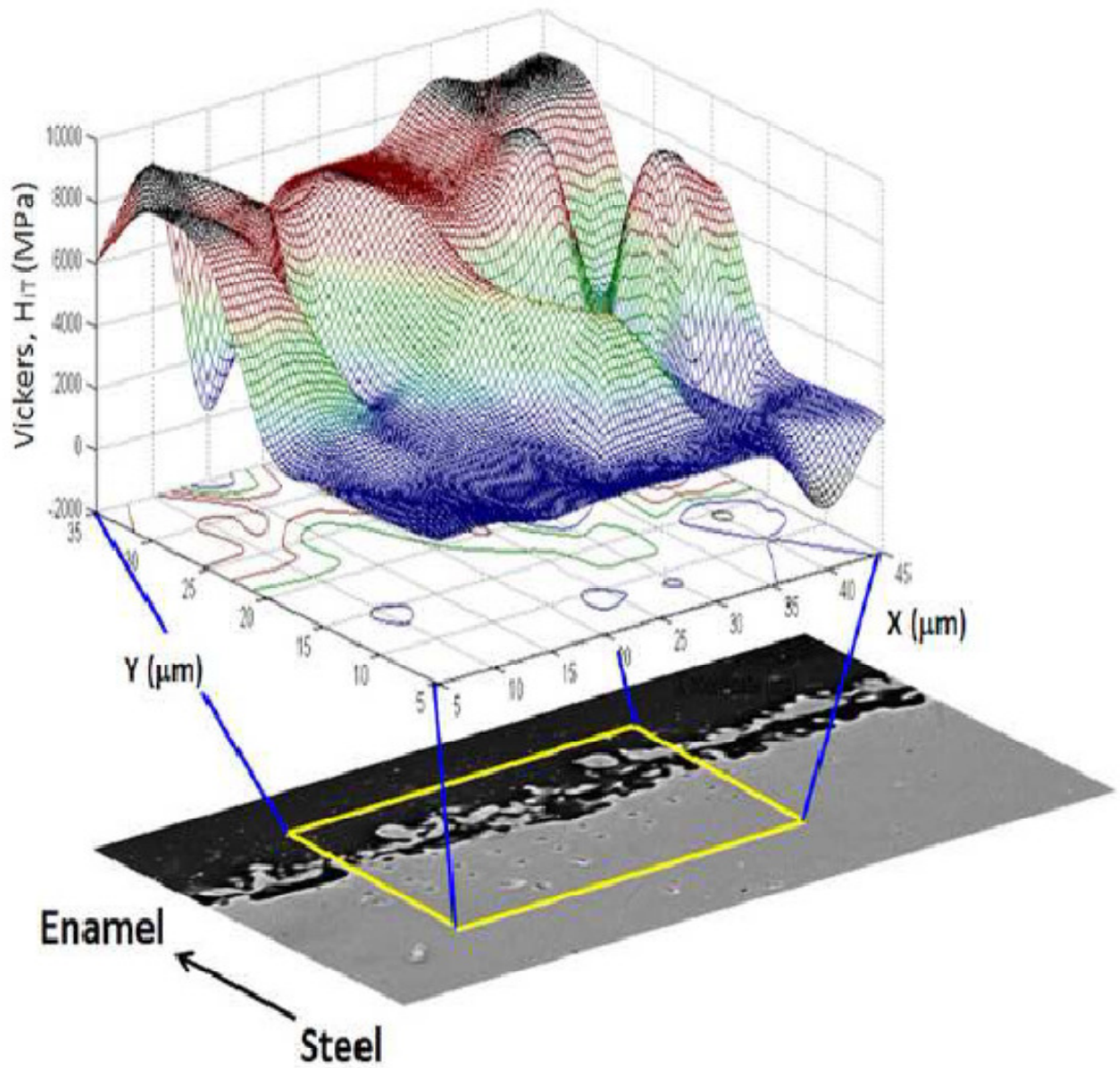


Figure 49. Vickers map by interpolation of Nano-indentations values: enamel-red; steel-blue; yellow/light blue-interface

The variability in this plot is largely due to the variation of concentration of metal oxides in the enamel interface. As an example, in Figure 50-B, we report the iron (Fe) and the silicon (Si) atomic concentration diagrams respect the position in the interface. A more evident diagram of the

hardness variation can be obtained by a mean value of the hardness along each line with respect to the material constitution.

Such a diagram is shown in Figure 50-C, where the mean values and the standard deviation of the HV hardness obtained by means of Nano-indentation are related to the measurement positions through the specimen thickness.

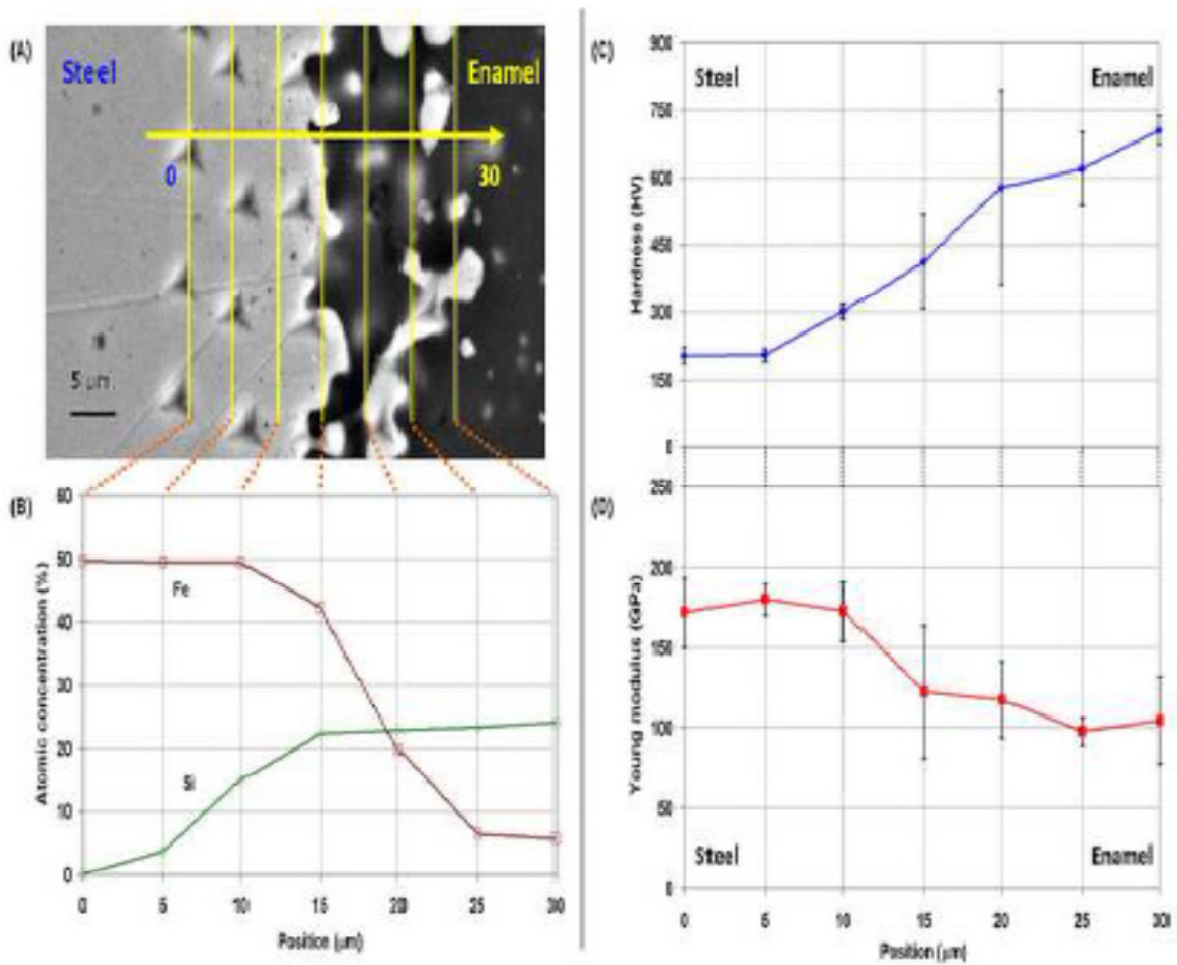


Figure 50. (A) detail of the indented area; (B) iron (Fe) and silicon (Si) percentage concentration versus position in the interface area; (C) Hardness and (D) Young Modulus trends versus position in the interface area

The increase of hardness from the steel to enamel is due to the fact that the interface-enamel has a higher amount of  $Fe^{2+}$  than the surface-enamel and, as already reported, it acts as a network modifier; this means that some properties, such as hardness, chemical, thermal and so on, decrease with the increase of iron content in the glass [34-36].

As reported by Romero et al. [30], glasses containing higher amounts of iron oxide (15-25 wt%) give Vickers Hardness values in the (571- 685) HV range in agreement with the values of Vickers

hardness obtained for the enamel-interface. On the contrary, the Young modulus, see Figure 50-D, showed a decreasing trend from the steel to the enamel layer.

Such behaviour can be explained by the fact that the Young Modulus of silicate glasses is usually 70GPa while for the low-carbon steel it is close to 150GPa ; increasing the glassy phase content in the interface thus decreases the Young modulus.

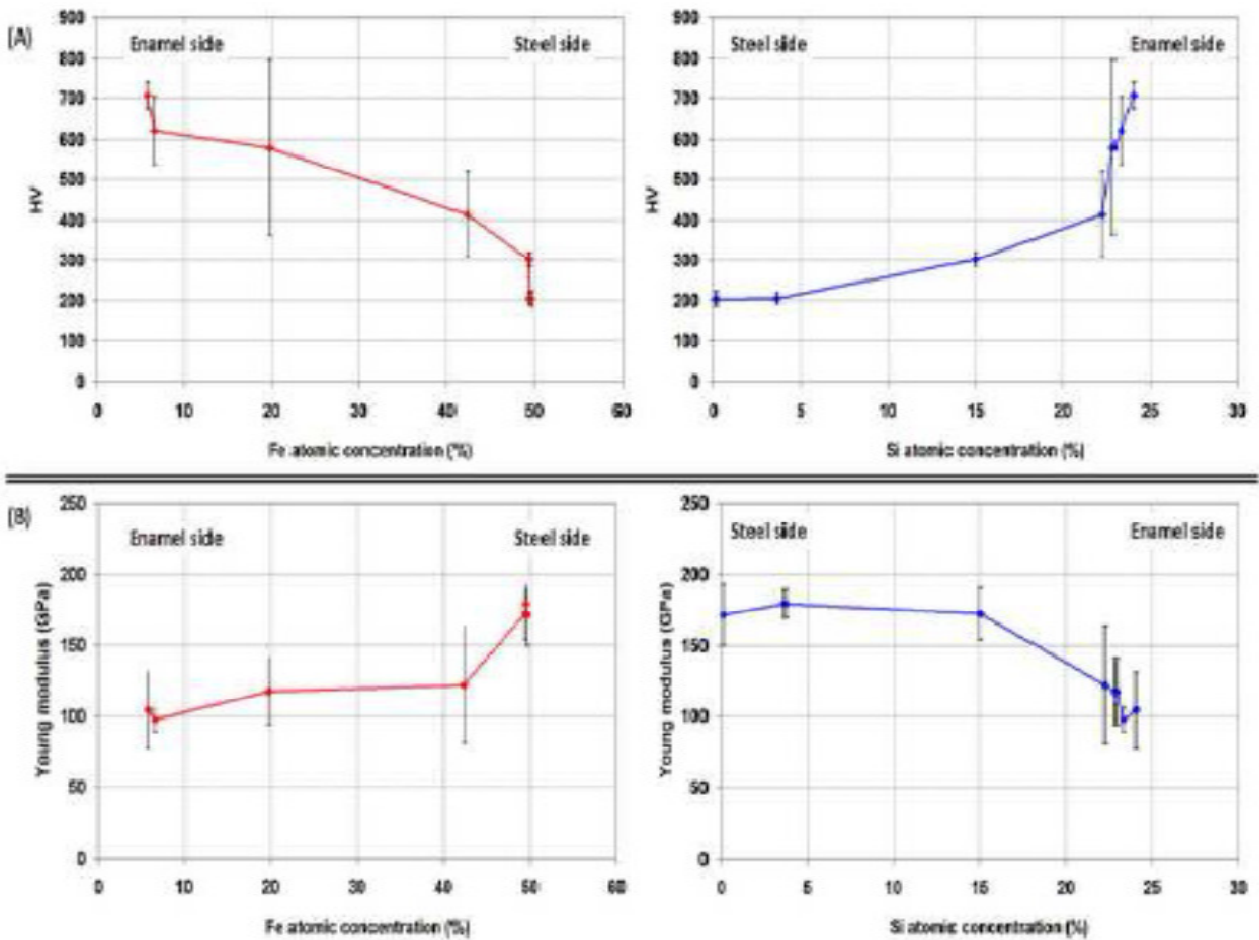


Figure51. (A) HV and (B) Young modulus trends with respect to the iron and silicon percentage

In Figure 51-A HV versus iron and silicon percentage concentrations are reported and the data show that micro-hardness increased from the steel to the enamel. Figure 51-A clearly shows a significant gradient in the interface Nano-indentation hardness going from the outer to the interior enamel (part in contact with the steel).

The outer enamel exhibits the highest hardness and was consistent with the fact that the enamel contains higher amounts of silicon, which is a former network ion. The hardness in the interior

enamel decreased significantly, and this reduction is due to the fact that the enamel contains high amounts of iron ion which is, as reported above, a network modifier ion.

Figure 51-B shows the Young modulus versus the iron and the silicon percentage content. On the contrary, with respect to what is observed in the case of the material hardness, the Young modulus decreases as the silicon percentage content increases and as the iron percentage content decreases.

As it was observed by P.M. Sorensen [29], the concentration of iron has a significant influence on the crystallization behaviour of the glass, and due to the fact that the enamelling is a high temperature process in an oxidizing environment, the iron, that diffuses from the steel plate, could promote the formation of stable crystalline phases [20] into the enamel coating so locally enhancing the mechanical performances and in particular the Young modulus as highlighted by the experimental results.

From a general point of view, it can be observed that the interface between the steel and the enamel is formed by a graded interface material, where due to a gradual variation of the elements from the steel to the enamel it is possible to obtain a gradual variation in the main material properties such as hardness and elasticity.

## **4.12 Characterization of samples obtained by electrophoretic deposition**

### **4.12.1 Yield deposition**

Yield deposition was an investigation about the setting parameters of electrophoretic deposition. Chen and Liu [37] shown the linearity between mass deposition, concentration of the particle and time. Specimens obtained in different condition were measured by digital calliper and scale (figure 52). Mass before and after deposition, area of deposition was the two important data. According to Ferrari at all [38] Van der Biest at all [14,39] electrophoretic deposition kinetics was determined for different masses of Densicer, voltage, mass of enamel in order to describe these variables.

From Figures 53 ; 54 ; 55 tests were carried out between 0-90 seconds to avoid problem of settling. In this range we have suitable condition of homogeneous mass deposit.

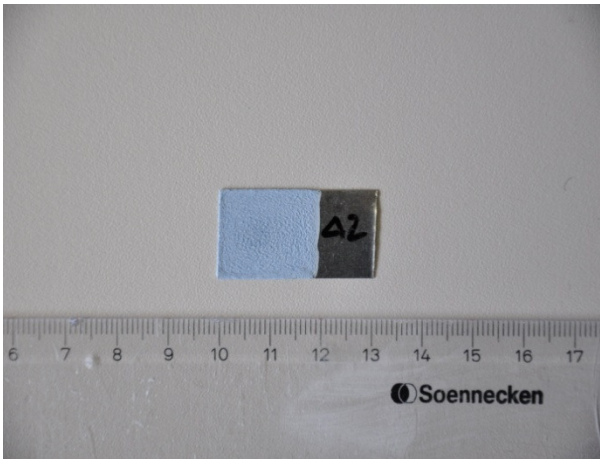
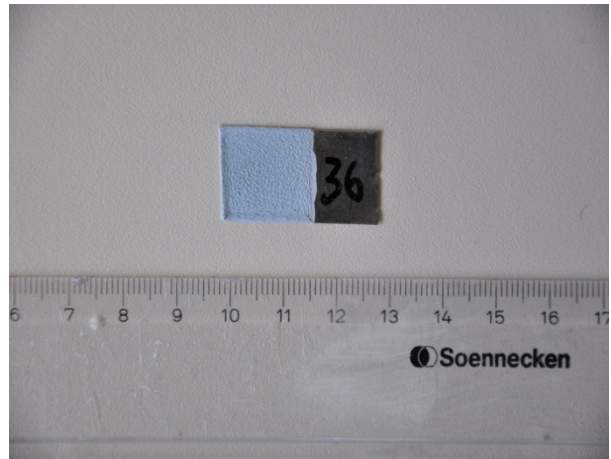
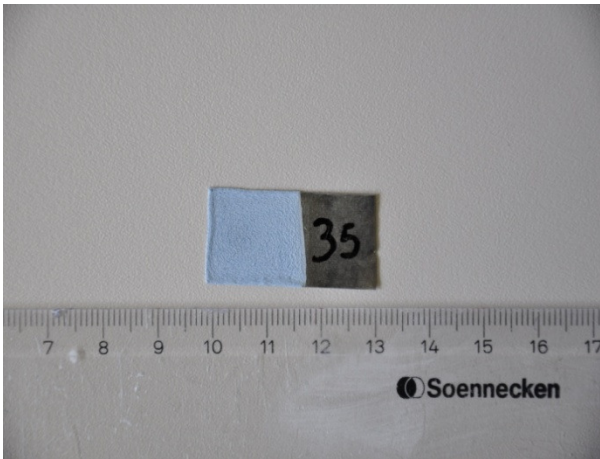


Figure 52. Sample obtained by EPD technique

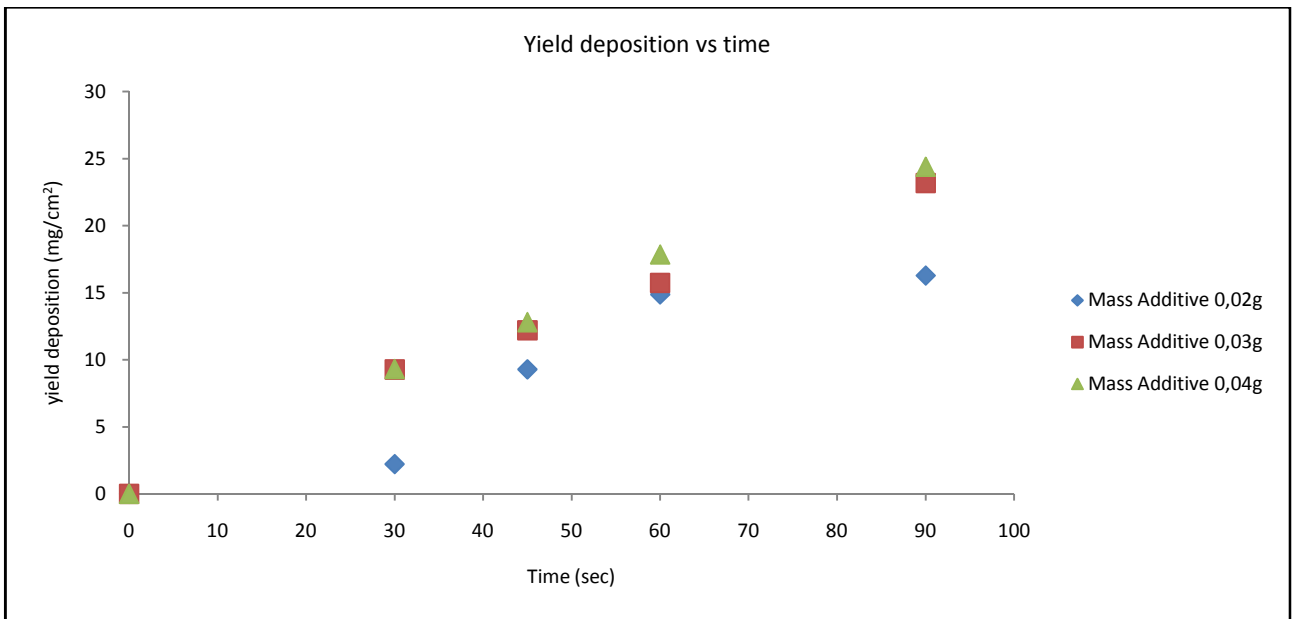


Figure 53. Yield deposition of Electrophoretic technique

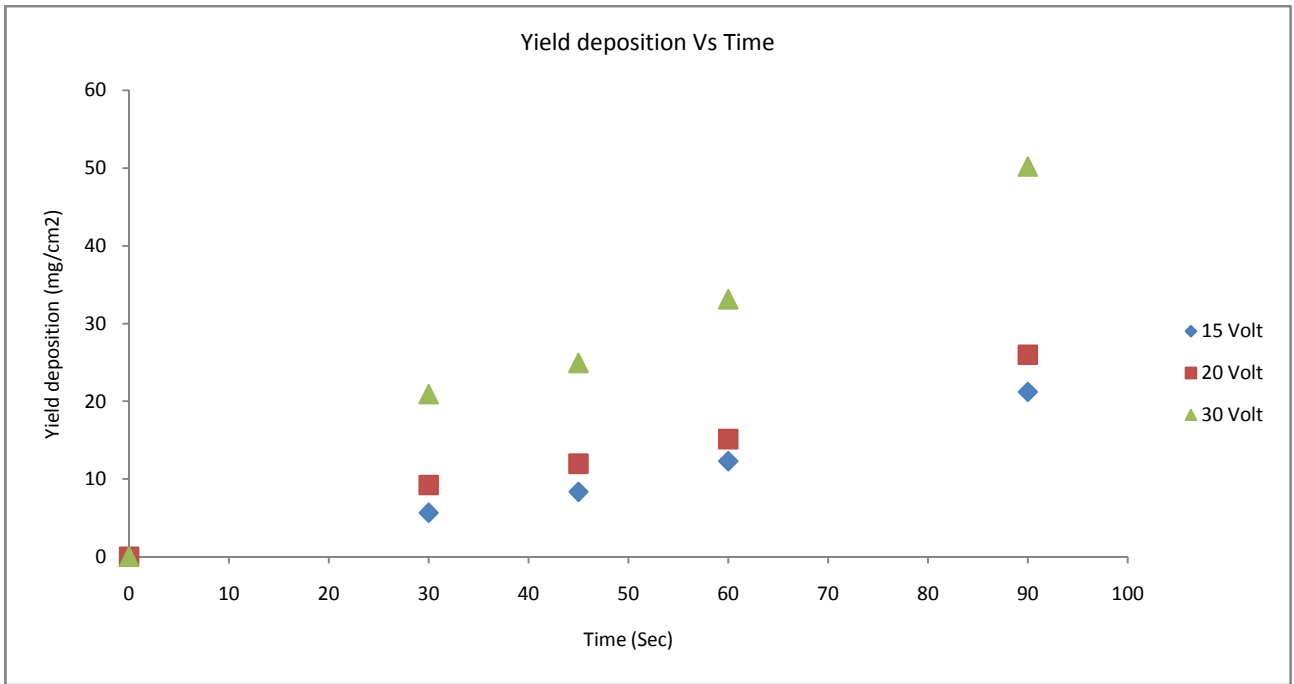


Figure 54. Yield deposition of Electrophoretic technique

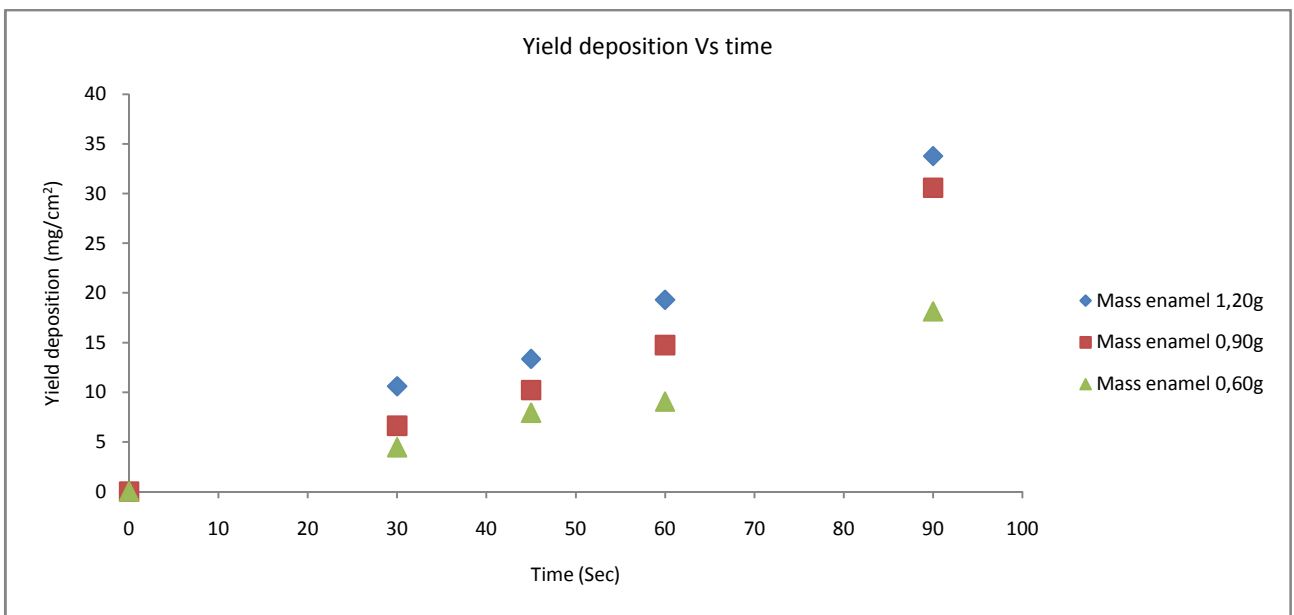


Figure 55. Yield deposition of Electrophoretic technique

	Figure 27	Figure 27 (g)	Figure 28	Figure 28 (Volts)	Figure 29	Figure 29 (g)
Value of R <sup>2</sup>	0,885	0,02	0,982	15	0,965	0,60
Value of R <sup>2</sup>	0,994	0,03	0,987	20	0,944	0,90
Value of R <sup>2</sup>	0,994	0,04	0,989	30	0,980	1,20
<b>Average</b>	<b>0,957</b>		<b>0,986</b>		<b>0,963</b>	

Table 16. Values of R<sup>2</sup>

From these trends (Figure 53 ; 54 ; 55) is reached different values of R<sup>2</sup> caused from different stabilities of suspensions, electric potential, different solid phase. In order to classify the kinetic mechanism of EPD (Table 16), it is possible shown the little gap about voltage and mass of enamel trends. Only the trend about mass of additive have a relevant gap between lower and higher R<sup>2</sup> because little mass of Densicer do not allow suitable stability to the suspension.

$$w = \int_{t_1}^{t_2} \mu \cdot E \cdot A \cdot C \cdot dt$$

Figure 56. Equation of Hamaker

Hamaker [40] and Avgustnik et al [41] (figure 56), was the first to correlate the amount of particles deposited during EPD with different influencing parameters.

Hamakers law relates the deposit yield (w) to the electric field strength (E), the electrophoretic mobility (μ), the surface area of the electrode (A), and the particle mass concentration in the suspension (C) through the following equation. In the apparatus of EPD technique are fixed and the solvent is water, the parameters (A) and (μ) are not variable of deposition mass

The weight of the deposited particles (w) in the EPD method is a function of E, t and C.

Mass of the deposited particles and the thickness of the coating can be readily controlled by the applied potential, concentration of the slurry, and deposition time in this technique. Ishihara et al. [42] and Chen and Liu [37] used other law for EPD technique, with linear correlation about zeta potential to mass deposition.

#### 4.12.2 Nano-indenter test of interface

Optical microscope allow to show the nano-indentation tests. Little area about  $2500 \mu\text{m}^2$  between steel and enamel was investigated by nano-indentation tests (figures 57, 58).

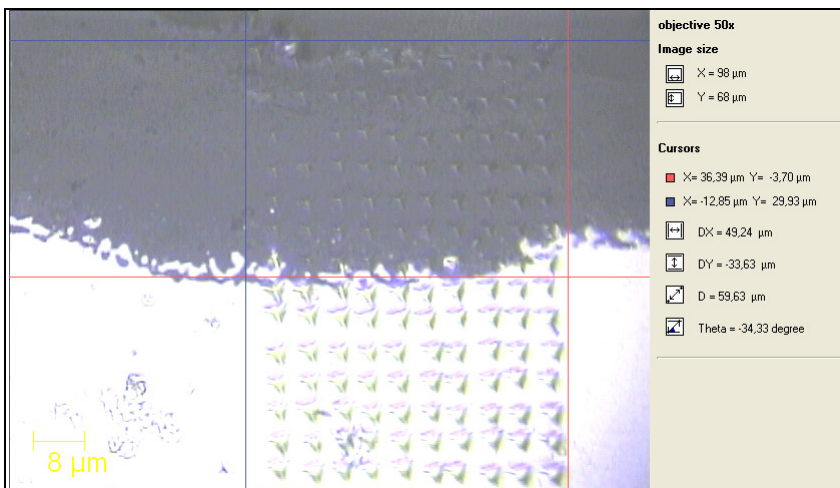


Figure 57. Complete area of Nano-indentation test

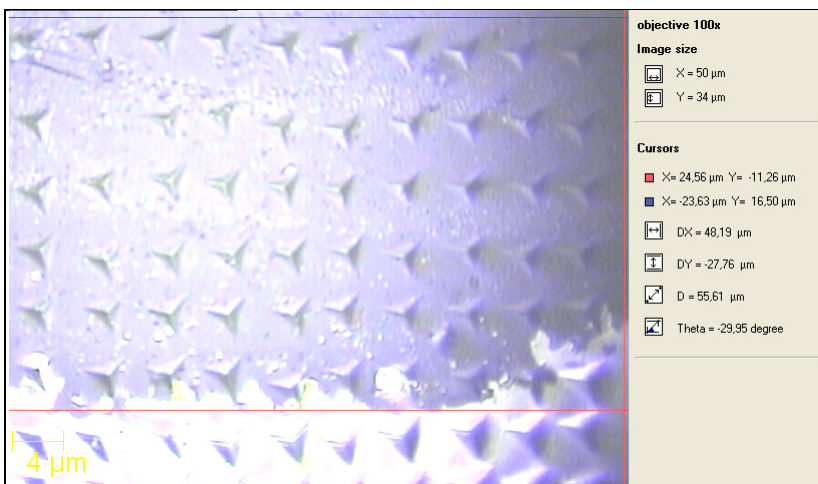


Figure 58. Nano-indentation at the interface steel-enamel

In order to classify different behaviour between enamel and steel, are shown two curves with Normal force versus Penetration depth. Different trends were shown from (Figures 59 and 60). According to Oliver, Pharr and Panich, Yong [43 - 46] this method consent to reach the hardness and elastic modulus of a material from indentation load displacement data obtained during one cycle of loading and unloading. About this modelling, deformation during loading is assumed to be both elastic and plastic in nature as the permanent hardness impression forms. During unloading, it is confirmed that only the elastic displacements are recovered ; it is the elastic nature of the unloading curve that make easier the analysis.

First curves (Figure 59) was obtained from indentation over AISI 316L because trend of Normal force and high area under the curve is typical of stainless steel.

Second curves (Figure 60) was obtained from vitreous enamel coating (AISI 316L) because values of Normal force is higher than the values of stainless steel and area of these curves is smaller than stainless steel [45]. According to Oliver, Pharr the hardness is relative small compared to the modulus, and this is typical of most metals. Different behaviour of elastic recovery is reached from vitreous coating [45-46].

Area below the curves (figures 59 and 60) is the energy needed to indent the material. Energy used to make an indentation is the area under the curves (figures 59 and 60).

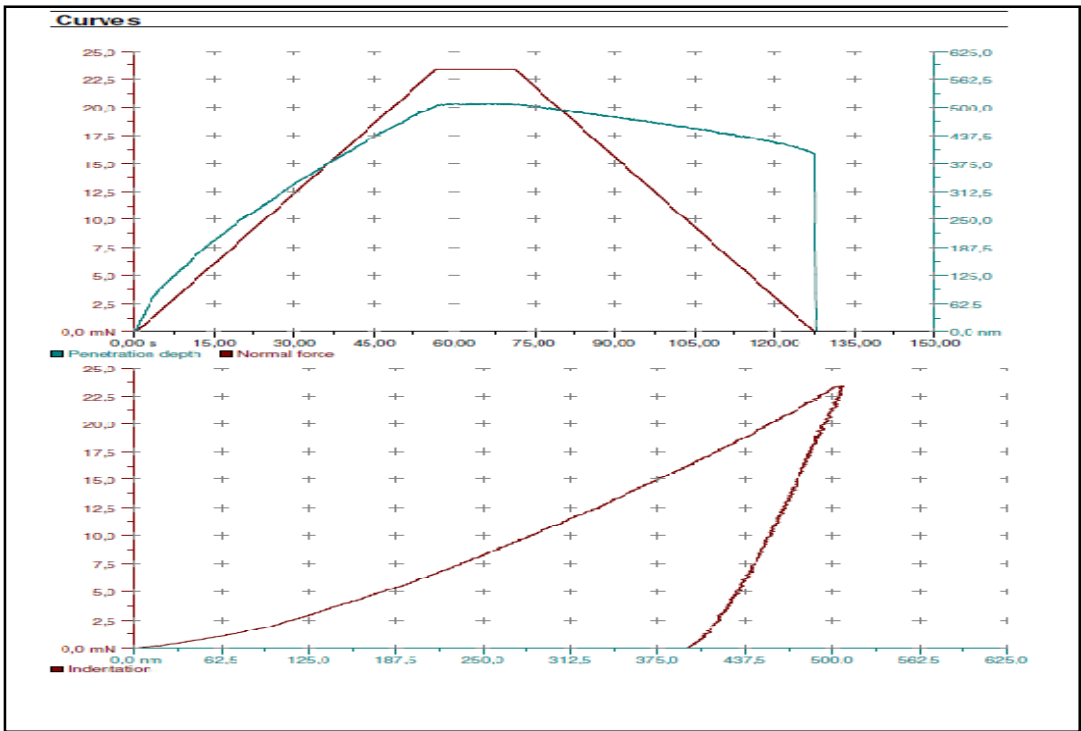


Figure 59. Nano-indentation over steel substrate AISI 316L after thermal treatment

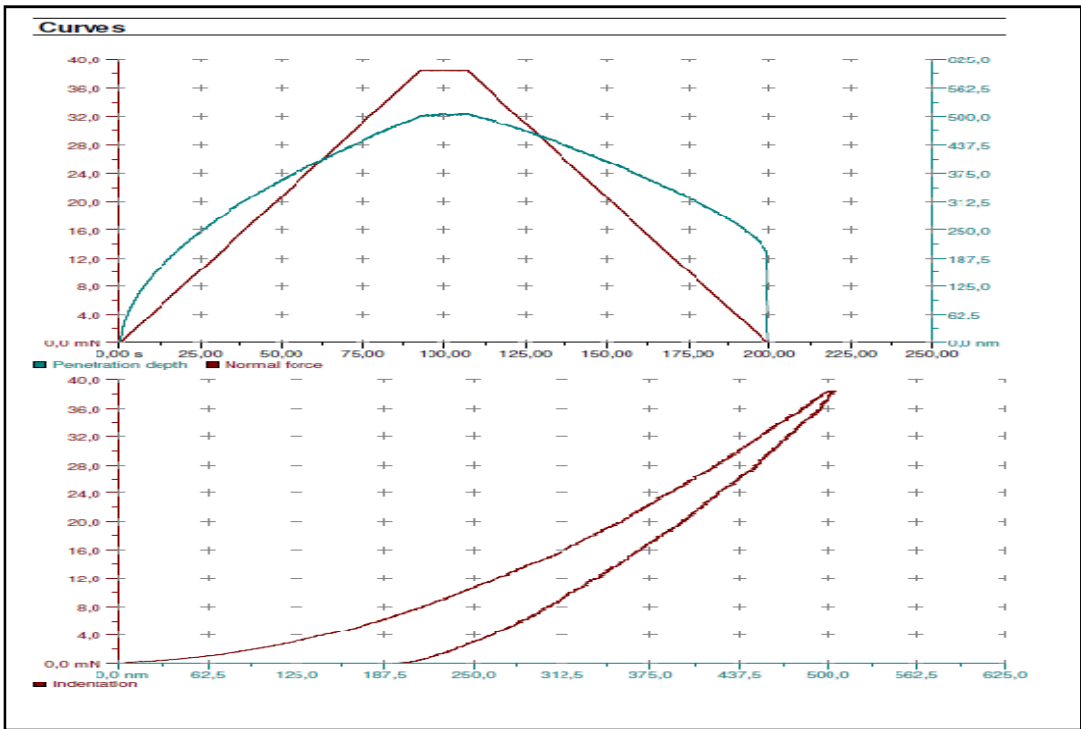


Figure 60. Nano-indentation over enamel SM014 after thermal treatment

From sample was obtained suitable results and was carried out two at thermal treatment at 800°C for 4 minutes (Figure 61 and 62). This sample was investigated by Nano-indentations, in order to

obtain mechanical properties such as : micro-hardness Hv and Young modulus. From each horizontal line of matrix (Figure 63) was obtained an average set of data about Young modulus and micro-hardness Hv. Investigation start in the steel area then finish in the vitreous area like Figure 35. The distance from each horizontal line is 5 microns, because less distance do not allow suitable measurements according to Oliver, Pharr [43 – 45]

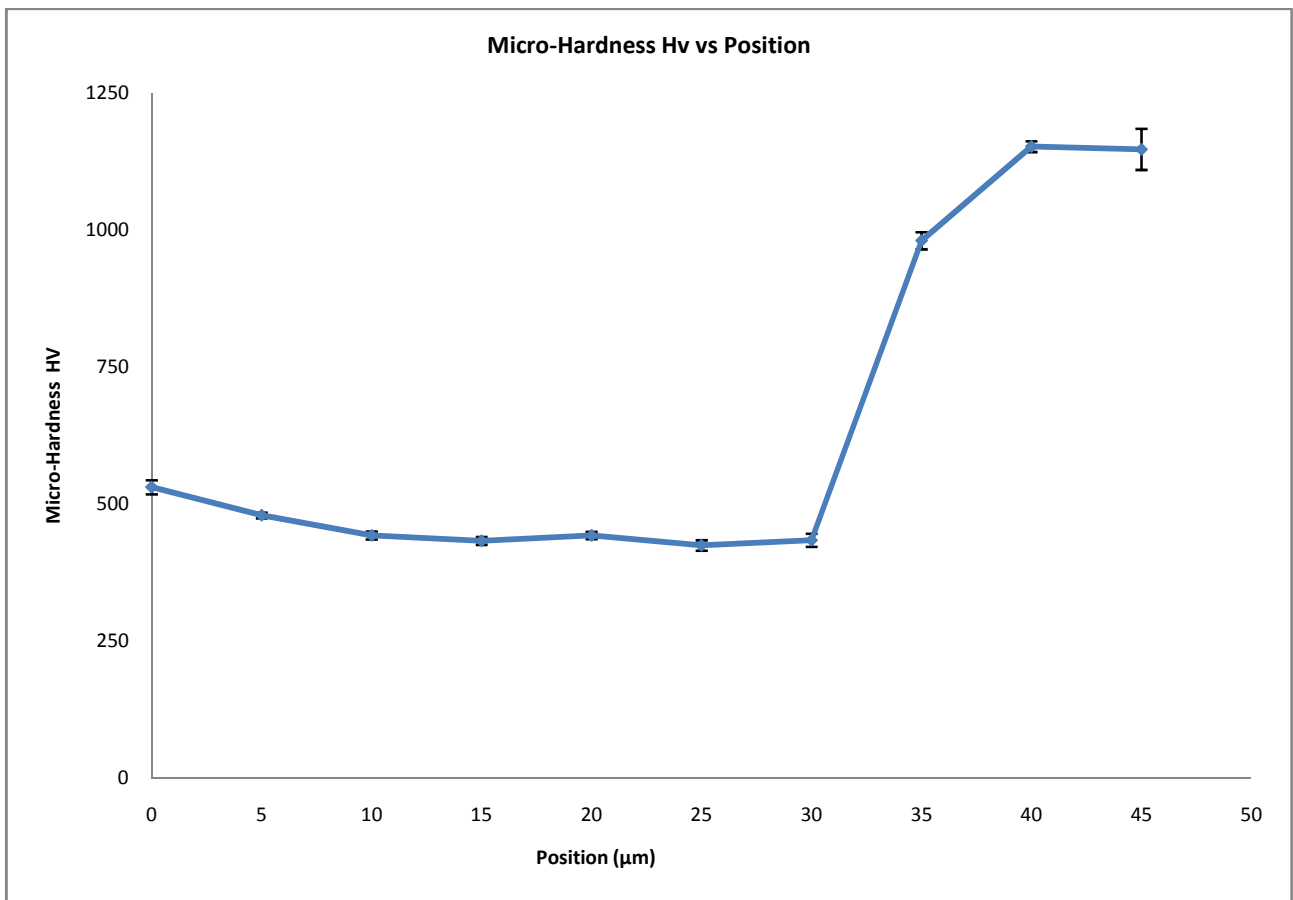


Figure 61. Micro-hardness Hv of sample with thermal treatment at 800°C

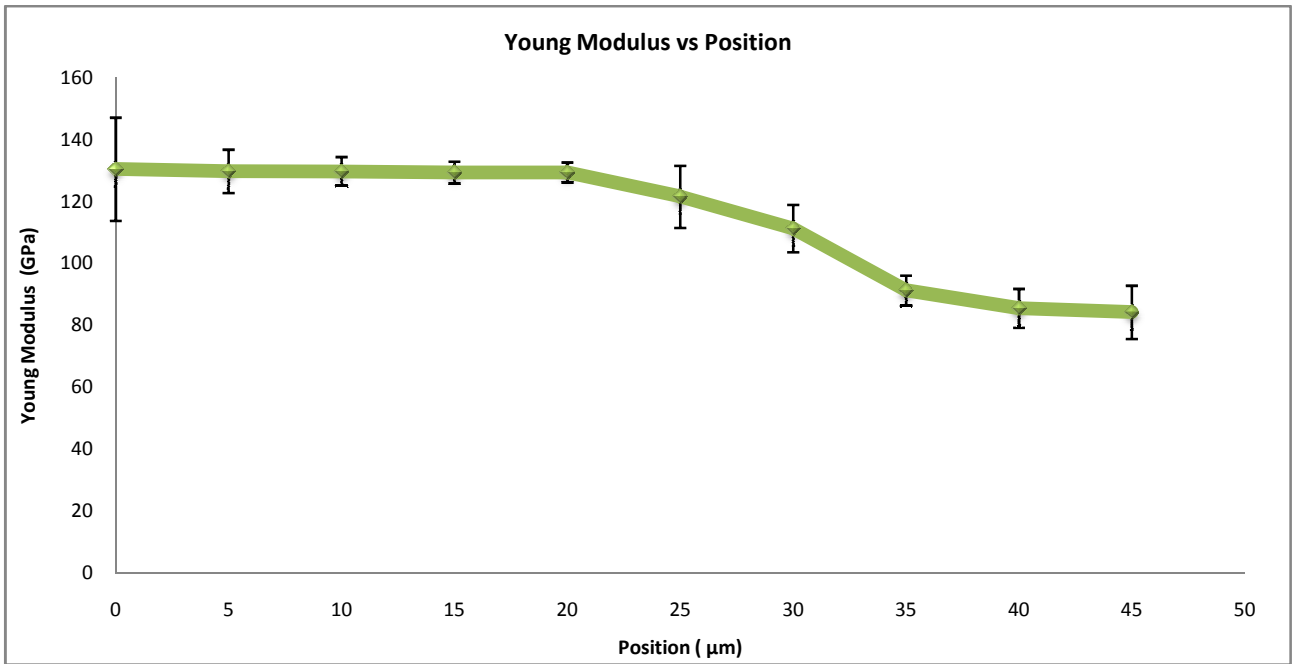


Figure 62. Young modulus of sample with thermal treatment at 800°C

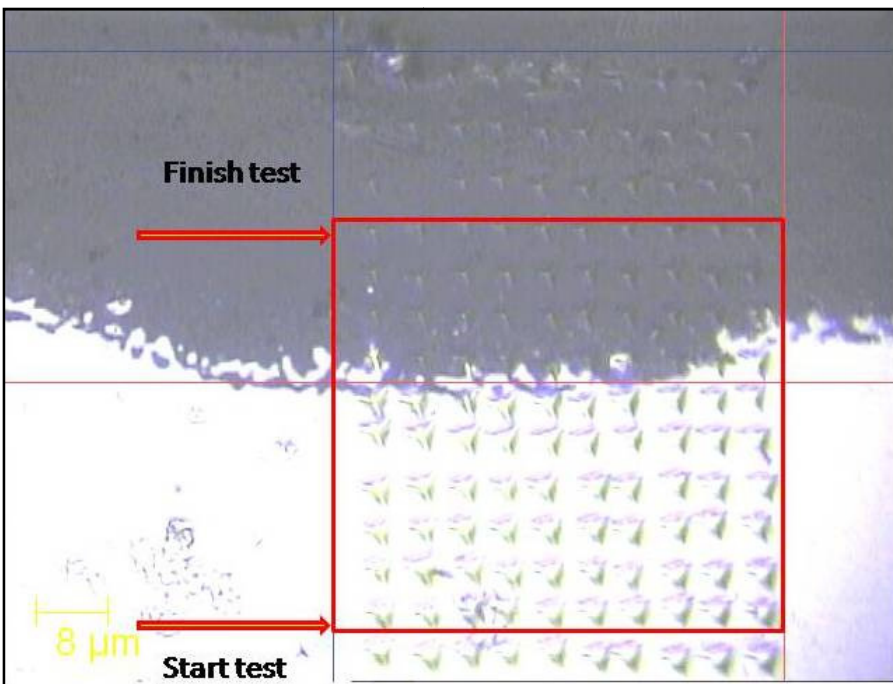


Figure 63. Area of test

Graphs of the hardness and Young modulus (Figures 61 and 62) trends can be obtained by a mean value of the hardness and Young modulus along each horizontal line with respect to the material constitution. Chaotic area typical of interface [1] is characterized from high value of error bar (Figure 61 and 62) to represent standard deviation of measurements for each horizontal line.

Figure 61 shown the positive trend, about micro-hardness, between between steel zone to Vitreous zone, and these results is according to Wang [21].

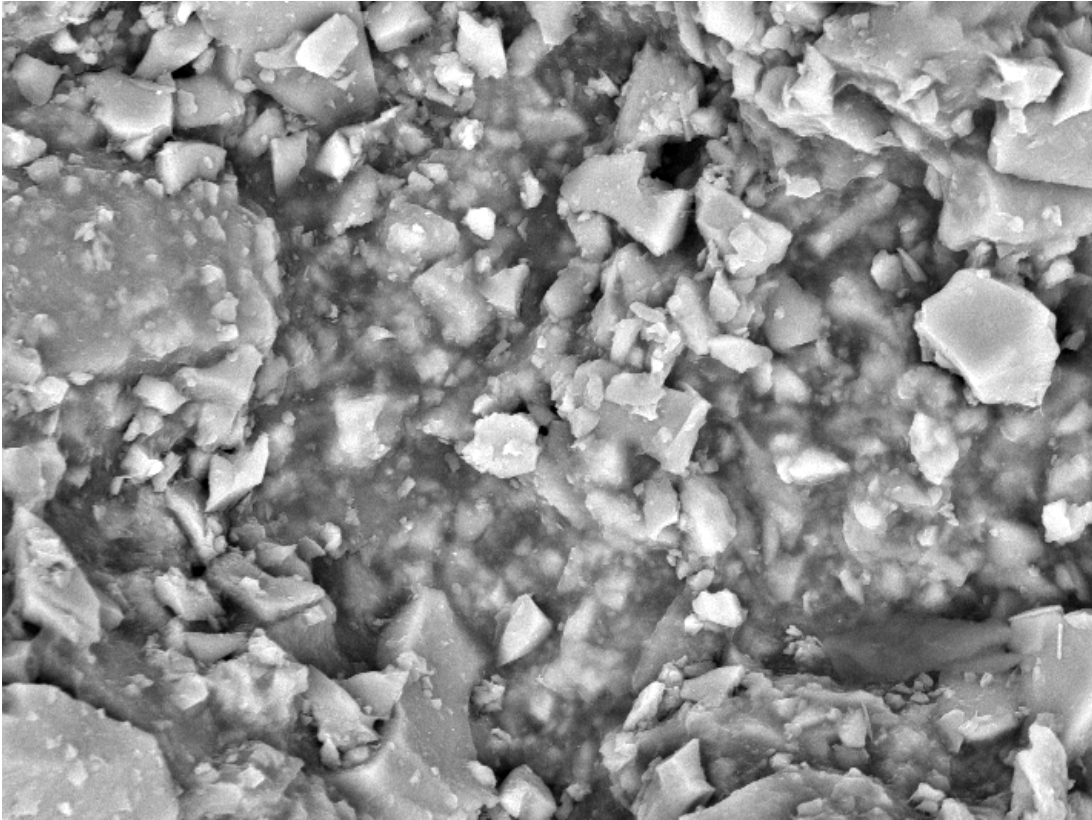
The increase of hardness from the steel to enamel is due to the fact that the interface-enamel has a higher amount of  $\text{Fe}^{2+}$  than the surface-enamel and, as already reported, it acts as a network modifier; this means that some properties, such as hardness, chemical, thermal and so on, decrease with the increase of iron content in the glass [34-36].

As reported by Romero et al [2, 30], glasses containing higher amounts of iron oxide (15-25 wt%) give Vickers Hardness values in the 571-685 HV range in agreement with the values of Vickers hardness obtained for the enamel-interface.

From steel area to enamel area Young modulus (Figure 62) decrease because stainless steel AISI 316L reach 150-200 GPa [47] and vitreous coating SM014 80-90 GPa [1].

#### **4.12.3 SEM of Electrophoretic deposition samples**

SEM images of deposits from suspensions with Densicer deposited by EPD technique before and after heat treatment at 800°C for 5 minutes are shown in Figure 5. In particular the green sample presents a quite uniform deposition even if large particles are well visible. After firing (Figure 64) the glaze shows a very homogeneous and compact material.



5  $\mu\text{m}$ . **BSD** 1000x **(a)**

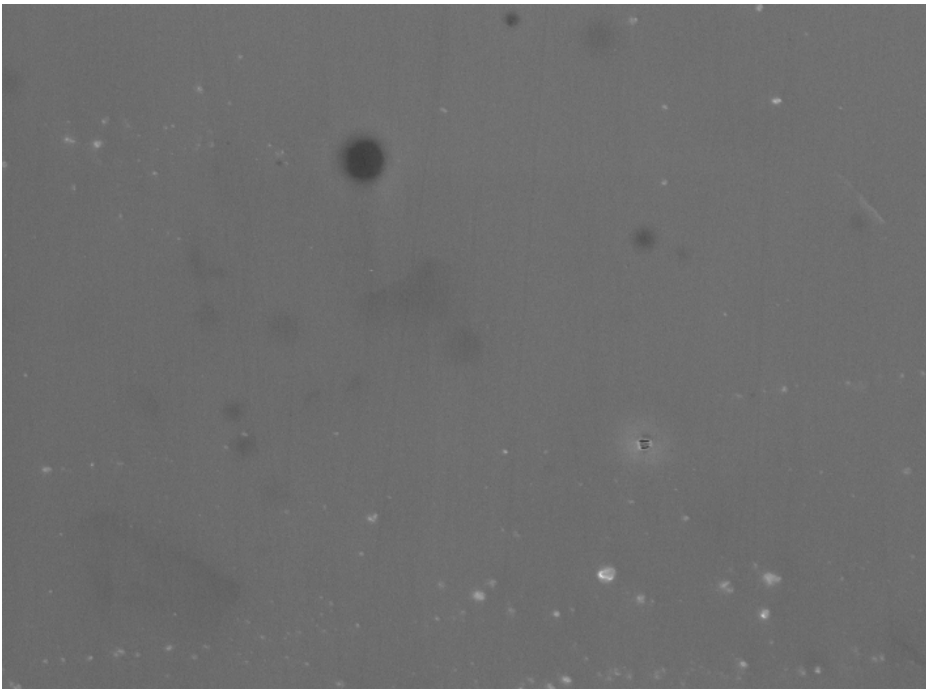


Figure 64. Vitreous glaze obtain by EPD From Densicer containing suspension (a) before firing (b) after firing.

5  $\mu\text{m}$ . **SED** 1000x **(b)**

Behaviour and relations between mechanical and structural properties with hand spraying and EPD technique. This properties was carried out from innovative technique such as : SEM, ESEM, Nano-Indentation test. These is very important also for Smaltiflex because it has not the technology to reach these data.

## References

- [1]. Andrea Zucchelli, Matteo Dignatici, Monia Montorsi, Riccardo Carlotti, Cristina Siligardi. ; Characterization of vitreous enamel-steel interface by using hot stage ESEM and Nano-indentation techniques ; journal of the European Ceramic Society
- [2]. Leila Samiee, Hossein Sarpoolaky, Alireza Mirhabibi ; Microstructure and adherence of cobalt containing and cobalt free enamels to low carbon steel ; Materials Science and Engineering A 458 (2007) 88–95
- [3]. From Smalto Porcellanato Tecnologia e Mercati numero 02/1996 anno XXXVIII inserto no. 2.
- [4]. De Pablos A., Duran A., Nieto MI. Adjusting of laboratory filature furnace for obtaining fibreglass Bol. Soc. Esp. Ceram. Vidr. (1997); 36 (5): 517-523.
- [5]. De Hoffa PH., Anusaviceb KJ. Creep functions of dental ceramics measured in a beam-bending viscometer Dental Materials (2004); 20: 297–304.
- [6]. Barbieri L, Leonelli C, Manfredini T, Siligardi C. Influence of viscosity on the crystallization of some anorthite-diopside glass precursors” J. Mater. Sci. Lett. (1993); 12: 294-296.
- [7]. Siligardi C, Lusvarghi L, Montorsi M, Vernia M. Sintering and Crystallization of CaO–Al<sub>2</sub>O<sub>3</sub>–ZrO<sub>2</sub>–SiO<sub>2</sub> Glasses Containing Different Amount of Al<sub>2</sub>O<sub>3</sub>, J. Am. Ceram. Soc., (2008) 91 [3]: 990–5.

- [8]. Zucchelli A, Minak G, Ghelli D. Low-velocity impact behaviour of vitreous enamelled steel plates, *International Journal of Impact Engineering* (2010); 37: 673-84.
- [9]. PROPRIETA' E CONTROLLI SU FRITTE, SMALTI E SMALTATURE, Tratto da Smalto Porcellanato Tecnologia e Mercati numero 01/1997 anno XXXIX inserto no. 4
- [10]. Tandon R., Green DJ. Residual stress determination using strain gage measurements *J. Am. Ceram. Soc.* (1990); 73 (9): 2628-33.
- [11]. Sarkar, P. and Nicholson, P. S., Electrophoretic sedimentation (EPD): mechanism, kinetics and application to ceramics. *J. Am. Ceram. Soc.*, 1996, 79, 1987–2002.
- [12]. Boccaccini, A. R. and Zhitomirsky, I., Application of electrophoretic and electrolytic sedimentation techniques in ceramics processing. *Curr.Opin. Solid State Mater. Sci.*, 2002, 6, 251–260.
- [13]. X. Yang, A. Jha, R. Brydson, R.C. Cochrane, The effects of a nickel oxide precoat on the gas bubble structures and fish-scaling resistance in vitreous enamels, *Materials Science and Engineering A366* (2004) 254–261
- [14]. Van der Biest, O. O. and Vandeperre, L. J., Electrophoretic sedimentation of materials. *Ann. Rev. Mater. Sci.*, 1999, 29, 327–352.
- [15]. Laxmidhar Besra , Meilin Liu ; A review on fundamentals and applications of electrophoretic sedimentation (EPD) ; *Progress in Materials Science* 52 (2007) 1–61
- [16]. Guven, N., Pollastro, R.M ; Molecular aspects of aqueous smectite suspensions. In: (Eds.), *Clay–Water Interface and its Rheological Implications. Clay Minerals Society Workshop Lectures*, vol. 4. Clay Min. Society, Boulder, Colorado, pp. 2–79

[17]. Heavens N. Electrophoretic deposition as a processing route for ceramics. In: Binner GP, editor. Advanced ceramic processing and technology, vol. 1. Park Ridge (NJ), USA: Noyes Publications; 1990. p. 255–83 [chapter 7].

[18]. STUDIO DELLE PROPRIETÀ MECCANICHE E TRIBOLOGICHE DI LAMIERE IN ACCIAIO RIVESTITE MEDIANTE SMALTI PORCELLANATI, Tratto da “Smalto porcellanato – Tecnologia & Mercati” N. 3/06 – Anno XLVIII

[19]. Tratto da “Smalto Porcellanato - Tecnologia & Mercati” – N. 2/1999 – Anno XLI, ACCIAI DA PROFONDO STAMPAGGIO PER L'INDUSTRIA DEI SANITARI

[20]. Barcova K, Mashlan M, Zboril R, Filip J, Podjuklova J, Hrabovska K, Schaaf P. Phase composition of steel-enamel interfaces: Effects of chemical pre-treatment Surface & coating (2006); 210: 1836-1844.

[21]. Deqing Wang, Effect of crystallization on the property of hard enamel coating on steel substrate, Applied Surface Science 255 (2009) 4640–4645

[22]. J. Lu, M. Chen, B. Zhu, G. Wu, China Enamel 11 (1990) 13.

[23]. A. Goel, D.U. Tulyaganov, S. Agathopoulos, J.M.F. Ferreira, Ceram. Int. 34 (2008) 505

[24]. A. Chelli, R. Poletti, Smaltiflex S.p.A., F. Bruscoli, G. Pasqualetti, F. Bruni, Colorobbia S.p.A. A. Zucchelli, L. Rossetti, F. Lotti, G. Minak, V. Dal Re, S. Curioni, Università di Bologna, Un approccio integrato dalla formatura e smaltatura all'assemblaggio nei cestelli, ELEMENTI IN ACCIAIO SMALTATO PER PRERISCALDATORI D'ARIA E GAS-GAS HEATERS

[25]. Shieu FS, Lin KC, Wong JC. Microstructure and adherence of porcelain enamel to low carbon steel, Ceram. Int. (1999); 25: 27-34.

[26]. J. I. Goldstein, D.E. Newbury, P. Echlin, D.C.Joy, A.D. Romigjr., C.E. Lyman, C. Fiori, E. Lifshin in “Scanning electron microscopy and x-ray microanalysis” Second Edition Plenum Press,

New York, 1994, pp 417-547

[27]. Dumm JQ, Brown PW. Dissolution of iron in silicate melts J. Am. Ceram. Soc. (1999); 82: 987-93,

[28]. X. Yang\*, A. Jha, R. Brydson, R.C. Cochrane, An analysis of the microstructure and interfacial chemistry of steel–enamel interface, Thin Solid Films 443 (2003) 33–45

[29]. Sorensen PM, Pind M, Yue YZ, Rawlings RD, Boccaccini AR, Nielsen ER. Effect of the redox state and concentration of iron on the crystallization behaviour of iron-rich aluminosilicate glasses J. Non-Cryst. Solids (2005); 351: 1246-53.

[30]. Romero M, Rincon JMa. Preparation and Properties of high iron oxide content glasses obtained from industrial wastes” J. Eur. Ceram. Soc. (1998); 18: 153-160.

[31]. Richmond JC., Moore DG., Kirkpatrick HB., Harrison WN. Relation between roughness of interface and adherence of porcelain enamel to steel. J. Am. Ceram. Soc. (1953); 36, [12]: 410–416.

[32]. Piscella P, Pelino M. Thermal expansion investigation of iron rich glass-ceramic J. Eur. Cer. Soc. (2008); 28: 3021-3026.

[33]. J. E. Shelby “Introduction to glass science and technology” The Royal Society of Chemistry Cambridge, UK, pp.48-68

[34]. Varshneya AK. Fundamentals of inorganic glasses” Academic Press, Inc., (1994), p. 61-86.

[35]. Barbieri L., Corradi A., Lancellotti I. Thermal and chemical behaviour of different glasses containing fly ash and their transformation into glass-ceramics J. Europ. Cer. Soc. (2002); 22:1759-1765.

[36]. Karamanov A, Pelino M. “Crystallization phenomena in iron-rich glasses” J. Non-Cryst. Solids (2001); 281: 139-151.

- [37]. Chen F, Liu M. ,Preparation of yttria-stabilised zirconia (YSZ) films on La<sub>0.85</sub>Sr<sub>0.15</sub>MnO<sub>3</sub> (LSM) and LSM–YSZ substrate using an electrophoretic deposition (EPD) process. *J Eur Ceram Soc* 2001;21:127–34.
- [38]. Begona Ferrari, Sergio Gonzalez, Rodrigo Moreno, Carmen Baudín ; Multilayer coatings with improved reliability produced by aqueous electrophoretic deposition ; *Journal of the European Ceramic Society* 26 (2006) 27–36
- [39]. Aqueous electrophoretic deposition in asymmetric AC electric fields (AC–EPD), Bram Neirinck, Jan Fransaer, Omer Van der Biest, Jef Vleugels, *Electrochemistry Communications* 11 (2009) 57–60
- [40]. Hamaker HC. Formation of deposition by electrophoresis. *Trans Farad Soc* 1940;36:279–83.
- [41]. Avgustinik AI, Vigdergauz VS, Zharavlev GI. Electrophoretic deposition of ceramic masses from suspension and calculation of deposit yields. *J ApplChem USSR (English Translation)* 1962;35(10): 2175–80.
- [42]. Ishihara T, Shimise K, Kudo T, Nishiguchi H, Akbay T, Takita Y. Preparation of Yttria-stabilised zirconia thin-films on strontium doped LaMnO<sub>3</sub> cathode substrate via electrophoretic deposition for solid oxide fuel cells. *J Am Ceram Soc* 2000;83(8):1921–7.
- [43]. W.C. Oliver, G.M. Pharr, A new improved technique for determining hardness and elastic modulus sing load and sensing indentation experiments, *J. Mater. Res.* 7(6) (1992) 1564-1582.
- [44]. W.C. Oliver, G.M. Pharr , Measurement of hardness and elastic modulus by instrumented indentation: Advances in understanding and refinements to methodology, *Journal of Materials Research*

[45]. W.C. Oliver, G.M. Pharr, An improved technique for determining hardness and elastic modulus using load and displacement sensing indentation experiments, J.Mater. Res, Vol 7, No.6, June 1992

[46]. Nurot Panich, Sun Yong, IMPROVED METHOD TO DETERMINE THE HARDNESS AND ELASTIC MODULI USING NANO-INDENTATION, KMITL Sci. J. Vol. 5 No. 2 Jan-Jun 2005

[47]. UNI EN 10028-7

## 5 Conclusions

The lower carbon steel (DC04ED) considered in the study is a cheap substrate, and the application of vitreous enamel coating represents the best choice to its possible application as a thermal exchanger.

Due to the fact that the enamel-steel interface is one of the most strategic and, at the same time, critical aspects that influence the quality and the behaviour of the enamel coating, the detailed analysis and characterization of the interface between enamel and steel becomes the key factor for the definitions of this possible application into the industrial field .

Recent experimental techniques, such as the nano-indentation test, and some consolidated techniques, such as the Environmental Scanning Electron Microscopy (ESEM) with the hot stage and the hot stage microscope, were used to investigate the microstructural and chemical features of the enamel-steel interface. The latter techniques are used in a non-conventional way to study these materials, but they provide useful information on enamelling and on its use.

The present study confirms the presence of the complex diffusion mechanism of the constituent materials occurring during enamel-steel interface creation and growth at high temperature. The presence of liquid-liquid phase separations was confirmed and supposed to be the main driving force for the nucleation and crystallization of iron rich phases in the interface area. These iron rich phases influence the adherence of the enamel as well as the hardness and the elastic properties of the interface. Through the nano-indentation techniques, the interface hardness and the Young modulus were analyzed and an increasing hardness trend from the steel side to the enamel one was observed. On the contrary, the elasticity of the interface decreased from the steel side to the enamel one.

In the second part of work, the electrophoretic deposition technique was used as an alternative method to coat the steel. This process is one of the latest methods introduced on an industrial-scale, according to the considerable advantages that it offers.

In this study, the industrial slurry used in the first part of work has been diluted and added with specific additives in order to obtain stable slip enamel.

The use of additives is a fast and suitable way to optimize the rheological behaviour of diluted vitreous enamel slurries to apply in EPD technique. Inorganic additives like Bentonite and coagulants are not appropriate, since the prepared slurries are unstable and the settling time is

not high enough to enable the particles to move and deposit on the deposition electrode during EPD.

The three carboxy methyl celluloses show similar settling times and viscosity values. Low molecular weight CMC shows high value of zeta potential, but it doesn't have a good performance as for the settling time, confirmed by rheological measurements. Densicer was the only additive that improved the stability time in order to delay the sedimentation of the enamel slurry. The composition of this additive led to a better performance with zeta potential, which is typical of organic compounds (like CMC), and the stability time, which is typical of inorganic compounds. All techniques used such as the zeta potential and the rotational rheometry confirmed a better performance of Densicer in comparison to other additives used.

It was possible to come to the conclusion that using Densicer as additive represents an innovative solution to deposit slurries with relative high glassy solid fraction during electrophoretic deposition in order to obtain vitreous coatings. The use of well-dispersed suspensions reduces the waste after the mass sedimentation and the cost of this type of enamelling. This part of the study showed also that the use of mixtures of additives as binder with dispersant did not improve the suspension stability, suggesting the absence of a synergy effect between the involved additives.

## 6. Acknowledgements

I would like to acknowledge to all of them that have contributed to the realization of the PhD school in the University of Modena, especially to:

My family : Ivano ,Manuela and Marco which have always supported me during all these years. My advisor, Professor Siligardi Cristina and Professor Montorsi Monia for them patience, incentive, financial and intellectual support during this PhD course. Particular regard at Professor Boccaccini Aldo to help me during my period in Germany and other two german friends such as Liverani Liliana (la zia), and Francesca Iannantuoni (honda).

Dr Zucchelli Andrea and Dr Pavese Matteo for them assistance on the mechanical sections of this work. Professor Storari Silvia and Professor Parillo Margherita to help me with English. Special regard to Professor Mariano Paganelli.

Colleagues from the laboratory and office for the long work discussions about sport, travel and work during all these years.

My friends Davide, Marco, Tax, Biri, Vale kate, Vally, Angela, Ilaria Sandro and Barbara, Marcello and other for their friendship and fantastic times spent together.

## List of Table

Table 1. Mechanical properties of different kind of materials.....	13
Table 2. Thermal properties of different kind of materials.....	14
Table 3. Specific data of degreasing process.....	21
Table 4. Additivies used for EPD technique.....	37
Table 5. Summary of peculiar temperatures for enamels studied.....	59
Table 6. Values of linear thermal expansion. ....	61
Table 7. Summary of DTA results. ....	65
Table 8. Chemical composition of SM014 enamel. ....	66
Table 9. Laser particle size tests. ....	67
Table 10. Hardness of Very low carbon steel. ....	70
Table 11. Zeta potential values (mV) for suspensions added with additive. ....	71
Table 12. Time of sedimentation for the suspensions studied added with 2wt% of additive (except Densicer).....	78
Table 13. Hardness of Very low carbon steel. ....	81
Table 14. Characterization of different thickness of vitreous enamel plate bulk.....	82

Table 15. Semiquantitative chemical analysis of the three different zones of the enamel (see Figure 30)[7]85	
Table 16. Values of $R^2$ .....	94

## List of Figure

Figure 1. One rotational thermal exchanger of thermal power station.....	2
Figure 2. Ljungstrom preheater .....	3
Figure 3. Test of corrosion carried out by Smaltiflex .....	4
Figure 4. Different behaviour between solid state and glass state.....	10
Figure 5. Glass structure .....	11
Figure 6. Viscosity vs Temperature and characteristic points.....	12
Figure 7. Effects of characteristic points .....	13
Figure 8. Melting of raw material .....	15
Figure 9. Frit glass during the cooling.....	16
Figure 10. Industrial washing machine.....	21
Figure 11. Dipping enamelling process, chain with specimens.....	23
Figure 12. Flow enamelling for tube application.....	24
Figure 13. SEM of interface of vitreous enamel steel .....	29
Figure 14. Interface enamel steel with presence of dendritic area .....	31
Figure 15. Production plant of glass frit .....	34
Figure 16. Quenching process to obtain the frit.....	35
Figure 17. Vitreous enamel steel plate after thermal treatment.....	36
Figure 18. Sample of vitreous enamel steel by EPD technique .....	38
Figure 19. Vitreous enamel steel obtained by EPD technique after dryer process .....	38
Figure 20. Comparison of stability of the same enamel SM014 with and without additives. From left side SM014 with Densicer, SM014 with Bentonite, SM014 without additive.....	39
Figure 21. Hot stage microscope .....	40
Figure 22. Characteristic temperature obtained from HSM investigation.....	40
Figure 23. 402MVD, Wolpert Wilson.....	45
Figure 24. Indentation tester, CSM instruments.....	49
Figure 25. Indentation tester CSM instruments.....	50
Figure 26. Indentation Tester with sample in resin.....	51
Figure 27. Hot stage microscope of Enamel SM014.....	58
Figure 28. Qualitative viscosity-temperature curve and the related ESEM taken during the heating of the enamel-steel system.....	60
Figure 29. Matching of linear thermal expansion. ....	62
Figure 30. Differential thermal analysis of enamel SM014 .....	63
Figure 31. Differential Thermal analysis of frit 1524.....	63
Figure 32. Differential thermal analysis of frit 8010.....	64
Figure 33. Differential thermal analysis of frit 8100.....	64
Figure 34. Differential thermal analysis of frit mix.....	65
Figure 35. Grain size distribution of industrial slurry SM014.....	67

Figure 36. X-ray diffraction of Enamel SM014.....	69
Figure 37. Very low carbon steel DC04ED .....	70
Figure 38. Flow curve (up and down) of slurries prepared with Densicer 0.10% .....	73
Figure 39. Flow curve (up and down) of slurries prepared with Densicer 0.10% at different times. ....	73
Figure 40. Flow curves (Viscosity vs. shear rate) for the slurries without additive and with Densicer 0,10% at the two measured time points (5' and 10').....	75
Figure 41. Time curves (Shear stress vs. time) for the slurries without additive (SM014 TQ) and with Densicer (SM014 Densicer) and bentonite (SM014 bentonite).....	76
Figure 42. Time curve, matching between two better additive like : Densicer and Bentonite. ....	76
Figure 43. Time curve of 10' minutes of industrial Slurry with Densicer .....	77
Figure 44. Test of time settling in three different condition : SM014 Densicer, SM014 with Bentonite, SMO14 without additive.....	79
Figure 45. ESEM "in situ" image of studied enamel during heating at different temperatures .....	80
Figure 46. SEM micrograph of cross sectioned enamel/steel interface.....	83
Figure 47. X-ray mapping of interface .....	84
Figure 48. SEM indentation matrix zone on enamel-steel interface at 1500X of magnification .....	87
Figure 49. Vickers map by interpolation of Nano-indentations values: enamel-red; steel-blue; yellow/light blue-interface .....	88
Figure 50. (A) detail of the indented area; (B) iron (Fe) and silicon (Si) percentage concentration versus position in the interface area; (C) Hardness and (D) Young Modulus trends versus position in the interface area.....	89
Figure51. (A) HV and (B) Young modulus trends with respect to the iron and silicon percentage .....	90
Figure 52. Sample obtained by EPD technique .....	92
Figure 53. Yield deposition of Electrophoretic technique.....	92
Figure 54. Yield deposition of Electrophoretic technique.....	93
Figure 55. Yield deposition of Electrophoretic technique.....	93
Figure 56. Equation of Hamaker.....	94
Figure 57. Complete area of Nano-indentation test .....	95
Figure 58. Nano-indentation at the interface steel-enamel .....	95
Figure 59. Nano-indentation over steel substrate AISI 316L after thermal treatment.....	97
Figure 60. Nano-indentation over enamel SM014 after thermal treatment.....	97
Figure 61. Micro-hardness HV of sample with thermal treatment at 800°C .....	98
Figure 62. Young modulus of sample with thermal treatment at 800°C .....	99
Figure 63. Area of test .....	99
Figure 64. Vitreous glaze obtain by EPD From Densicer containing suspension (a) before firing (b) after firing.....	101

## Contents

1 Introduction and objective .....	2
1.1 Introduction.....	2

1.2 Problems about final application of vitreous enamel steel.....	3
1.3 Objective.....	5
1.3.1 Specific objectives .....	5
References.....	6
2. State of the Art .....	8
2.1 Glassy.....	8
2.1.1 Method and manufacture of glass .....	9
2.1.2 Glass properties.....	9
2.2 Porcelain enamel : definition composition and properties.....	14
2.2.1 Definition .....	14
2.2.2 Composition.....	15
2.2.3 Properties .....	16
2.3 Porcelain enamels.....	18
2.4 Substrates for enamelling applications .....	18
2.5.1 First treatment for low carbon steel .....	20
2.5.1.1 Deagresing .....	20
2.5.1.2 Pickling for very low carbon steel.....	21
2.4.1.3 Nickeling .....	22
2.4.1.4 Water.....	22
2.4.1.5 Dry .....	22
2.5 Enamelling .....	22
2.5.1 Wet enamelling .....	23
2.5.1.1 Dipping.....	23
2.5.1.2 Flow coating.....	24
2.5.1.3 Spray enamelling .....	25
2.5.1.5 Electro-enamelling.....	25
2.5.2 Dry enamelling.....	26
2.5.3 Coating steel .....	27
2.6 Dry process for wet enamelling.....	27
2.7 Thermal treatment process.....	28
References.....	32
3. Materials and Methods .....	34
3.1 Enamel SM014.....	34
3.2 Carbon steel.....	35
3.3 Vitreous enamel steel by hand-spray system.....	36

3.4 Vitreous enamel steel by Electrophoretic technique .....	37
3.5 Characterization Methods .....	39
3.5.1 Characterization of enamels.....	39
3.5.1.1 Thermal analysis .....	39
3.5.1.2 Chemical analysis.....	43
3.5.1.3 Particle size distribution .....	43
3.5.1.4 Density.....	44
3.5.1.5 X- Ray diffraction (XRD) .....	44
3.5.2 Characterization of carbon steel .....	45
3.5.2.1 Mechanical characterization .....	45
3.5.2.2 Measurements of roughness.....	45
3.5.3 Characterization of the slurry for EPD.....	46
3.5.3.1 Zeta potential .....	46
3.5.3.2 Rheological characterization .....	47
3.5.3.3 Settling after preparation of suspension for EPD.....	47
3.5.4 Vitreous enamel steel by hand-spraying system: surface characterization.....	48
3.5.4.1 ESEM with hot stage.....	48
3.5.4.2 Indentation tester.....	48
3.5.5 Vitreous enamel steel by hand-spraying system: interface characterization .....	49
3.5.5.1 SEM/EDS characterization .....	49
3.5.5.2 Indentation tester.....	50
3.5.6 Characterization of the vitreous enamel steel obtained by EPD.....	51
3.5.6.1 Indentation tester.....	51
3.5.6.2 Scanning electron microscope (SEM) .....	52
References .....	53
4 Result and discussion.....	57
4.1 Hot stage microscopy .....	57
4.2 Optical dilatometer.....	61
4.3 Differential thermal analysis .....	62
4.4 Chemical analysis.....	66
4.5 Grain size distribution.....	66
4.6 Density.....	68
4.7 X-ray diffraction .....	68
4.8 Characterization of steel.....	69
4.8.1 Optical observation .....	69

4.8.2 Micro-hardness.....	70
4.8.3 Measurements of roughness.....	71
4.9 Investigation of Enamel SM014 for electrophoretic deposition technique .....	71
4.9.1 Zeta potential .....	71
4.9.2 Rheological characterization .....	72
4.9.3 Settling after preparation of suspension for EPD.....	77
4.10 Vitreous enamel steel by hand-spraying system : surface characterization .....	79
4.10.1 ESEM with hot stage.....	79
4.10.2 Micro-hardness.....	81
4.10.3 Nano Indenter test .....	82
4.11 Vitreous enamel steel by hand-spraying system: interface characterization .....	83
4.11.1 SEM and EDS observation.....	83
4.11.2 Nano indenter test .....	87
4.12 Characterization of samples obtained by electrophoretic deposition.....	91
4.12.1 Yield deposition .....	91
4.12.2 Nano-indenter test of interface .....	95
4.12.3 SEM of Electrophoretic deposition samples.....	100
List of Table.....	110
List of Figure .....	111
References.....	102
5 Conclusions.....	107
6. Acknowledgements .....	109